University of Zurich[UZH]

Dynamics of rockfall hazard and risk from past to future: a case study in Täsch (VS), Switzerland

GEO 511 Master's Thesis

Author
Michael Fehlmann
10-729-309

Supervised by
PD Dr. Christian Huggel
Dr. Daniel Trappmann[1]
Prof. Dr. Markus Stoffel[2]
Dr. Michael Bründl[3]

Faculty representative
Prof. Dr. Andreas Vieli

September 2016
Department of Geography, University of Zurich

[1]University of Bern, Institute of Geological Sciences, Baltzerstrasse 1-3, CH-3012 Bern
daniel.trappmann@dendrolab.ch
[2]University of Geneva, Institute for Environmental Sciences, 66 boulevard Carl Vogt, CH-1205 Geneva
Markus.Stoffel@unige.ch
[3]WSL Institute for Snow and Avalanche Research SLF, Flüelastrasse 11, CH-7260 Davos Dorf
bruendl@slf.ch

Abstract

Switzerland is exposed to a multitude of natural hazards. Mass movements such as snow and rock avalanches, landslides or rockfalls affect more than 6% of the country. To protect human lives, property and the environment from resulting damages, hazard and risk assessments provide an essential basis. However, such assessments are often only applied and representative for a certain time period, typically for present conditions. By contrast, multi-temporal analyses can provide valuable information about hazard and risk developments and their driving factors. The main purpose of this study is therefore to develop a consistent methodology to assess long-term developments of rockfall hazard and accompanying risk. To test the developed method, it was applied at Täschgufer, a highly active rockfall slope in the southern Swiss Alps, where release zones of rockfall are located in periglacial environments. Thereby, hazard and risk maps were created for distinct time periods (1880, 1940, 2010 and 2060), depicting spatial patterns of past and likely future developments.

In accordance with well-established concepts of hazard and risk in Switzerland, a general analytical framework was developed, integrating field observations, event reports, dendrochronological and socio-economic data as well as statistical and process-oriented models, and then adjusted to the different time periods. For the analysis of past time periods, information about rockfall frequencies was derived from dendrochronological data of 255 sampled trees at the slope, and past exposure of infrastructure and people was inferred from historical maps. Furthermore, dendrochronological data allowed the establishment of a relation between annual rockfall frequencies and mean annual summer temperatures over several decades of the 20^{th} century. Future rockfall hazard and risk were then estimated based on both climate and socio-economic scenarios. Results show that past development of rockfall risk in Täsch was mainly driven by socio-economic factors, more precisely by increasing exposure of infrastructure and people in the late 20^{th} century. From present to 2060, however, projected rockfall risk is estimated to be equally driven by climatic and socio-economic factors, leading to an increase in rockfall risk by a factor of 2.2 over all scenarios. Therefore, it is suggested that a lacking climate signal in past losses from natural hazards does not necessarily imply the same finding for the future under continuing climate and socio-economic change.

Existing disaster loss studies are mainly focusing on regional to global scales but risk has typically many local-scale characteristics. This local study points out the importance of protection measures and the spatial distribution of infrastructure and people for local risk evolution. Future developments of such factors are highly uncertain, and can be influenced by local risk management. Also, future climate impacts on rockfall frequencies and magnitudes are site-specific and further research is needed to reduce related uncertainties.

Contents

List of Figures

List of Tables

1 Introduction

1.1 Context

Switzerland is a country exposed to many natural hazards. Especially in the Alps and Pre-Alps, mass movements such as snow and rock avalanches, landslides or rockfalls affect 6% of the country (Raetzo et al. 2002). Although generally small masses are involved in a single rockfall (Stoffel et al. 2006), it is one of the most common and most intensely studied hazards of the cliff zone in mountainous regions (Schneuwly & Stoffel 2008). Rockfall can be defined as the free falling, bouncing or rolling of individual or a few rocks and boulders, with volumes involved being generally smaller than 5 m^3 – and potentially endangers infrastructure and people in alpine settlements, which are concentrated in confined areas in Switzerland (Fuchs et al. 2004, Schneuwly & Stoffel 2008).

To assess natural hazards and risks and to protect human lives, property and the environment from damage, hazard and risk maps are useful tools. Since 1991, cantons in Switzerland are required to establish hazard maps. These maps denote hazard-prone areas and provide a basis for land-use planning, whereby for example construction in substantially endangered areas is prohibited (Raetzo et al. 2002). However, when it comes to the implementation of protection measures for already built infrastructure within such areas, risk maps can be more informative, as they indicate the potential financial damage resulting from hazardous events (van Westen et al. 2006).

Assessments and maps of natural hazards and risks, however, are often only representative for a certain time period, typically for present conditions, since they integrate many dynamic aspects of the natural and the man-made environment. In the case of rockfall, changes in the natural environment (e.g. rockfall activity) can be expected to go along with climate change (Stoffel & Huggel 2012, Stoffel et al. 2014). The man-made environment can change due to the implementation of protection measures (e.g. deflection dams or protection forest) (Dorren et al. 2007, Stoffel et al. 2005), changing land-use practices or changing vulnerabilities (Mechler & Bouwer 2015, Nussbaumer et al. 2014). Regarding risk management, it is important to understand hazard and risk as dynamic concepts and to assess the relative importance of these changes (Keiler & Fuchs 2008).

In the context of multi-temporal hazard and risk assessments, the following three challenges have been identified. First, a generally accepted framework for quantifying natural hazards and risks over time is lacking at present, and only few process-oriented approaches exist that investigate changes of both the natural and the man-made environment and their interactions

(Bouwer 2013, Mechler & Bouwer 2015). Second, hazard and risk developments are typically investigated only within a few decades in the past and the future (Bouwer 2011, 2013). Probably due to limited data availability, long-term hazard and risk assessments are rarely carried out (Schneuwly & Stoffel 2008), but would be interesting especially with regard to a better understanding of potential climate impacts (Bouwer 2011, 2013). Third, most studies are focusing on regional to global scales and suffer from limited capabilities in investigating spatial patterns, which are important for hazard and risk development (Neumayer & Barthel 2011). To depict such patterns on the local scale, standard procedures for hazard mapping exist in Switzerland (Lateltin 1997), while the creation of risk maps is less common and less standardized.

1.2 Research questions and structure of thesis

In this context, the main purpose of this study is to assess long-term changes (1880–2060) in rockfall hazard and risk at Täschgufer, a highly active rockfall slope in the the southern Swiss Alps, and to create hazard and risk maps for distinct time periods, depicting spatial patterns of these changes. More specifically, the following research questions are addressed.

1. How can information from different sources (e.g. field observations, event reports, dendrochronological and socio-economic data, statistical and process-based models) be combined within a consistent, transparent methodology to assess developments of hazard and risk for distinct time periods in the past (1880, 1940 and 2010)?

2. How and how strong are rockfall hazard and risk in the study area affected by different factors such as climate change, building of deflection dams, protection forest and changing construction activity?

3. On which scientific basis can plausible future climate and exposure scenarios (2060) be defined and implemented into the assessment of hazard and risk?

4. By combining different climate and exposure scenarios and evaluating their influence on rockfall hazard and risk, which conclusions can be drawn with respect to future research and risk management in the study area?

The study is structured along the following chapters: Chapter 2 summarizes the current state of research on mechanisms relating rockfall activity and climate and presents expected future changes of rockfall activity in Switzerland. Chapter 3 introduces fundamental concepts of hazard and risk and points out some peculiarities regarding the rockfall hazard. Chapter 4 characterizes the study area and Chapter 5 provides an overview of the data used to assess rockfall hazard and risk in this area. Chapter 6 describes the methodology of the quantitative hazard and risk analysis in more detail, including the mapping of rockfall hazard and risk. Chapter 7 presents obtained estimates and maps for hazard potential, damage potential and risk for all investigated time periods (1880, 1940, 2010 and 2060), which are discussed with respect to the research questions in Chapter 8. Chapter 9 draws the most important conclusions of the study and provides an outlook for future research.

2 Rockfall and climate in periglacial environments

Research into relations between climate, permafrost and the stability of alpine rock faces was initiated in the 1990s (Haeberli et al. 1997, Wegmann et al. 1998) and gained in importance since the summer 2003. During this extreme summer, when monthly mean temperatures from June to August were the hottest on record in the Alps (Schär et al. 2004), a greatly increased rockfall activity could be observed in many alpine areas. Many of the events originated from steep bedrock at high elevations and north-exposed slopes, which are often influenced by permafrost (Figure 2.1). In the absence of heavy precipitation or earthquakes, thawing of permafrost close to the surface was therefore thought to have played a major role in triggering these events (Gruber et al. 2004, Schiermeier 2003). The hypothesis gained much public attention and triggered further research. Although the important role of permafrost was confirmed in other extreme summers 2006 and 2015, the related mechanisms are more complex and make the interpretation of observations difficult.

Figure 2.1: Massive ice visible at the detachment surface of a rockfall event, which was triggered in summer 2003 just below the Carrel hut on the Matterhorn (3830 m a.s.l). A similar event nearby during summer 2006 also revealed massive ice (Gruber & Haeberli 2007).

The aim of this chapter is to summarize the current state of research on mechanisms relating rockfall activity and climate. Therefore, triggering mechanisms of rockfall events and their climate sensitivity is described on different scales of time and depth, and some peculiarities regarding spatial patterns in alpine terrain are pointed out. On this basis, the interpretation of observations is critically discussed. Finally, expected changes of rockfall activity in Switzerland are presented based on results of a recent study.

2.1 Triggering mechanisms and climate sensitivity

Triggering mechanisms of rockfall events can be described with the disposition concept (Figure 2.2). The disposition of a rockfall release area denotes its susceptibility to rockfall events. The actual triggering of an event then follows an external stress on the system, which exceeds the threshold given by the disposition. The basic disposition, the variable disposition and the triggering events are typically variable on shorter time scales each, which is described in more detail in the following (Kienholz et al. 1998).

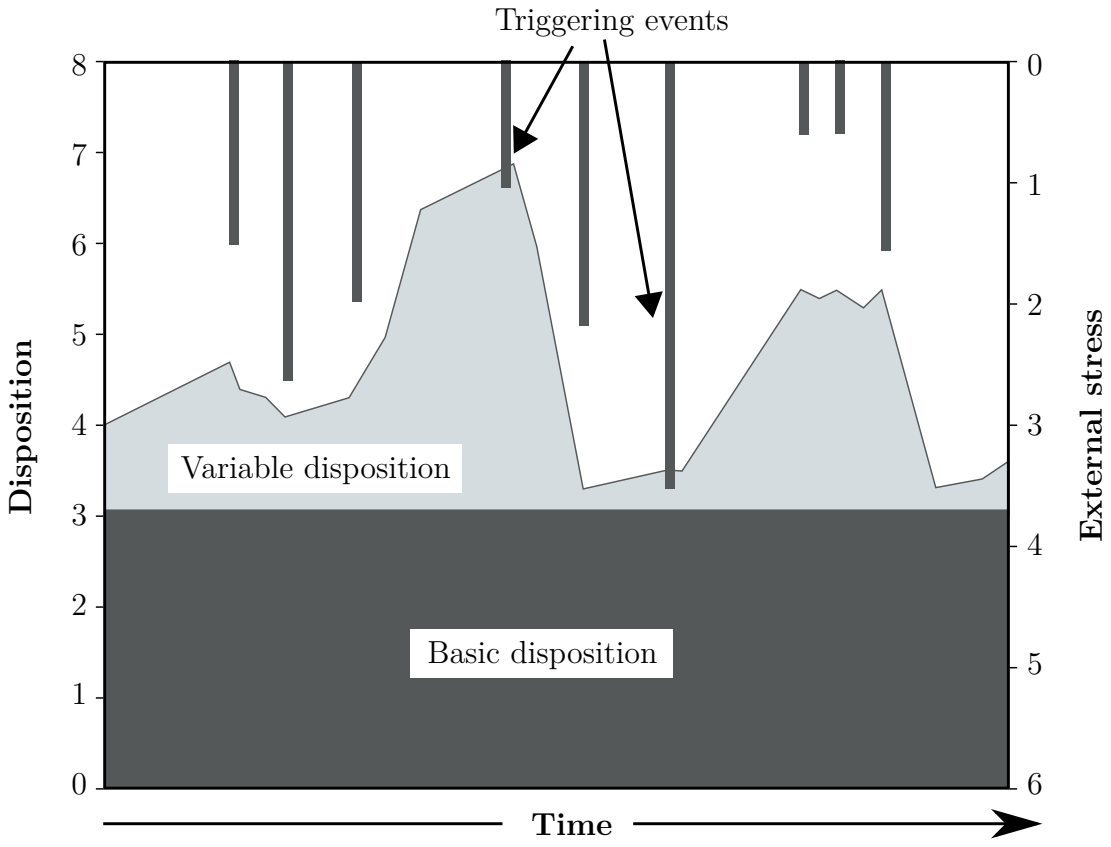

Figure 2.2: The disposition concept: The basic disposition is more or less constant, the variable disposition can change at shorter time scales, while a triggering event is a momentary stress on the system. If the stress on the system exceeds the threshold given by the disposition, an event is triggered (Kienholz et al. 1998).

2.1.1 Basic disposition

The basic disposition determines, where rockfall can basically occur and which volumes can be expected. It is mainly given by topographic an geological factors, which are only variable at very long time scales (decades to centuries). Besides the slope gradient, lithology plays an important role, determining physical and chemical weathering of rocks, which is a basic prerequisite for their loosening and detachment. Furthermore, existing fractures within the rock mass control water infiltration, which can intensify chemical weathering, increase hydrostatic pressure and promote ice formation under appropriate thermal conditions (Allen & Huggel 2013, Fischer et al. 2012).

The basic disposition is hardly influenced by climate. An exception is related to deglaciation and debuttressing of steep lateral slopes, which can promote slope failure. Furthermore, ice segregation may affect the stability of steep bedrock permafrost by slowly widening fractures and thus preparing the way for later failure during degradation, or by expanding fractures past a critical value (Gruber & Haeberli 2007).

2.1.2 Variable disposition

The variable disposition describes shorter variations (days to decades) of the susceptibility of a cliff and determines primarily, when and how often rockfall events can be triggered. Thereby, properties of existing fractures are important, along which a rock mass can be destabilized. As fractures in perennially frozen rock are likely to contain ice, their properties depend on temperature. Thereby, ice strength decreases towards the bulk-melting point. A stability minimum was found at temperatures between -1.5 and 0 °C, where the existence of liquid water reduces the cohesion of ice (Davies et al. 2001). Ice apparent in fractures can also have a cementing effect related to ice-rock interlocking and adhesion, which is reduced or lost during warming or thaw (Gruber & Haeberli 2007).

The variable disposition is strongly influenced by climate, since atmospheric warming can lead to permafrost-degradation in rock bodies, whereat the following processes are relevant.

Deep permafrost-degradation is related to the adjustment of the temperature profile at depth to atmospheric warming and a potential rise of the lower permafrost boundary, which could cause large and deep-seated instabilities (Harris et al. 2009). Due to the large timescale of heat diffusion, by which a surface warming propagates downwards, this process can be delayed by centuries to millennia, and thereby might be hard to clearly distinguish from the basic disposition. The warming of the 20^{th} century, in this perspective, has only reached a depth of some tens of meters at steep slopes and high elevations (Haeberli et al. 1997). A modeling of subsurface temperatures at the Matterhorn shows that even with further warming over the next 200 years, substantial permafrost can possibly remain a few decameters below the surface (Noetzli & Gruber 2009). However, the extent of so-called warm permafrost (about -2 to 0 °C) would significantly increase in volume and vertical extent (Figure 2.3).

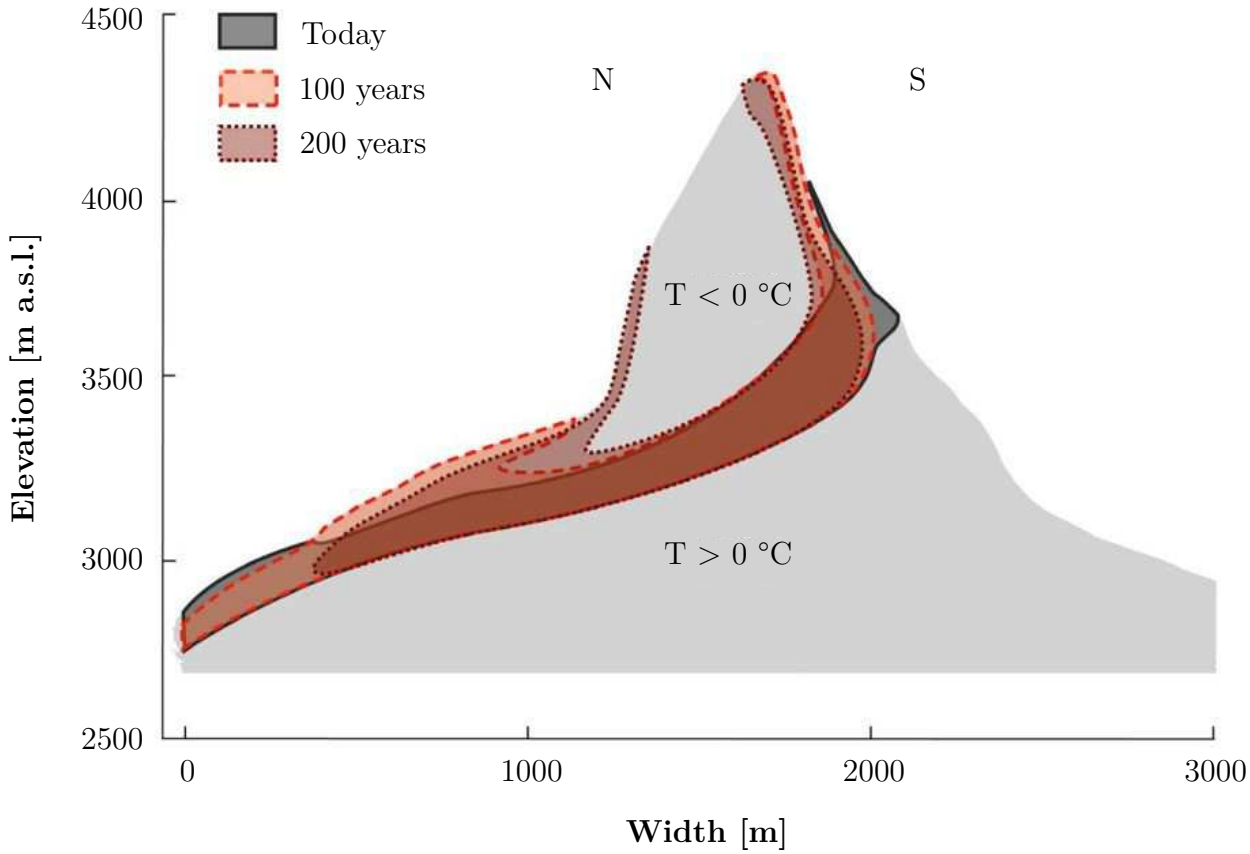

Figure 2.3: Modeled temperature range of -2 to 0 °C in a north-south cross section of the Matterhorn for today, in 100 and in 200 years. A linear warming scenario of +3 °C per 100 years was assumed (Noetzli & Gruber 2009).

Active layer thickening refers to the thickening of the seasonally frozen layer above the permafrost body, by which new volumes of rock will be subject to critical temperature ranges or thaw (Harris et al. 2009). The increased rockfall activity during summer 2003 was interpreted as a phenomenon of active layer thickening (Figure 2.4). The rapid and immediate response thereby might have been favoured by convective and advective heat diffusion processes, such as water circulation (Gruber & Haeberli 2007), and rapid thawing in complex topography (Noetzli & Gruber 2009).

2.1.3 Triggering events

A triggering event is a momentary stress on system (minutes to days) and in the case of rockfall mostly related to pressure. Pressure can be associated with repeated freeze-thaw cycles and the related volume expansion of freezing water (9%), which can loosen material in the uppermost decimeters of a rock surface (Gruber & Haeberli 2007). Furthermore, water input from heavy rainfall events or melting of snow and ice increases the hydrostatic pressure within fissures, which may also trigger larger events (Huggel et al. 2010). The sensitivity to

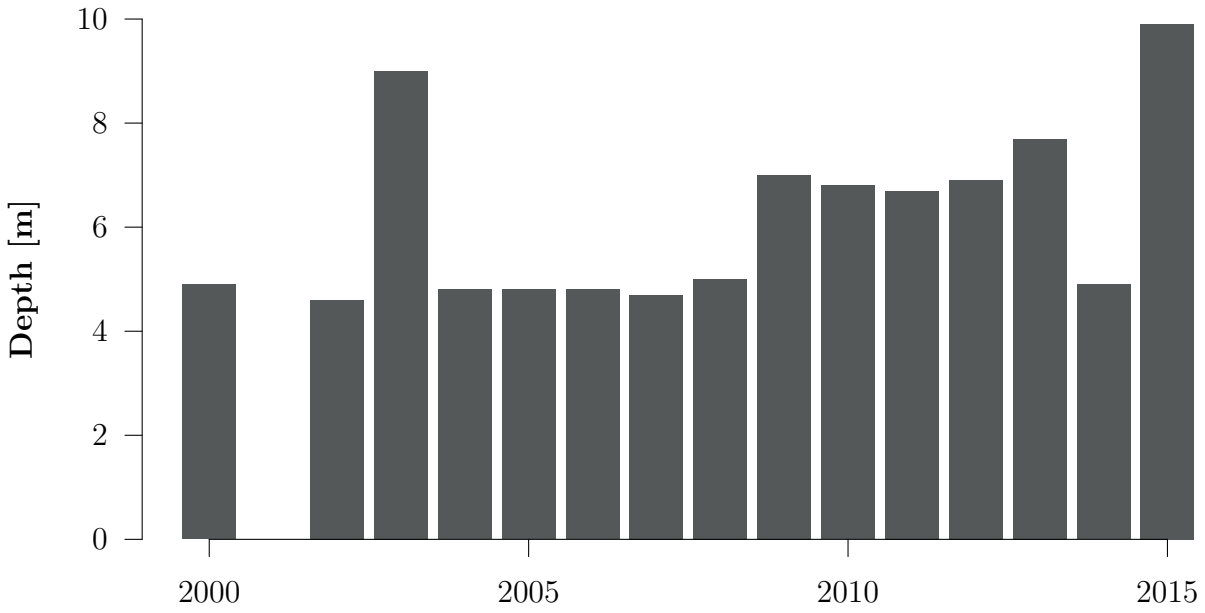

Figure 2.4: Active layer depth at the 14 m deep borehole Schilthorn (2910 m a.s.l.) in the last 15 years. In summer 2001 no data is available (PERMOS 2016).

water input is most relevant in spring, when rock masses are loose due to the influence of frost during winter, and less relevant in summer and autumn, when fissures begin to close again (Gruner 2008). There exist several other possible triggering events (e.g. root pressure, wind, earthquakes), which are however of minor importance.

Triggering events are influenced by climate in several aspects. Increasing atmospheric temperatures can cause changes in the frequency of freeze-thaw cycles, which is related to the frequency of rockfall events (Sass 2005). However, a linear relationship cannot be assumed, because loosened material is often released only in combination with water supply. Furthermore, water input is affected by changes in the frequency and intensity of heavy precipitation events or the timing of snowmelt in spring.

2.1.4 Spatial patterns

In addition to different scales of time and depth, spatial patterns of the above processes need to be considered. Regarding the influence of permafrost, the temperature field at depth is to a large degree determined by surface conditions (Gruber et al. 2003). The spatial distribution of ground surface temperatures in mountainous terrain is highly complex and variable at different scales. In a first approximation, ground surface temperatures vary with elevation, since they are coupled to air temperatures. For instance, the occurrence of permafrost at elevations below 2500 m a.s.l. is unlikely and other processes become more important than in more elevated, periglacial areas (Gruner 2008). On steep rockwalls, net short-wave solar radiation exerts another major control and depends on the exposition

of these slopes (Gruber et al. 2003). For instance, freeze-thaw cycles are more frequent at south-exposed slopes than at north-exposed slopes of comparable elevation. Also, three-dimensional effects, such as a heat flux from the southern to the northern flank of a mountain peak, can affect permafrost distribution at depth (Noetzli & Gruber 2009). The situation is most complex on flat terrain, where ground surface temperatures are additionally influenced by snow redistribution, shading from surrounding terrain and differing ground properties (Gubler et al. 2011).

2.2 Interpreting results

It is often difficult to interpret observed rockfall events with respect to the involved mechanisms or the influence of climate, as different processes are acting on different temporal and spatial scales (Huggel et al. 2010). This holds especially true for the influence of permafrost on slope stability in periglacial environments, despite the theoretical understanding of related mechanisms (Gruber & Haeberli 2007). However, a considerable number of rockfall events originating from alpine permafrost areas have been described and investigated in the past 30 years (Stoffel & Huggel 2012), whereby the visibility of ice at several detachment surfaces supports the relevance of thawing ice-filled fractures. During summer 2003, increased rockfall activity could for the first time be attributed with some certainty to the summer heat wave, while the presence of fractures might also have been relevant for the fast response of active layer thickening to atmospheric warming (Gruber & Haeberli 2007, Gruber et al. 2004). More recently, the additional influence of enhanced surface melt of snow and ice during such heat waves was pointed out, which enhances hydrostatic pressure and reduces shear strength in fractures (Allen & Huggel 2013). Finally, the important role of permafrost on slope stability could be confirmed in summer 2015 by a recent study of Magnin et al. (2015) in the Mont Blanc massif. Of the 161 rockfall events mapped in the area (Figure 2.5), 96% originated at negative mean annual rock surface temperatures and only 4% at temperatures between 0 and 1 °C. Ice could be observed in 46 cases (30%) directly at the detachment surface.

The robust inference of a trend in rockfall activity from these observations and its linkage to climate change is difficult due to the low frequency of events and increased observation activity during recent times (Huggel et al. 2012). A regional study of large rock slope failures between 1900 and 2010 in the Alps however indicates increased frequency of rock slope failures in the 1940s, and particularly since the 1990s, going along with higher mean annual air temperatures in both periods (Huggel et al. 2012). It is interesting that this pattern is consistent with a local study in the Mont Blanc massif, which investigated rockfall activity over the past 100 years with help of a rich archive of historical photographs (Huggel et al. 2012). In another local study, Stoffel et al. (2005) also showed that the temperature increase of the past 30 years goes along with increased rockfall activity in Täsch (VS), based on dendrochronological evidence. However, the robust relation of seasonal or annual air temperatures and rockfall activity has not yet been proven, and the relevant physical processes require further understanding (Huggel et al. 2012).

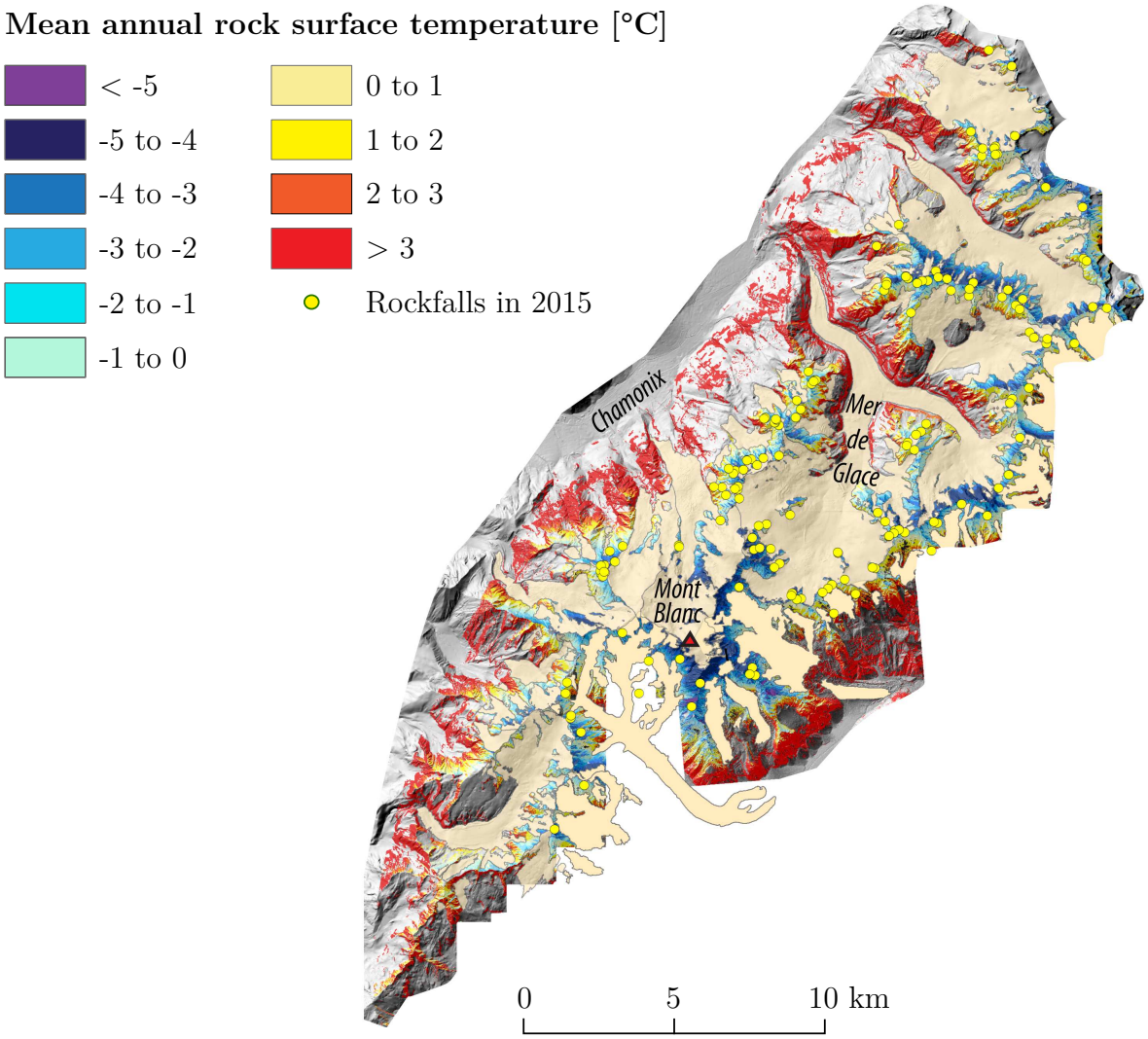

Figure 2.5: Mean annual rock surface temperatures and observed rockfall events in the Mont Blanc massif 2015 (Magnin et al. 2015).

2.3 Future projections

In the framework of a recent study (Mani & Caduff 2015), climate sensitivity of rockfall release areas in Switzerland could be estimated with a fine spatial resolution. The aim of the sensitivity analysis was thereby not to make an accurate prediction for a distinct time period, but to identify possible changes in rockfall activity in different scenarios. Therefore, a moderate scenario with a time horizon of 2060 and an extreme scenario with a time horizon of 2085 were defined on the basis of the Swiss Climate Change Scenarios CH2011 (Section 5.3) and additional analyses of heavy precipitation events. In these scenarios, changes in rockfall frequencies and magnitudes were estimated based on changes in the availability of loose material and water input (Figure 2.6).

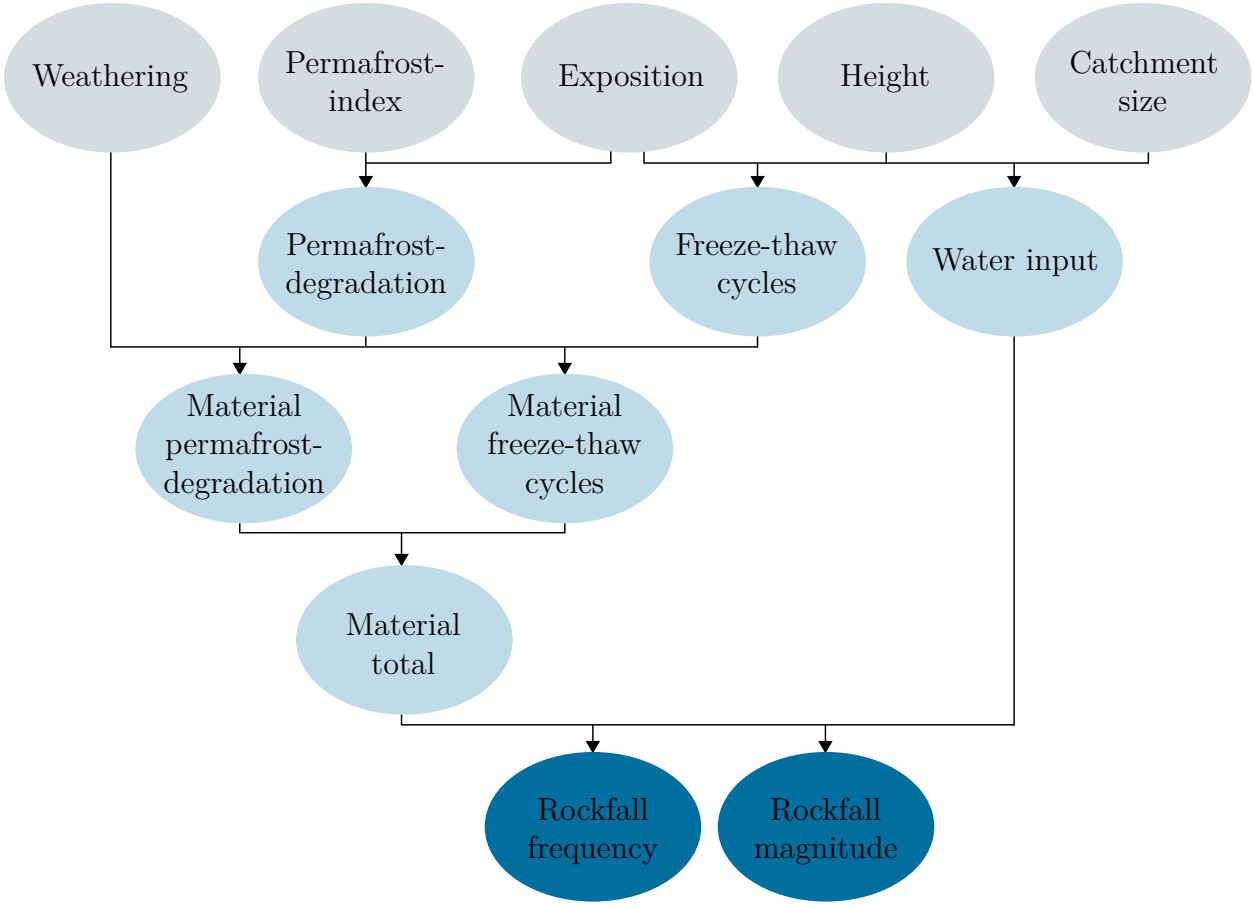

Figure 2.6: Changes in rockfall frequency and magnitude were estimated based on combined changes of indicators describing the availability of loose material and water input. Regarding the availability of loose material, both permafrost-degradation and changes in freeze-thaw cycle are weighted equally (Mani & Caduff 2015).

A map of expected changes in rockfall frequency in the extreme scenario reveals distinct spatial patterns (Figure 2.7). In many areas in northern and central Switzerland, no changes are expected due to a limited number of release areas. An increase in rockfall activity is however expected in the Alps. Future atmospheric warming can not only lead to permafrost-degradation at high elevations, but also goes along with more frequent freeze-thaw cycles in these regions, both factors increasing the availability of loose material. Furthermore, loose material is expected to be mobilized more frequently by heavy rainfall events and increased snowmelt in winter and spring. In contrast, a decreasing rockfall activity is expected in the main valleys of the Alps and Pre-Alps as well as in southern Switzerland, mainly due to a decreasing number of freeze-thaw cycles at lower elevations.

It might be surprising at first sight, that increasing rockfall magnitudes, meaning volumes of individual rockfall events, are only expected in very few regions according to the study (Mani & Caduff 2015). Other authors argue that in the perspective of these timescales, increasing

block sizes due to deep-seated permafrost-degradation are not unlikely (Gruber & Haeberli 2007). Such effects could not be accounted for in the study of Mani & Caduff (2015) due to lacking information on the jointing of rock bodies. An increase in rockfall magnitudes is therefore limited by the increase in rockfall frequencies. Where loose material is more frequently mobilized, smaller magnitudes are expected for individual events. Increasing magnitudes for individual events could be expected in regions, where increasingly available loose material is mobilized less frequently, for example due to decreasing water input.

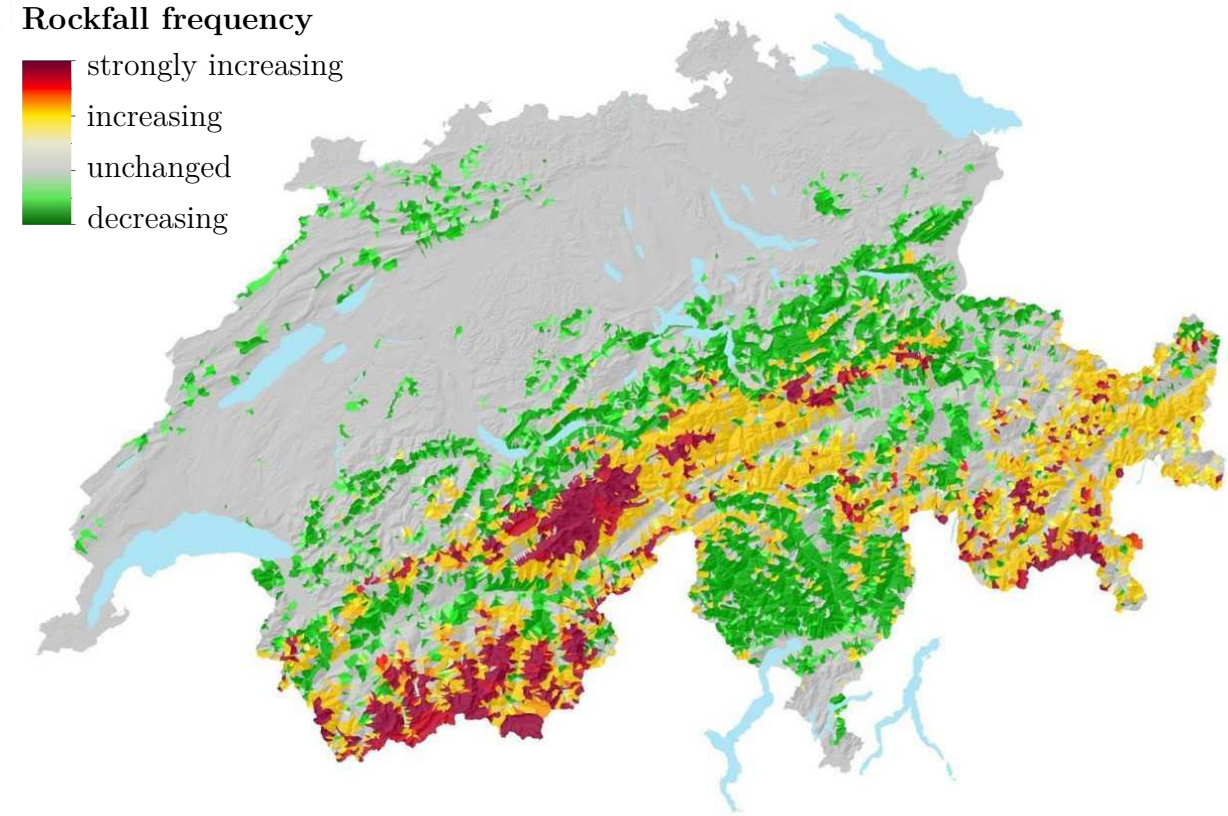

Figure 2.7: Expected sensitivity of rockfall release areas in Switzerland within the extreme scenario (2085) (Mani & Caduff 2015).

To summarize, considerable changes in rockfall activity due to climate change can be expected in Switzerland. A moderate to strong increase is expected in the Alps, while a decrease is expected in the Pre-Alps and in southern Switzerland. Increasing rockfall magnitudes can be expected based on theoretical considerations, but are difficult to quantify based on available data. These expectations are consistent with the statement that rock slopes in cold high-mountain regions are probably among the systems most sensitive to climate change (Stoffel & Huggel 2012). The reasons for this have not only to be sought in the degradation of permafrost, which is naturally confined to high alpine areas, but also in increasing frequencies of freeze-thaw cycles and an accentuation of heavy rainfall and snowmelt events in the future.

3 Concepts and models

In this chapter, fundamental concepts of hazard and risk are introduced. After introducing the general concept of risk, its two main components, namely hazard potential and damage potential, are discussed in more detail. While these concepts can be applied to any type of natural hazard, some peculiarities regarding their quantification and mapping in the case of the rockfall hazard are pointed out. In this context, the rockfall model applied in this study is presented. Finally, concluding remarks are made about the assessment of sensitivity and temporal aspects in risk analyses as a basis for risk management.

3.1 Risk

Risk in general terms is the the potential of an undesired consequence (Bründl 2009). In the case of natural hazards, such a potential is determined by both the natural system (hazard potential) and the human system (damage potential) (Figure 3.1). Hazard potential, on one hand, describes the potential of a natural process to cause damage in the area at interest, for example the potential of a rockfall event to reach a village at the valley floor. Damage potential, on the other hand, describes the potential of the human system to suffer damage from such a hazardous process (Alcántara-Ayala 2002), for example the potential of people being injured, property being damaged or economic activity being disrupted from a rockfall event in a village (van Westen et al. 2006).

The perception of both hazard and damage potential as well as their inclusion into risk analyses and management has changed historically. Until the late 1960s, risk from natural hazards was mainly perceived as the consequence of dangerous, uncontrollable natural processes and it was thus mainly tried to improve process understanding and prediction of these hazards, as well as to cope with their consequences. In the 1970s, risk from natural hazards was increasingly interpreted in a social context and concepts such as vulnerability (Section 3.4) were developed (Alcántara-Ayala 2002). Although nowadays the inclusion of social aspects into risk analyses is considered important in literature (Keiler & Fuchs 2008, Keiler et al. 2006), it remains a major challenge not only in terms of data availability but also on a conceptual level (Künzler et al. 2012, Peduzzi & Herold 2005). Thus, still today many practical risk assessments strongly focus on the analysis of hazard potential (Keiler & Fuchs 2008).

Figure 3.1: Risk at the intersection of the natural and the human system (photo: M. Fehlmann).

3.2 Hazard potential

The analysis and assessment of hazard potential is a classical task in geomorphology (Alcántara-Ayala 2002) and basically has to provide information about the magnitude and frequency of expected events (event analysis) as well as their potentially destructive impact on the area of interest (impact analysis) (Bründl 2009, Jaboyedoff et al. 2005).

Having identified potentially hazardous processes, the event analysis formally describes expected events in terms of several event scenarios, each of them associated with a certain magnitude and frequency. The magnitude is a measure of the event dimension in its triggering zone. For example, the magnitude of an earthquake is given by the energy released at its hypocenter, and the magnitude of a rockfall is given by the volume of a block in the release area. It has been found empirically that the magnitude of many natural events is related to their frequency, meaning that smaller events in general occur more often than larger events. This behaviour can mathematically be captured by Magnitude-Cumulative Frequency (MCF) distributions or power laws, in the general form of Equation (3.1). Thereby, the exceedance frequency F(M), meaning the number of events equal or larger than a certain magnitude M, is proportional to this magnitude to the power of some constant exponent b (Malamud 2004).

$$F(M) = a \cdot M^{-b} \tag{3.1}$$

This behaviour is also referred to as scale-invariant, because it is often statistically stable over several orders of magnitudes. The value of the exponent b thereby depends on the process at investigation. It has been known for some time, for example, that the number of earthquakes with a released energy E or greater in different geographic regions or even across the world is proportional to $E^{-0.8 \text{ to } 1.0}$ (Malamud 2004). Similarly, universal constants for rockfall events are proposed by some authors (Hergarten 2012). However, in the case of rockfall, it seems not yet to be clear to what extent the value of b depends on the specific geological and geomorphological context, such as the lithology or the fall height, which influence rock fragmentation and thereby rock volume distributions (Hergarten 2012, Ruiz-Carulla et al. 2015). Power laws for the rockfall hazard can be established by analyses of the release area with remote sensing techniques (Carrea et al. 2015, Guerin et al. 2014), analyses of rockfall deposits on the slope (Ruiz-Carulla et al. 2015), rockfall inventories (Dussauge-Peisser et al. 2002) or models (Hergarten 2012). Although event scenarios might alternatively be based on geological surveys or documentations of historical events at the valley floor (Bründl 2009, Lateltin 1997), power laws are thought to play a crucial role in hazard assessments in the future (Malamud 2004).

The derivation of several rockfall scenarios from a MCF distribution is visualized in Figure 3.2. When speaking of event scenarios, the exceedance frequency F(M) is often expressed in terms of the so-called return period T(M), which is defined by the time interval at which a certain magnitude M or greater is released and can simply be approximated by the inverse of F(M) (Bründl 2009). Furthermore, given several event scenarios j, the frequency of each scenario $F(S_j)$ can be calculated by the difference of the exceedance frequencies of both its maximum and minimum magnitude. For reasons of comparability, in Switzerland typically three scenarios with return periods of 30–100 years ($F(S_j) = 0.23$), 100–300 years ($F(S_j) = 0.066$) and >300 years ($F(S_j) = 0.033$) are considered (Bründl 2009).

Having defined several event scenarios for a process with corresponding magnitudes and frequencies, the impact analysis describes how these scenarios affect the surrounding environment. The physical impact of the process at each location in its propagation zone is thereby referred to as intensity, the exact measure of which depends on the process at investigation (Bründl 2009). For example, the intensity of a flood is given by the flooding height or the flow velocity (Bründl 2009), the intensity of an avalanche by its impact pressure, and the intensity of a rockfall by its total (translational and rotational) kinetic energy (Lateltin 1997). It is worth emphasizing that, in contrast to the magnitude, process intensity is spatially variable and in general decreases with increasing distance from the triggering zone. In the case of rockfalls, however, maximum intensities are typically reached at some distance from the release area (Jaboyedoff et al. 2005). In Switzerland, similar to the definition of event scenarios, process intensities are classified into three classes of low, medium and high intensity depending on process-specific threshold values, which in the case of rockfall cor-

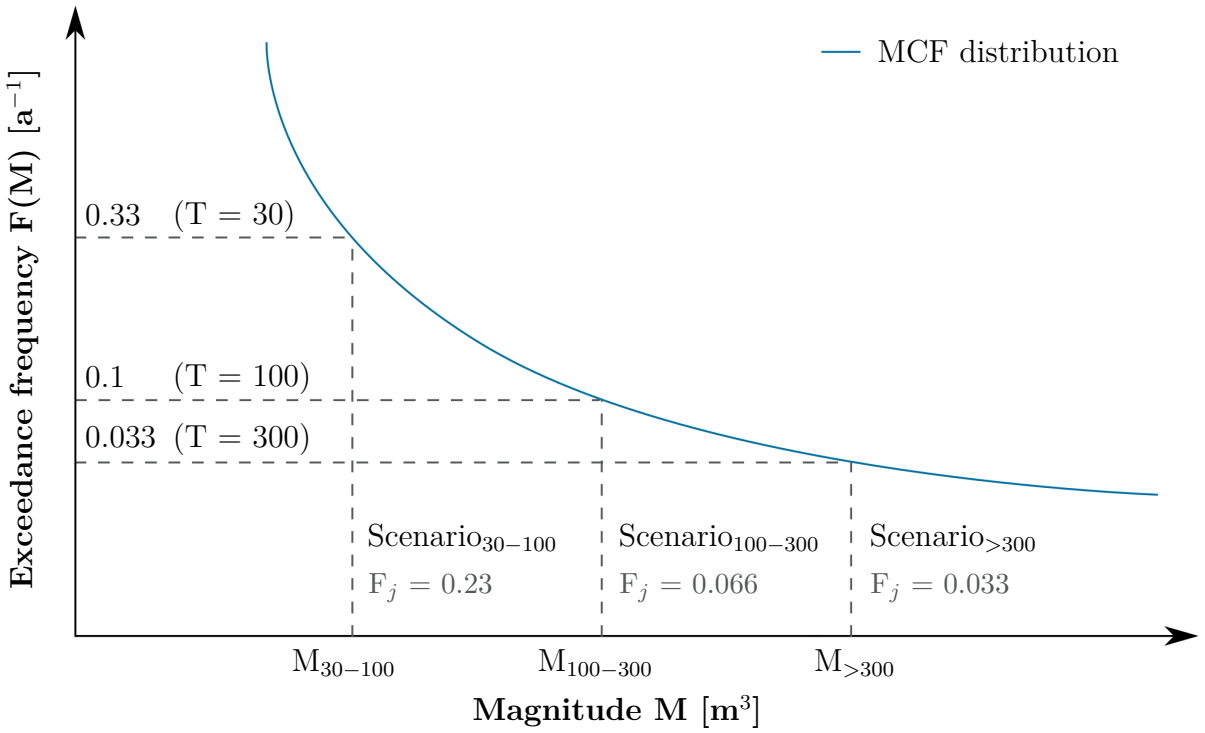

Figure 3.2: Derivation of event scenarios from a MCF distribution: A MCF distribution assigns an exceedance frequency F(M) or return period T(M) to each magnitude M. The frequency of a scenario F(S_j), which typically represents a magnitude range, can be calculated by the difference of the exceedance frequencies of both its maximum and minimum magnitude (Bründl 2009).

respond to 30 and 300 kJ of its kinetic energy (Lateltin 1997). Information about process intensities for each event scenario is obtained from direct observations and event documentations, simple mapping approaches in combination with rules of thumb or frequently with help of conceptual or process-based models (Bründl 2009, Jaboyedoff et al. 2005). Regardless of the applied methodology, the impact analysis results in a set of intensity maps for distinct event scenarios (Bründl 2009).

Hazard mapping is the process of combining and visualizing the two previously discussed aspects on a single map with the aim of providing authorities with important information concerning land-use planning (Abbruzzese et al. 2009). The Swiss hazard mapping scheme, which can be applied in this form to all kind of different processes, is shown in Figure 3.3. On the x-axis, the exceedance frequency of each event scenario is given by its return period $T(M)$. On the y-axis, corresponding intensities I at a specific location are given. For each scenario and location, the resulting hazard matrix defines the hazard degree, and the final hazard map is coloured according to the worst case from all scenarios. The red colour represents the high hazard zone, where new urban development is forbidden and protective measures must be taken for existing buildings. The blue colour represents the moderate hazard zone, where development is permitted under restrictions. The yellow colour represents the low

hazard zone, where development is allowed without restrictions. On the final hazard map, it is no longer apparent, which scenario the resulting hazard degree is a result of, or in other words, how frequent a certain intensity value is reached at a certain location. Since this information is crucial to determine the risk at a certain location, separate intensity maps for each scenario are a necessary prerequisite for detailed risk analyses and can only be replaced by hazard maps in a very limited way (Bründl 2009, Lateltin 1997).

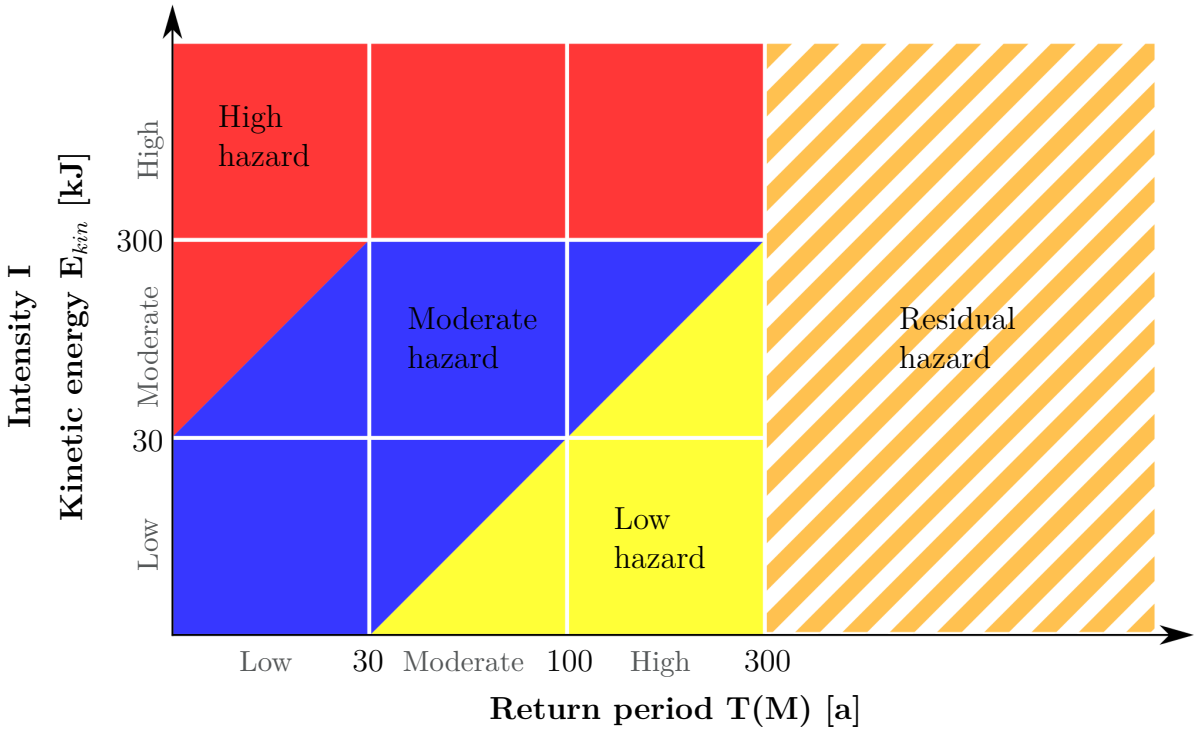

Figure 3.3: The Swiss rockfall hazard mapping scheme: The rockfall hazard is determined according to both the return period T(M) of a certain rockfall magnitude M and its intensity I. The intensity of a rockfall event is given by its total (translational and rotational) kinetic energy E_{kin} at each point in space (Lateltin 1997).

For rockfall hazard mapping at the local scale, currently a number of qualitative and quantitative approaches are available (Abbruzzese & Labiouse 2014). Latest developments mostly have been oriented towards quantitative approaches based on trajectory modeling, which are thought to provide a sounder and more objective basis than qualitative approaches (Abbruzzese & Labiouse 2014). In case of the rockfall hazard, the implementation of the above discussed concepts is subject to certain peculiarities. Regarding the return period of events (x-axis of the hazard matrix), it is important to not only consider the exceedance frequency of a certain magnitude, but also the so-called propagation probability, which denotes the probability that a rockfall – once released – reaches a certain location at the slope. This probability can be obtained from multiple model results and takes into account that blocks released in a certain scenario only affect parts of the slope and are deposited or stopped by trees along their way. Considering a fixed return period for each location in a scenario might

therefore not be adequate. In this study, it was accounted for a spatially varying return period in each scenario by applying the Swiss hazard scheme to each point in space. The x-axis of the Swiss hazard mapping scheme is thereby interpreted in a continuous way to allow for a numerical solution (Abbruzzese & Labiouse 2014). Regarding the intensity (y-axis of the hazard matrix), rockfall models usually provide a probabilistic energy distribution for each location according to multiple model runs rather than a single energy value. While some approaches consider the whole energy distribution at each location (e.g. Cadanav methodology), this distribution is represented by a certain quantile in other approaches (e.g. Matterock methodology) (Abbruzzese et al. 2009). Finally, methods for rockfall hazard mapping are often well described for two-dimensional modeling, while work is in progress to transfer methodologies to outputs of three-dimensional rockfall models (Abbruzzese & Labiouse 2014).

3.3 Rockfall models

As described above, numerical models are increasingly used for the impact analysis, predicting the area inundated by the process at investigation as well as spatial patterns of process intensities (Bründl 2009). Rockfall models thereby typically calculate individual rockfall trajectories on a three-dimensional slope or a two-dimensional slope profile. In the following section, the rockfall model Rockyfor3D, which is used in this study, is described and compared to the newly developed rockfall model RAMMS::Rockfall, which was also shortly tested during this work (Table 3.1).

Table 3.1: Comparison between the rockfall models Rockyfor3D and RAMMS::Rockfall.

Aspect	**Rockyfor3D**	**RAMMS::Rockfall**
Mechanics	Rebound mechanics	Rigid-body approach
Algorithms	Deterministic, stochastic	Deterministic
Rock motions	Jumping, rolling	Jumping, rolling, sliding, skipping
Forest	Contact with individual trees	Homogeneous drag layer
Computation	Fast	Slow

Rockyfor3D is a simulation model, which has been developed since 1998 and especially focuses on interactions between rockfall and forest. The model calculates individual rockfall trajectories on a three-dimensional slope. It thereby simulates classical, parabolic free falling of rocks through the air, as well as their interaction with the slope surface or trees. To describe these complex interactions, like in most other rockfall models, simple rebound mechanics are applied to the entire rock body, which is represented by a simplified spherical shape. To account for the wide variation of possible jump distances and heights, which can be observed even in homogeneous terrain, physically-based, deterministic algorithms are combined with stochastic approaches, which makes Rockyfor3D to be a so-called probabilistic, process-oriented rockfall model. For example, free flying of rocks is calculated according

to standard algorithms, while stochastic methods are used to determine possible restitution coefficients and thus energy loss during ground contact. Thereby, as will be in more detail discussed in Section 5.2, the height of obstacles that falling rocks collide with is chosen randomly from three representative roughness parameters and is again varied by ±10% to better represent the variability of surface roughness observed in nature. Random numbers are also applied when calculating deviations of blocks from their original fall direction after contact with the ground (0–60°) or trees (0–76°). Forest is represented in Rockyfor3D by individual trees, which is discussed in more detail in Section 5.2 (Dorren 2016).

Another recently developed rockfall model is the RAMMS::Rockfall process module developed by the Institute for Snow and Avalanche Research (SLF) and the Swiss Federal Institute of Technology (ETH) in Zurich and officially released after a period of calibration and testing in April 2015. In contrast to common rebound models, a hard-contact, rigid-body approach is followed, which applies contact forces to the edges and corner points of the rock body. The primary advantage of this approach is that the influence of rock shape is accounted for, which facilitates a natural modeling of the four primary modes of rock motions (e.g. jumping, rolling, sliding and skipping) without the use of random, stochastic methods. The statistical variation of jumps is thereby automatically defined by the rock shape and orientation during ground contact. Different shapes and sizes can easily be specified, either from an available library or from point clouds of real rock geometries, which can be obtained from laser scans during field investigations. In contrast to the Rockyfor3D model, the statistical spread of rock run-out and dispersion is thus generated only by changing the initial conditions. This clear separation between stochastic initial conditions and deterministic boundary conditions simplifies the construction of engineering-based hazard scenarios and the interpretation of model results. Also, in contrast to the Rockyfor3D model, forest is represented by a homogeneous layer with mean drag properties in the RAMMS::Rockfall module. Below the drag layer height, which roughly corresponds to the height of the forest, a resisting force acts on the rock's center of mass, which is proportional to the rock velocity (Bartelt et al. 2015).

Several reasons suggested the application of the model Rockyfor3D in this study. A practical advantage of Rockyfor3D is the faster computation time due to stochastic algorithms. Since more individual rockfall trajectories can be simulated within the same computation time, their lateral spread over the entire slope is guaranteed, which facilitates automatic mapping procedures. Furthermore, multiple model runs can be run automatically with help of a batch file, which facilitates the assessment of multiple scenarios. The main reason to apply Rockyfor3D, however, is the detailed representation of the forest in the model, which allows for a more accurate assessment of its protective effect. Furthermore, with individual trees being represented in the model, results can more easily be validated with dendrogeomorphological data. A disadvantage of Rockyfor3D is certainly the negligence of rock shape when simulating ground contact, especially in the case of flat rocks, which can be observed in the study area and may reach long run-out distances.

3.4 Damage potential

For the description of damage potential, different approaches exist, while exposure, value and vulnerability of the human system are essential concepts to be taken into account (Künzler et al. 2012, Nussbaumer et al. 2014, Thouret et al. 2013).

Exposure denotes the presence of infrastructure, environmental services and resources, economic, social or cultural assets as well as people and livelihoods in places that could be adversely affected (Cardona et al. 2012). In risk analyses, it is in general distinguished between exposed objects and people (Bründl et al. 2015). The presence of objects such as buildings, streets and railways as well as the extent of forests, meadows or agricultural land can be inferred from maps, aerial photographs or field investigations (Fuchs et al. 2004), while the presence of people is often more difficult to assess. In Switzerland, the Federal Statistical Office (FSO) provides the number of permanent residents at the resolution of a hectare, while for research purposes the exact number of persons per domicile is available. Furthermore, the number of persons in hotels, guest houses or clinics might be estimated according to the number of beds and their degree of utilization (Fuchs et al. 2004).

As risk is generally expressed as an expected monetary loss per unit of time, usually one year, the value of exposed objects and persons is typically monetized (Bründl 2009). Regarding object values, insurance companies can provide valuable information. Where mandatory cantonal building insurances exist in Switzerland, detailed information about reinstatement values is available (Fuchs et al. 2004). Otherwise, common average values can be assumed for different object categories and assigned to the exposed objects according to their volume. Object categories can be mapped in the field, and object volumes can be estimated by mean number and mean height of floors or derived from products like swissBUILDINGS3D (Section 5.5). Over- or underestimations for individual objects are thereby cancelled out when integrating risk over entire areas or hazard zones (Keiler & Fuchs 2008). Regarding people, it is hardly possible to value human lives. However, to account for the exposure of people in risk analyses and compare it to the exposure of objects, a monetary value is nevertheless assigned to each person, which corresponds to the willingness of a society to pay for the prevention of a fatality. In Switzerland, this value is set to 5 Mio CHF per person and corresponds to the situation where the victim has a low self-responsibility of taking the risk. It is worth emphasizing that this value does not represent the value of a human life, but depends on the capabilities of a society, the social acceptance of taking risks and the specific situation (Bründl 2009).

The term vulnerability is widely used and defined differently in different applications (Hegglin & Huggel 2008). In the following, it is understood as the propensity of objects and people at risk to suffer different degrees of loss or amount of damage, depending on their particular physical, social, economic, cultural, and political weakness (Alcántara-Ayala 2002, Künzler et al. 2012). Commonly, it is further distinguished between physical and social vulnerability, which is described below.

Physical vulnerability depends on the physical resistance of an object or person towards a certain hazardous event. The physical vulnerability of buildings, for example, depends on construction materials, building structure as well as physical protection measures such as avalanche deflectors or protection walls (Fuchs et al. 2004, Keiler et al. 2006). Furthermore, it is a function of process intensity, since objects and persons become more vulnerable towards higher physical impacts. This dependency is depicted by so-called vulnerability functions (Figure 3.4), which describe the expected degree of loss with increasing process intensity for different object categories and processes (Keiler et al. 2006). According to the Swiss hazard mapping scheme (Section 3.2), a vulnerability function might also be represented by a set of vulnerability values for discrete intensity classes (Bründl et al. 2015).

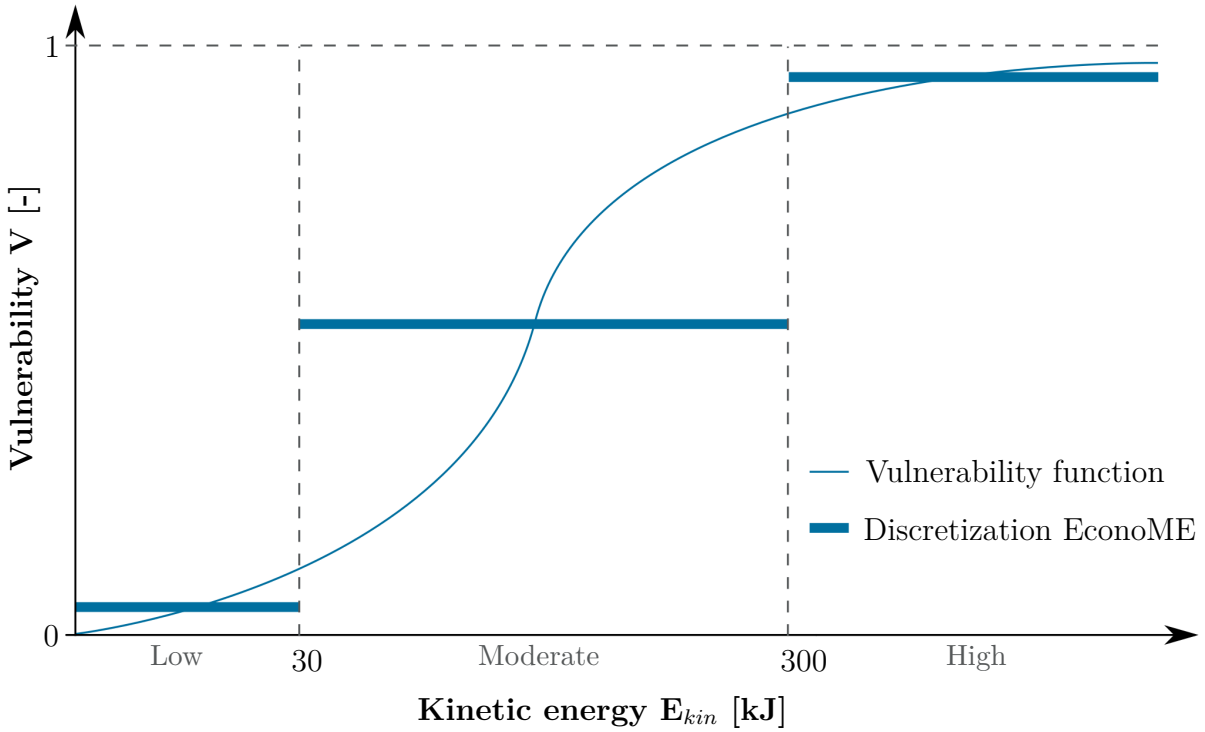

Figure 3.4: Schematic example of a vulnerability function, indicating higher physical vulnerability with higher process intensity. According to the Swiss hazard mapping scheme, the function might also be represented by a set of vulnerability values for discrete intensity classes (Bründl 2009).

Social vulnerability can be understood as the ability of a person or a group to cope with loss (Nussbaumer et al. 2014) and takes into account social, political, cultural or economic criteria that affect the resilience of an object or a person towards a certain hazard. Common measures for social vulnerability include demographic (e.g. age, gender, nationality, ethnicity) and socio-economic indicators (e.g. income, insurance cover, wealth, poverty, educational level), while the choice of appropriate indicators strongly depends on the study area (Künzler et al. 2012, Nussbaumer et al. 2014). A further aspect of social vulnerability concerns the ability of a society to cope with the negative

consequences of a natural hazard, as for example to rebuild infrastructure after a hazardous event (Thouret et al. 2013). However, in practical risk analyses, such indirect effects are often neglected (Bründl 2009).

For damage potential mapping, less standardized procedures exist than for hazard mapping. Usually, exposed objects and persons are classified into semi-quantitative classes by combining their values with several indicators of physical or social vulnerability into a damage potential index. Such procedures are not yet well developed and require standardization and weighting of different indicators as well as the final classification of the index (Künzler et al. 2012, Nussbaumer et al. 2014), all of which is highly subjective. Furthermore, as described above, physical vulnerability is not independent of process intensity, and therefore differs among several event scenarios. To avoid this problem and to simplify damage potential mapping, a constant vulnerability value (e.g. min, max, mean) might be equally assumed for all objects and persons (Fuchs et al. 2004, Nussbaumer et al. 2014).

3.5 Sensitivity and temporal aspects

Following the above considerations, a risk analysis integrates data from various sources and a considerable number of assumptions, resulting in highly subjective and uncertain estimates of risk. However, having developed a consistent methodology integrating various aspects of risk, the aim of a profound risk analysis is in fact to investigate the sensitivity of risk towards these factors rather than providing an absolute risk estimate. Furthermore, having identified factors controlling risk at a certain location, past and future changes of risk can be assessed as a basis for risk management (Keiler & Fuchs 2008).

A sensitivity analysis provides information about how sensitive the resulting risk estimate is towards changes in certain parameters. It thereby allows for the assessment of weak points, uncertainties and interdependencies in the risk analysis, which is characterized by complex, non-linear relationships (Keiler & Fuchs 2008). The influence of a certain parameter is obtained by changing its value while holding all other parameters constant (Fuchs et al. 2004).

The analysis of temporal aspect is closely linked to a sensitivity analysis, but investigates effects of observed and anticipated rather than hypothetical changes in parameters of the natural and human system over time. Thereby, risk development at a certain location and its causes can be assessed. Changes in the natural system might be implemented by changing magnitudes and frequencies of expected events (Bouwer 2013). Changes in the exposure of infrastructure and people can be obtained from old maps, aerial photographs, information about building phase, construction plans or descriptions (Keiler et al. 2006). Future changes of both systems are often defined in terms of scenarios, which are thought to take account for the substantial uncertainties in these developments (Bouwer 2013). By including either already existing or planned protection measures, such as deflection dams, protection forest, or hazard zones and legal construction obligations, their effects can be evaluated as a basis for planning and risk management (Fuchs et al. 2004, Keiler et al. 2006).

4 Study area

Rockfall hazard and risk are investigated at Täschgufer, a highly active rockfall slope in the the southern Swiss Alps (Figure 4.1). The slope descends from the Leiterspitzen summit (3214 m a.s.l.), which belongs to the Mischabel nappe, to the village of Täsch at the valley floor (1430 m a.s.l.). Mean slope gradients thereby gradually decrease from 48° in the upper part to 20° in the lower part of the slope. Below the summit, rockfall is frequently triggered from the heavily disintegrated paragneissic rockwalls. The main rockfall release areas are located between 2300 and 2600 m a.s.l., where the bedrock is highly fractured with many joints. It is likely that these areas are affected by permafrost as it is suggested by the map of the potential permafrost distribution in Switzerland (FOEN 2016). Furthermore, the presence of contemporary permafrost is confirmed on the southern edge of the slope between 2400 and 2500 m a.s.l., where ground ice was encountered during construction work. Rockfall fragments occurring at Täschgufer normally consist of small and medium-sized boulders ($\oslash \approx 80$ cm), the volume of single fragments normally not exceeding 2 m^3. As recently confirmed by dendrochronological analyses, almost 90% of the intra-annual rockfall at Täschgufer occurs in April to May, while long-term rockfall activity apparently increased during the past 30 years. Besides frequent rockfall activity, one rockslide is noted in chronicles, the age of which was estimated with lichenometry to be at least 600 years BP. Furthermore, small debris flows occur at the slope. Single events generally amount to a few cubic meters and move downslope in well-defined channels. In contrast, snow avalanches have never been witnessed at the slope. The forest at Täschgufer predominantly consists of L. decidua Mill. trees, accompanied by single Picea abies (L.) Karst. and Pinus cembra ssp. sibirica trees. Although the regional timberline is located at the approximately 2300 m a.s.l in the immediate neighbourhood, continuous forest cover reaches only 1780 m a.s.l. in the most heavily affected areas of the active rockfall slope. In this part of the slope, surfaces are sparsely wooded and large areas remain free of vegetation (Stoffel & Perret 2006, Stoffel et al. 2005, 2006).

The village of Täsch is located about 5 kilometers north of Zermatt, a famous tourist destination at the upper end of the Matter valley. Since Zermatt is car-free, the road from Täsch to Zermatt is closed to normal traffic. However, car drivers can park their cars in the large Matterhorn Terminal in Täsch and continue their journey by the frequent train shuttles of the Matterhorn-Gotthard railway, leaving every 20 minutes from Täsch railway station. As will be pointed out later (Section 6.4.2), the socio-economic development of Täsch is strongly coupled to developments in Zermatt. Since the early 19^{th} century, hotels opened in Täsch, followed by the construction of numerous holiday flats and chalets. Many of the employees in Täsch work in the service sector, including many immigrant workers, who are employed in

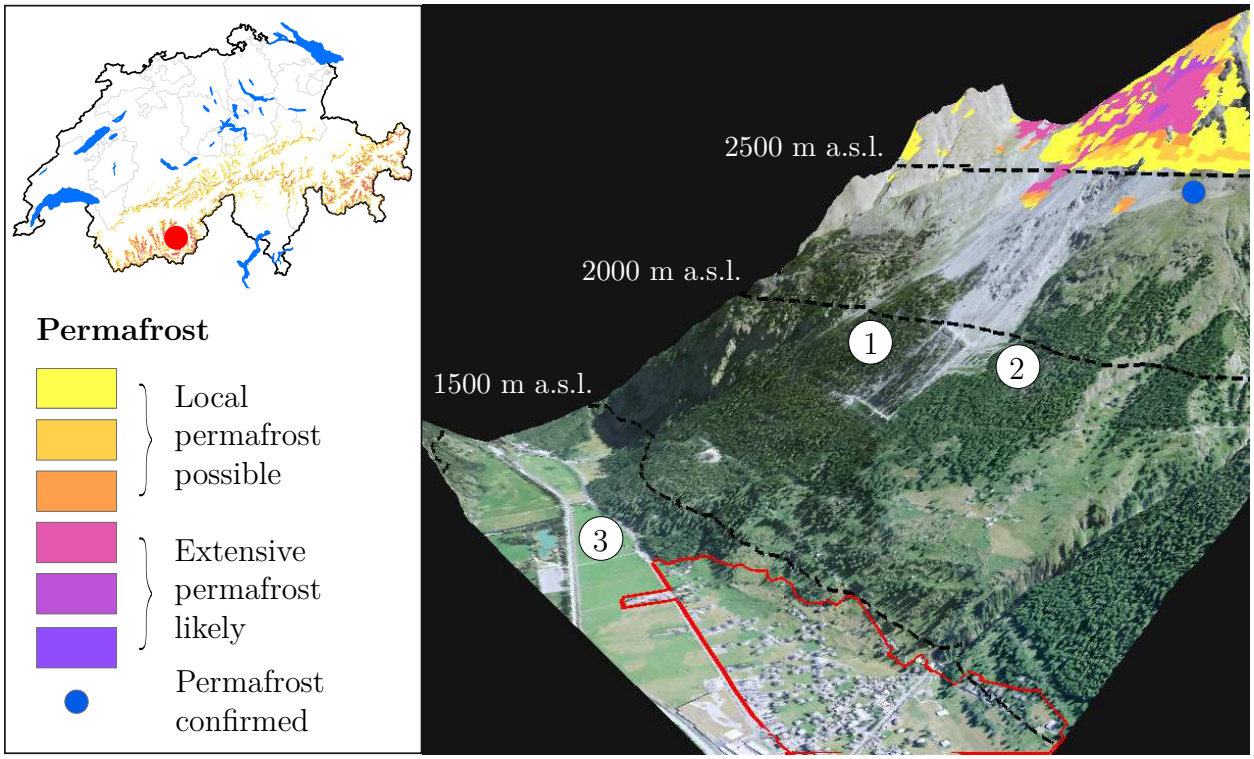

Figure 4.1: The rockfall slope Täschgufer in the southern Swiss Alps: Below the Leiterspitzen summit, permafrost is likely according to the map of the potential permafrost distribution in Switzerland (FOEN 2016), and was locally confirmed on the southern edge of the slope. Fieldwork for the event analysis was conducted at sites 1–3, which is further described in Section 5.1. Current building zones are delineated in red and shown in more detail in Figure 4.2.

.

Zermatt at low wages and live in Täsch due to the relatively low rents. Especially since the early 1990s, the foreign population in Täsch has steadily increased, contributing to 53.7% of total population in 2015 according to the current Buildings and Dwellings statistic (BDS) (Section 5.5). Despite recent growth of the village, construction in Täsch is very much limited by both current building zones and hazard zones (Figure 4.2). Thereby, construction of new buildings in Switzerland is generally only allowed within current building zones, and might be subject to structural obligations within current hazard zones (Section 3.2).

Two records of rockfall events in the recent past illustrate how rockfall might cause damage to roads, hiking trails and farm infrastructures at the valley floor. On October 6, 1985, single blocks reached the valley floor, damaging agricultural buildings in Täsch (Stoffel et al. 2005). On August 3, 2013, massive blocks reached the golf course in the northern part of the village and blocked the road between Täsch and Randa, which hence had to be temporarily closed in both directions (Gsponer 2013). To protect the village from such events, several active and passive protection measures had been adopted in Täsch in the late 20th century, including the building of seven deflection dams and a gallery, which protects the frequently travelled

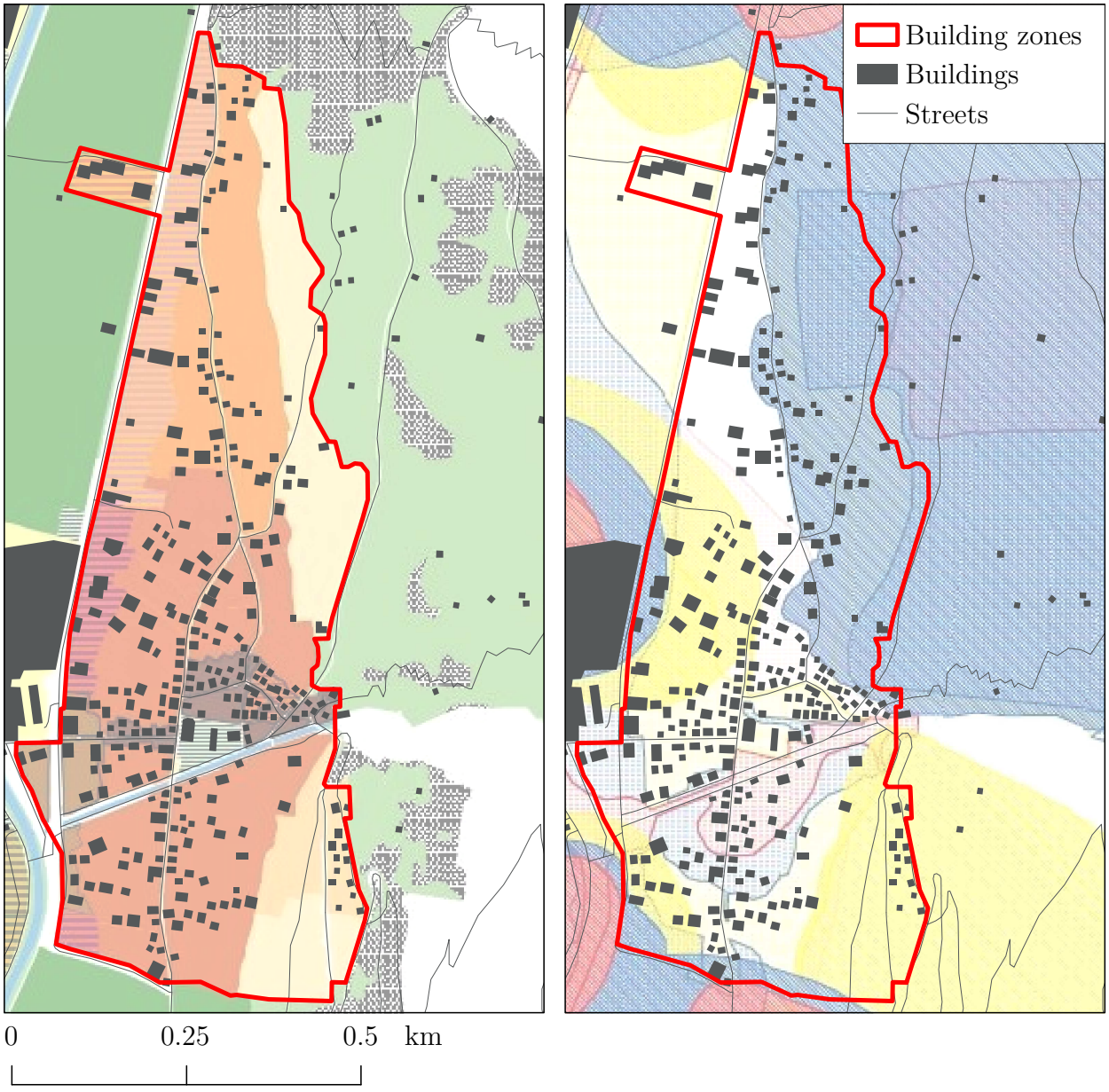

Figure 4.2: Current building zones (left) and hazard zones (right) in Täsch, which confine construction activity. Processes depicted by the hazard zones include rockfall, avalanches and flooding of the Vispe and the Täschbach.

Europaweg, a hiking trail crossing the slope of Täschgufer. Five deflection dams were erected in 1988 and 1989, while two large deflection dams completed the construction works on the slope in the late 1990s (Stoffel et al. 2005). Also, construction within endangered areas is limited by the hazard zonation, which started in the 1990s.

5 Data

Risk analyses integrate different information from various data sources. Lack of data is often a problem in developing countries as well as in high alpine environments (Huggel et al. 2015), while in Switzerland a variety of data is provided by federal, cantonal and communal institutions. Table 5.1 provides an overview of the data used in this study, divided into positions for the assessment of hazard potential (1–3) and damage potential (4–6) respectively, which are described in the following sections.

Table 5.1: Overview of the data used in this study, divided thematically into positions for the assessment of hazard potential (1–3) and damage potential (4–6).

Position	Data purpose and description	Source
1	**Event analysis: Rockfall scenario definition**	
	Dendrochronological data	[6]
	Rockfall deposits	[8]
	Historical records	[5]
2	**Impact analysis: Rockyfor3D parameters**	
	swissALTI3D: Digital elevation model (DEM) 2×2 m [Edition 2015, zone nr. 1328, data status 2009]	[1]
	Release areas: Extent and lithology	[8]
	Terrain roughness and soil types	[8]
	Forest cover	[8]
3	**Future hazard potential scenarios**	
	Observations from meteorological stations	[3]
	Swiss Climate Change Scenarios CH2011	[7]
4	**Topographic maps and aerial images**	
	Topographic Atlas of Switzerland 1:50'000 (Siegfried Map) [Edition 1881, sheet nr. 533 (Mischabel), data status 1881]	[1]
	National Map 1:50'000 (LK50) [Edition 1941, sheet nr. 284 (Mischabel), data status 1941]	[1]
	National Map 1:25'000 (LK25) [Edition 2012, sheet nr. 1328 (Randa), data status 2009]	[1]
	Aerial image: flight date 02-09-1941, nr. 19410640010081	[1]
	Aerial image: flight date 02-09-1941, nr. 19410640130079	[1]

Position	Data purpose and description	Source
5	**Infrastructure**	
	Objekt category	[8]
	swissBUILDINGS3D	[1]
	[Edition 2015, Täsch, variable data status]	
	Buildings and Dwellings statistic (BDS)	[2]
	[Edition 2015, Täsch, data status 2015]	
	VECTOR25	[1]
	[Edition 2008, Täsch, data status 2005]	
	Traffic densities 2010	[4]
6	**Future damage potential scenarios**	
	Expert interview	[5]
	Communal hazard and building plans	[5]

[1]: Swiss Federal Office of Topography (swisstopo)
[2]: Swiss Federal Statistical Office (FSO)
[3]: Swiss Federal Office of Meteorology and Climatology (MeteoSwiss)
[4]: Cantonal Departement for Traffic, Building and the Environment (VS)
[5]: Community of Täsch
[6]: Swiss Tree-Ring Laboratory (dendrolab.ch)
[7]: Center for Climate Systems Modeling (C2SM)
[8]: Field observations and measurements

5.1 Event analysis: Rockfall scenario definition

As outlined in Section 3.2, the definition of plausible rockfall scenarios is based on information about the magnitudes and frequencies of expected events. In this study, various types of observations are considered at different sites along the rockfall slope Täschgufer, namely dendrochronological data, observed rockfall deposits on two deflection dams and records of historical events (Figure 5.1).

Dendrochronological data (site 1) were provided by the Swiss Tree-Ring Laboratory (dendrolab.ch) and allow for an estimation of past rockfall frequencies. Core samples from 255 trees were analysed in the laboratory and growth disturbances (GDs), which are assumed to be the consequence of rockfall events, were detected at yearly resolution with methods of tree ring analysis (Stoffel 2006). However, the observed number of GDs in past years is not a direct indicator of rockfall activity, since – especially in sparsely forested areas – some blocks do not leave any traces behind. To account for this underestimation, the observed number of GDs needs to be corrected for the forest density, or in other words, the exposed diameter of trees along a cross-section of the slope in each year, and the expected block di-

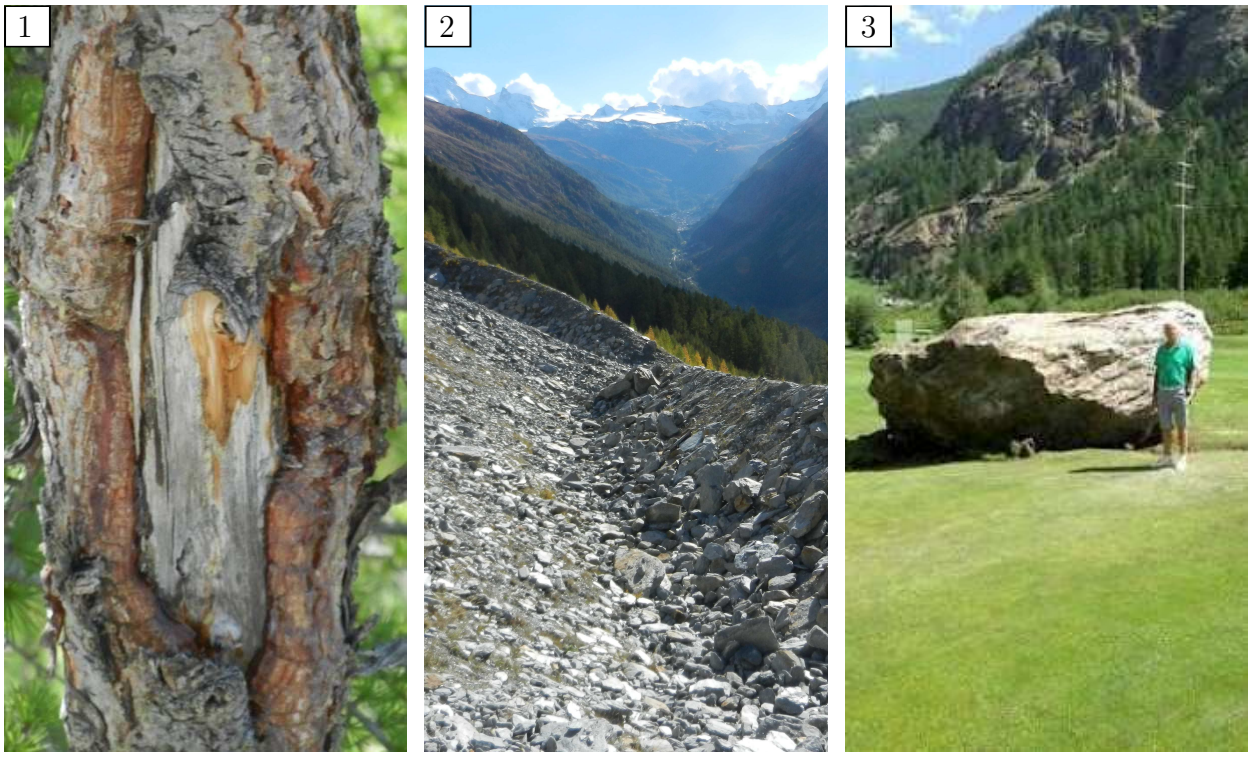

Figure 5.1: Data used for the event analysis: Dendrochronological data (site 1), rockfall deposits (site 2) and records of historical events (site 3). Site numbers refer to Figure 4.1.

ameter, resulting in an estimate of the so-called range corrected impacts (RCI) (Trappmann et al. 2014). RCI values describe the expected number of rockfall events per year and are thought to be reliable when more events are actually observed (GDs) than probably missed (Trappmann et al. 2013), which is the case since 1944 in the available dataset.

Block deposits on two deflection dams (site 2) provide not only information about frequencies, but also about magnitudes of expected events, the latter of which cannot be derived from tree ring analyses (Trappmann et al. 2014). The 480 m long dam at site 2 was considered to be suitable for the assessment of block deposits, since it has not been cleared since its construction in 1996 and represents a considerable part of the slope. Thereby, the volume of all deposited blocks larger than 0.05 m^3 was estimated by measuring their axes in each dimension and applying a shape correction factor (average 0.8) to the resulting product (Matsuoka & Sakai 1999). In total, 1168 blocks were counted on the upper dam, the maximum observed volume being 5.4 m^3. Similar to observed GDs in tree rings, the number of observed block deposits on the deflection dam underestimates the frequency of rockfall events since 1996, since some blocks were certainly not retained by the dam. To estimate the number of missed events, deposited blocks were counted on a second deflection dam, which was built in 1989 and lies around 80 m below the upper dam, covering 160 m of the slope. The 106 blocks observed on this dam, with a maximum volume of 3.1 m^3, are thought to roughly represent all the blocks missed by the corresponding segment of the upper dam.

As particularly the largest block volumes are not retained by the deflection dams and thus are not observable with the above method, documentations of rockfall events reaching the valley floor were considered to estimate the maximum magnitudes to be expected at the damage potential. The largest of the few documented events in Täsch was a rockfall in 2013, a fragment of which reached the golf course to the north of Täsch (site 3) and was blasted shortly afterwards. The volume of the deposited block is reported to be 30–40 m^3, representing only a fragment of the total released rockfall volume of 100 m^3 (Gsponer 2013). Since the rockfall was triggered slightly further north to the investigated release area and block volumes are expected to be somewhat smaller at the latter, the maximum magnitude at the valley floor was assumed to be 20 m^3.

5.2 Impact analysis: Rockyfor3D parameters

As outlined in Section 3.3, the impact of expected events along the slope is assessed with the rockfall model Rockyfor3D in this study, which relies on a set of input parameters characterizing the physical properties of the rockfall slope, which are visualized in Figure 5.2 and described in the following.

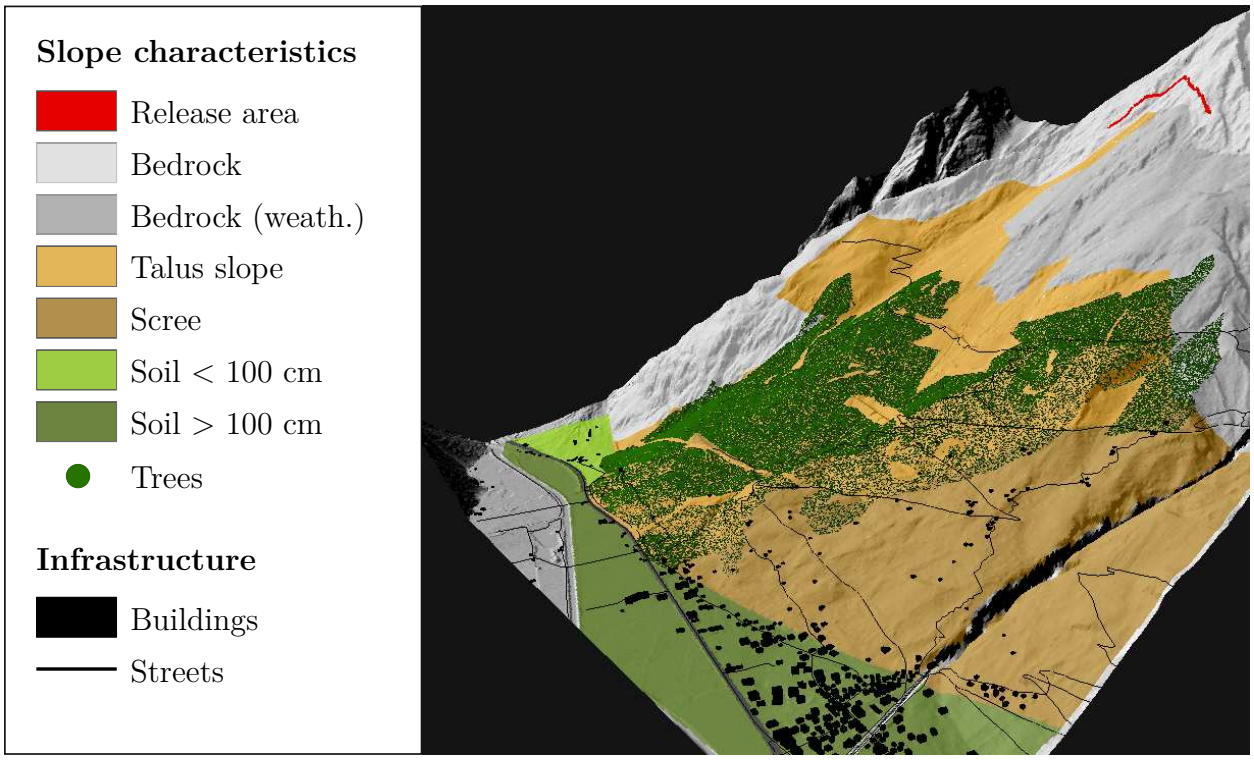

Figure 5.2: Model input parameters specified for the impact analysis: Slope characteristics at Täschgufer were determined in the field within homogeneous polygons according to the parametrization in Rockyfor3D.

The digital elevation model swissALTI3D provided by Swiss Federal Office of Topography (swisstopo) shows the terrain structure of Switzerland without vegetation and buildings at a horizontal resolution of 2×2 m. The product is derived from airborne laser scanning (LIDAR) below 2000 m a.s.l. and photogrammetry above 2000 m a.s.l., the latter of which being the dominant procedure in the study area. The product is updated according to new LIDAR data and aerial images every 6 years and continuously improved. The most recent edition released in 2015 represents the study area on the basis of data from 2009 (swisstopo 2016*d*). The resolution of the product is very suitable for rockfall models, since important terrain features such as gullies and cliffs are typically well represented and thus the kinematics can be simulated accurately. While resolutions coarser than 5×5 to 10×10 m are not recommended, praxis has proved that also a finer resolution of 1×1 m does not significantly improve the quality of the results despite much larger data volume and processing time (Bartelt et al. 2015, Dorren 2016).

The extent of the release area was determined with help of highly resolved photographs of the slope as well as images from Google Earth, on which active parts of the slope were identified. The observed lithology in the field is gneiss, according to which a mean rock density of 2.7 gcm^{-3} was assumed. Furthermore and in line with observed rockfall deposits, the block shape was assumed to be rectangular. As described in Section 3.3 though, the assumed block shape is only relevant for the calculation of the block volume from its dimensions, but is assumed to be spherical for the calculation of contacts with the ground and trees (Dorren 2016). Modeled block dimensions and volumes are variable according to the different rockfall scenarios, which is further described in Section 6.2.1.

The movement of a block along the slope is determined by terrain roughness and soil types, which were determined and mapped in the field for homogeneous polygons according to the parametrization in Rockyfor3D. Terrain roughness can be thought of small scale variability of elevation, which is not represented in the DEM. In Rockyfor3D, it is given by three parameters, defining the mean obstacle heights within 10, 20 and 70% of a homogeneous area, or in other words, the heights of representative obstacles a falling block collides with in 10, 20 and 70% of the ground contacts. Furthermore, Rockyfor3D distinguishes eight different soil types, determining energy transfer during ground contact, which were additionally assigned to the homogeneous polygons (Dorren 2016).

Finally, it was chosen to represent forested areas in Rockyfor3D by the mean number of trees and the distribution (μ, σ) of their diameters at breast height (BHD). These parameters were estimated based on measurements at 10 representative sites (20×20 m) within the homogeneous polygons. This statistical method was favoured over the automatic detection of individual trees from LIDAR data, which is supported by Rockyfor3D, but resulted in an underestimation of forest density compared to observations. With the chosen method, forest layers covered by dominant large trees (e.g. brushwood vegetation), which can have a significant protective function, are generally better represented in the model than with help of LIDAR data (Dorren 2016).

5.3 Future hazard potential scenarios

Future rockfall scenarios are constructed by linking rockfall activity to temperature data, which is described in more detail in Section 6.4.1. The basis for this procedure is given by long-term temperature observations as well as estimates of future temperature changes in the study area, which are shown in Figure 5.3.

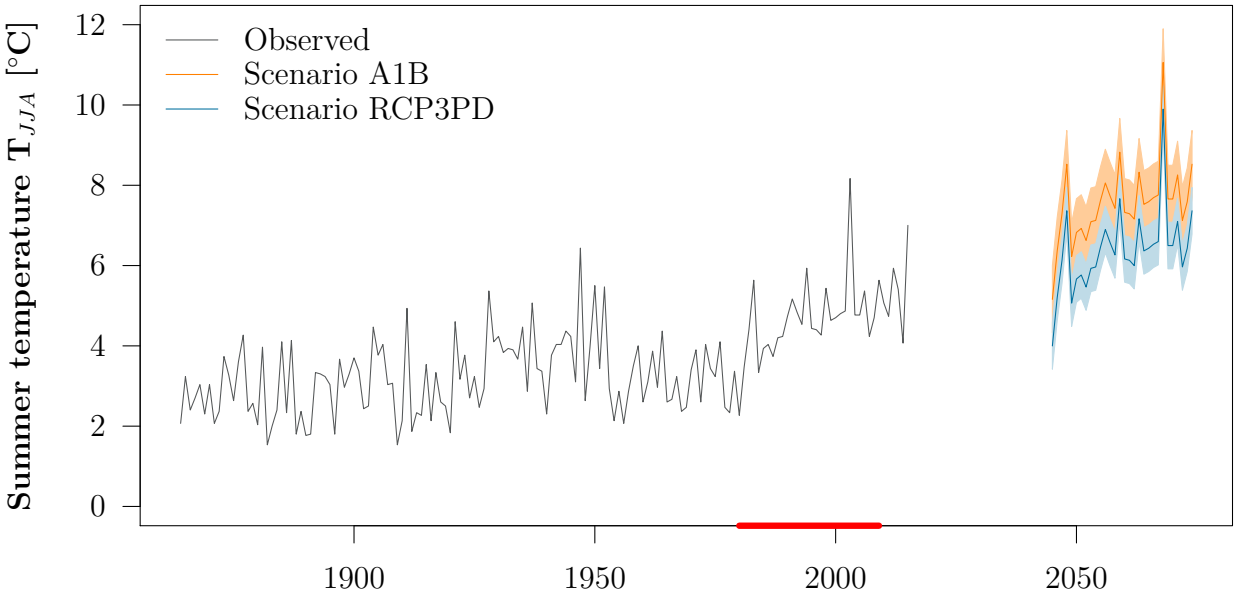

Figure 5.3: Observed mean annual summer temperature T_{JJA} from 1864–2015, as well as future temperature series constructed according to the Swiss Climate Change Scenarios CH2011 (region: CHS, scenario period: 1945–1975, emission scenarios: RCP3PD, A1B). Scenarios are constructed according to the delta change method by adding a constant value to observed temperatures in the reference period 1980–2009 (red). Both scenarios are given by a lower, medium and upper estimate.

Long-term temperature series are available from the meteorological stations of the Swiss Federal Office of Meteorology and Climatology (MeteoSwiss). The station Grächen, which is located at 1605 m a.s.l. around 14 kilometers north to the study area in the Matter valley (LV03: 630747/116058), was considered to be suitable for the analysis due to the the available long-term temperature record. Homogenized, monthly mean values of air temperature (2 m above the ground) are available from 1864–2015. Temperatures are corrected to the mean height of the delineated rockfall release area at 2700 m a.s.l. by assuming a temperature gradient of -0.77 °C per 100 meters and aggregated by season (JJA).

Future temperature series are constructed according to the Swiss Climate Change Scenarios CH2011, which are derived from regional climate models and intended to serve as a reference at a coarse temporal and spatial resolution. The CH2011 data were obtained from the Center for Climate Systems Modeling (C2SM) (C2SM et al. 2011). Scenarios of seasonal mean tem-

perature are considered for the region of Switzerland south of the Alps (CHS), the scenario period 2045–2074 (2060), and two greenhouse gas emission scenarios (A1B, RCP3PD). The emission scenario A2, for which estimates are also available, is not considered since it does not significantly differ from the emission scenario A1B in the medium-term. For each emission scenario, changes of mean summer temperatures (JJA) are given in terms of a lower, medium, and upper estimate relative to the reference period 1980–2009. Future temperature series are constructed according to the delta change method by adding these changes for a given season to the observed temperature series in the reference period. Thereby, there is still a chance that the actual climate change signal will be above the upper estimate or below the lower estimate in a given season. Also, the true climate change signal can be located in different categories (i.e. lower, medium, upper) across different seasons (C2SM et al. 2011).

5.4 Topographic maps and aerial images

The basis for analysing the exposure of infrastructure and people is provided by historical and current maps as well as aerial images, which are shown in Figure 5.4.

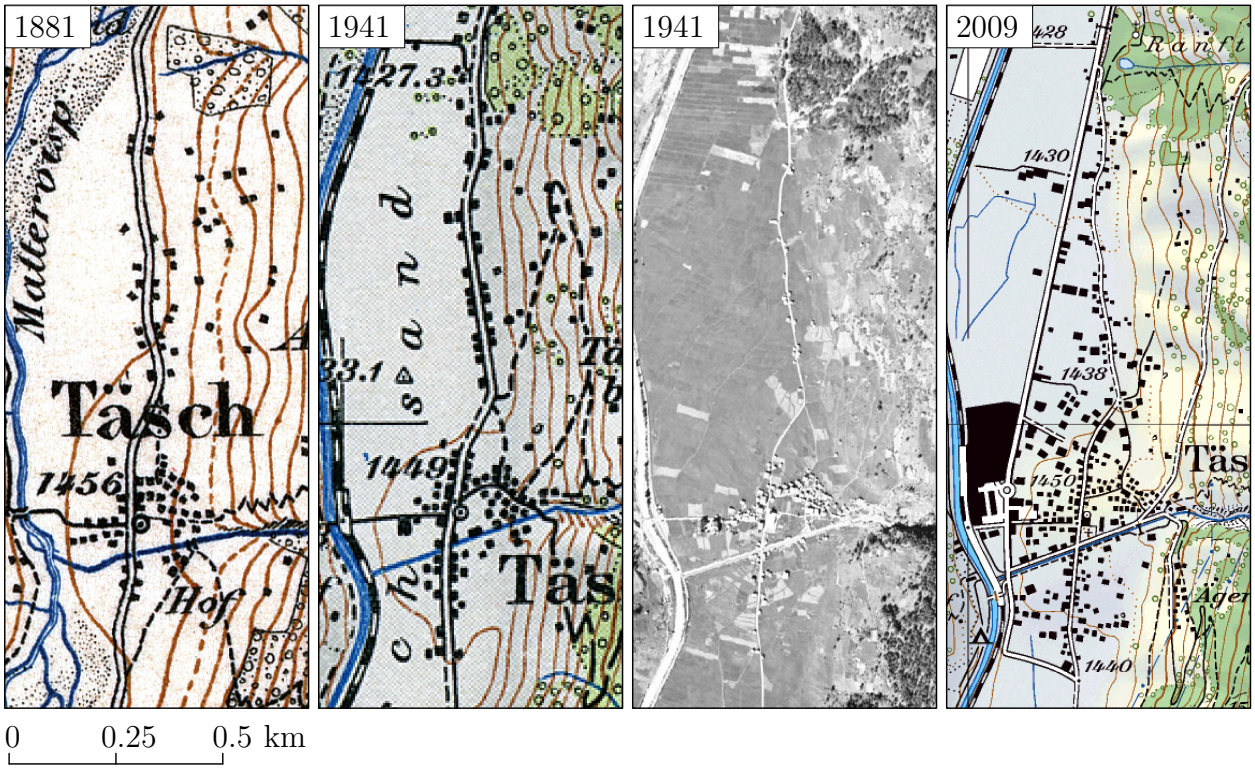

Figure 5.4: Historical and current maps considered in the analysis, namely the Topographic Atlas of Switzerland (1881), the historical National Map LK50 (1941) and the most recent National LK25 (2009). An aerial photograph (1941) is used to check the degree of detail depicted in the National Map LK50.

Historical and current maps are provided by swisstopo and were chosen to represent the past time periods of the analysis as close as possible and with a reasonable resolution. The Topographic Atlas of Switzerland (Siegfried Map) was produced between 1870 and 1926 on the basis of original surveys of the first Topographic Map of Switzerland (Dufour Map) and represents alpine regions at a scale of 1:50'000, while deviations of points from their correct locations are not exceeding 35 m. In this study, the first edition of the Mischabel sheet is used, which was produced in 1881. In the first half of the 20$^{\text{th}}$ century, the Siegfried and the Dufour Map were subsequently replaced by the National Maps, published by swisstopo in varying scales. In this study, the mid 19$^{\text{th}}$ century is examined by the first edition of the Mischabel sheet at the scale of 1:50'000 (LK50), produced in 1941. The current time period is examined on the current sheet (Randa) available at a scale of 1:25'000 (LK25) and produced in 2009. For the National Maps of Switzerland LK50 and the LK25, an accuracy of 5–15 m respectively 2.5–7.5 m can be assumed (swisstopo 2016*b*,*c*).

To assess the general degree of detail and generalization of these maps, aerial photos were used, available at regular intervals since the early 20$^{\text{th}}$ century for the entire country from swisstopo. Two aerial images from 1941 were of particular interest to compare with the National Map (LK50) of 1941, which are both available in black and white at a scale of 1:20'000 (swisstopo 2016*a*).

5.5 Infrastructure

Information about the value of exposed buildings and streets is difficult to derive from maps and was assessed with a combination of different data sources. To assess the values of buildings, a combination of the dataset swissBUILDINGS3D (object values) and the Buildings and Dwellings statistic (BDS) (number of persons) is used. To assess the values of streets, a combination of the VECTOR25 dataset (object values) and information about traffic densities (number of persons) is used.

The dataset swissBUILDINGS3D from swisstopo shows the building volume for every building footprint in Switzerland with a simple prismatic shape. Building footprints are based on the VECTOR25 dataset, a product derived from the National Map of Switzerland LK25, and building heights are calculated from the difference between two terrain models (DOM and DTV-AV), depicting the terrain structure of Switzerland with and without vegetation and buildings. Being derived from several data sources with different acquisition dates (VECTOR25: 1994–2006, DOM and DTM-AV: 2000–2007), differences in the data up to 10 years are possible. Also the accuracy depends on the accuracy of the individual datasets being 3–8 m for the position accuracy of building footprints from VECTOR25 and $\pm$1.5 m for the building heights derived from the two terrain models (swisstopo 2010).

The BDS provided by the Swiss Federal Statistical Office (FSO) is based on the Federal Register of Buildings and Dwellings (FBD) in combination with data from the harmonised communal and cantonal population registers and the structural survey. It provides infor-

mation about the structure of the whole building and dwelling stock and about the living conditions of the population (e.g. occupation density per room or dwelling, floor space per person). Various statistical analyses require the combination of building and dwelling data with data on persons and households. The building and dwelling variables may present missing data which can make analysis of statistical results difficult. The FSO provides completed data, while substitutions are made for the missing data. In principle, the statistical substitution method applied maintains the existing statistical distribution of variables. This enables statistical analyses to be made on the basis of these data, provided that the scale of the geographical units is not too small (FSO 2016*a*).

To get information about values of streets, the classification of streets in the latest version (2008) of the VECTOR25 dataset is used, which is based on the National Map of Switzerland LK25. VECTOR25 reproduces man-made and natural features in a flexible vector format and is available for entire Switzerland in homogeneous data format and quality. The accuracy of 3–8 m is again given by the accuracy and generalization of the National Map of Switzerland LK25.

Information about traffic densities in the study area was provided by the Cantonal Departement for Traffic, Building and the Environment of the canton Valais. More specifically, annual traffic frequencies are available for 2007–2015 from an automatic counting station at St. Niklaus (LV03: 628000/113600), representing the mean daily traffic volume, which is 4039 vehicles per day in 2010.

5.6 Future damage potential scenarios

To assess future developments of damage potential, meaning the development of population and the built environment in Täsch, different types of information were considered. On the basis of an expert interview, which was conducted with a local authority of Täsch in March 2016, three qualitative land-use scenarios could be defined. These scenarios were quantified on the basis of observed developments in the building zones of Täsch, which could be derived from data of the BDS (Section 5.5). New buildings were then allocated according to the extents of the current communal zone plan and current hazard zones (Figure 4.2), which were provided by the community of Täsch. The exact procedures of linking these types of information is in detail described in Section 6.4.2.

6 Methods

In this chapter, the methodology of the quantitative risk analysis is described in more detail. Following the structure of Chapter 3, the mathematical description of risk is given before the quantification and mapping of its components, namely hazard potential and damage potential, is described. As the risk analysis is performed for the time periods of 1880, 1940, 2010, and 2060, the chapter concludes by describing temporal changes of these components and their quantification.

6.1 Risk

The collective rockfall risk in the study area is calculated according to Equation (6.1), which is well established in engineering since the 1990s (Bründl 2009, Fuchs et al. 2004, Keiler et al. 2006) and visualized in Figure 6.1. Thereby, the monetary annual risk $R_{i,j}$ is calculated for each raster cell i and rockfall scenario j according to the frequency of the rockfall scenario $F(S_j)$, the probability that the raster cell is exposed to this scenario $P_{i,j}$, as well as the value A_i and the vulnerability $V_{i,j}$ of the objects and persons in the raster cell. The collective risk R for the whole study area is then the sum of these risks over all raster cells i and scenarios j (Equation (6.2)). This general risk formula integrates all aspects of hazard potential and damage potential discussed in Chapter 3, the exact implementation and mapping of which is presented separately in the following sections.

$$R_{i,j} = F(S_j) \cdot P_{i,j} \cdot A_i \cdot V_{i,j} \tag{6.1}$$

$$R = \sum_i \sum_j R_{i,j} \tag{6.2}$$

6.2 Hazard potential

In the following, the quantification of both the frequency of a scenario at and its impact at a certain location are described. As outlined in Section 3.2 and implemented in Equation (6.1), the frequency of a scenario at a certain location is given by the frequency of the scenario $F(S_j)$ at the release area and the spatially variable propagation probability $P_{i,j}$. The impact at a certain location is given by the total kinetic energy of the rock, which in turn determines the physical vulnerability $V_{i,j}$ (Section 3.4). At the end of this section, the integration of both of these aspects into the hazard map is presented.

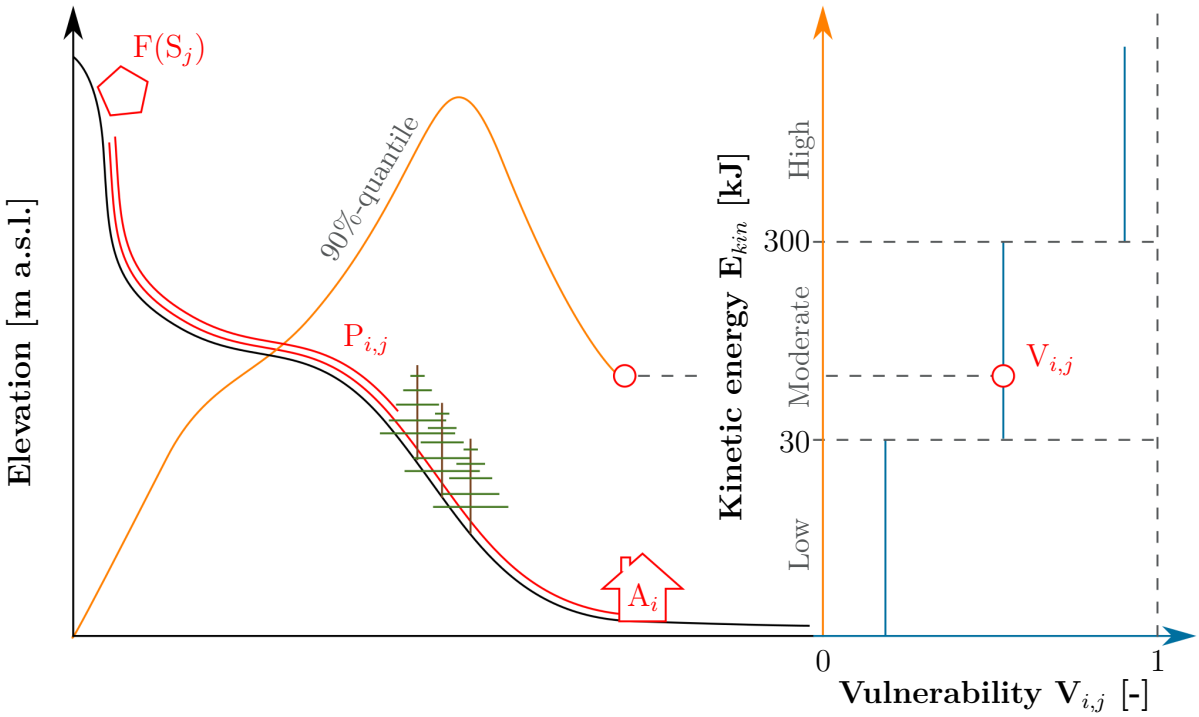

Figure 6.1: Visualization of the general risk formula for the rockfall hazard: Risk for each raster cell i and rockfall scenario j is calculated according to the frequency of the rockfall scenario F(S_j), the probability that the raster cell is exposed to the scenario $P_{i,j}$, as well as the value A_i and the physical vulnerability $V_{i,j}$ of the objects and persons in the raster cell. Physical vulnerability is thereby a function of the kinetic energy of the rockfall (Section 3.4).

6.2.1 Frequency of a scenario

The frequency of a rock fall scenario F(S_j) at the release area is associated with a certain block volume and can be derived from MCF distributions. Thereby, the MCF distribution (Equation (6.3)) describes the exceedance frequency F(M), meaning the number of blocks larger than volume v, which are expected to be released per year (Lari et al. 2014).

$$F(M) = a \cdot \left(\frac{v}{v_0}\right)^{-b} \tag{6.3}$$

The parameters of Equation (6.3) refer to observed frequencies and magnitudes and are estimated according to different data sources (Section 5.1). The total number of blocks a, which is expected to be released per year, was assessed with two similar but independent approaches described below. Weighting both approaches equally, the final value of$a$ was set to 104 blocks per year.

In a first approach, the number of deposited blocks on the 19-year-old upper deflection dam was corrected for the number of simulated trajectories reaching the dam, and for the estimated percentage of missed blocks (16%) according to deposits on the lower dam.

The resulting estimate is a rockfall activity of 1955 blocks in 19 years or 103 blocks per year.

In a second approach, the number of observed GDs in tree rings within the last 19 years was corrected for the number of simulated trajectories reaching the sampled trees, and the estimated missed events passing the trees without leaving any visible signs behind (Section 5.1). The resulting estimate is a rockfall activity of 2005 blocks in 19 years or 105 blocks per year.

The exponent b of 1.085, representing the volume distribution of the rockfall events, is estimated from rockfall deposits on the upper deflection dam and equal to the slope of a linear regression between the observed block volumes v and the corresponding cumulative number of blocks F(M) in a log-log representation (Figure 6.2 (left)) (Ruiz-Carulla et al. 2015). The minimal volume v_0 is set to 0.05 m^3, since smaller volumes were neither considered when counting the deposits on the deflection dams, nor thought to have caused GDs in trees, because such blocks do not reach the area of the sampled trees according to model results. The maximal volume is not explicitly accounted for in Equation (6.3), but is given by the range of values that the equation is applied to. As described in Section 5.1, the maximum volume expected to reach the the valley floor was chosen to be 20 m^3 according to the largest observed rock deposit of the rockfall event in 2013.

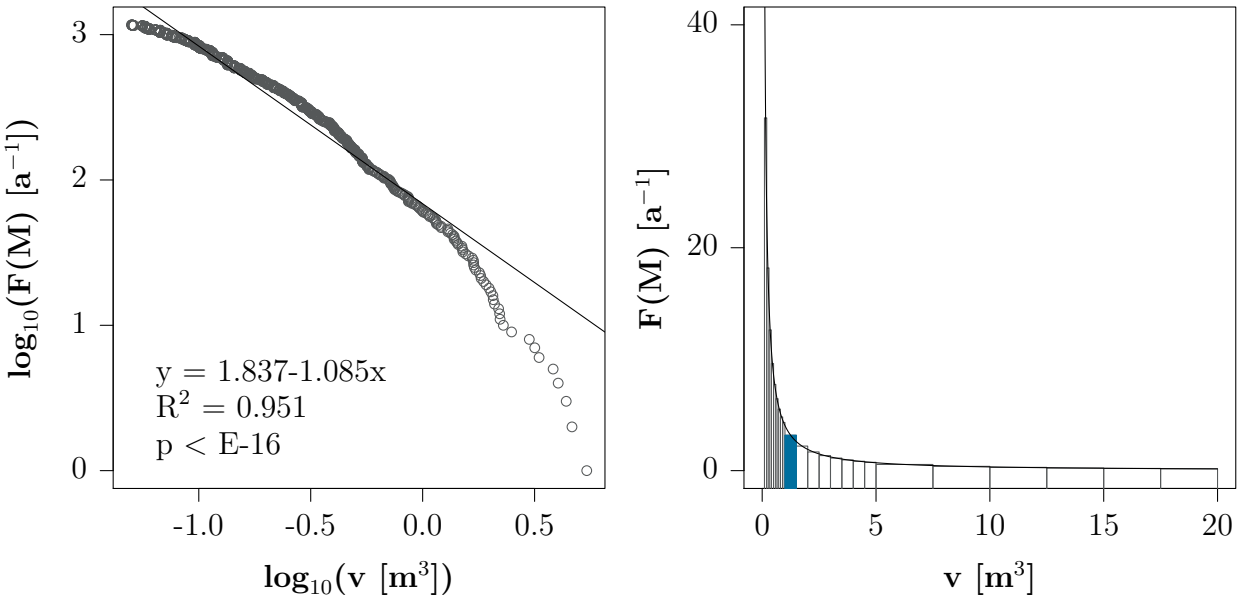

Figure 6.2: Derivation of b (left) and resulting MCF distribution (right) at Täschgufer: For rockfall modeling, 23 rockfall scenarios and their frequencies were derived from the MCF distribution. For example, the frequency of the highlighted scenario (1–1.5 m^3) is 1.44 blocks per year.

To adequately represent the resulting MFC distribution in the rockfall modeling, 23 rockfall scenarios between 0.1 and 20 m^3 were defined and are shown in (Figure 6.2 (right)). The

frequency of each scenario $F(S_j)$, which is relevant for the risk calculation, was calculated according to Equation (6.4), where M_j and M_{j+1} correspond to the volume range of the scenario. For example, $F(S_j)$ of the highlighted scenario (1–1.5 m^3) is 1.44 blocks per year.

$$F(S_j) = F(M_{j+1}) - F(M_j) \tag{6.4}$$

To assess the probability $P_{i,j}$ that a particular raster cell is affected by the released blocks, each rockfall scenario was simulated with the rockfall model Rockyfor3D. Thereby, the block volume released from each source cell was randomly sampled within the volume range of the scenario, and block dimensions were chosen to fit the dimensions of observed deposits within this range. For volumes larger than 5.4 m^3, which were not observed in the field, the dimensions of the largest observed block were applied. To ensure statistically stable results, 100 trajectories were calculated from each source cell, among which the block volume was again randomly varied by ±5%. The spatial probability $P_{i,j}$ can then be calculated according to Equation (6.5), which describes the number of trajectories passing through each raster cell $traj_{i,j}$ with respect to the total simulated trajectories $traj_{tot}$ (74'800). Figure 6.3 shows the resulting distribution of $P_{i,j}$ for the above discussed scenario (1–1.5 m^3). As blocks are distributed and deposited in spatial patterns along the slope, clearly certain raster cells (e.g. cells in preferential fall paths or near the release area) are affected more likely than others.

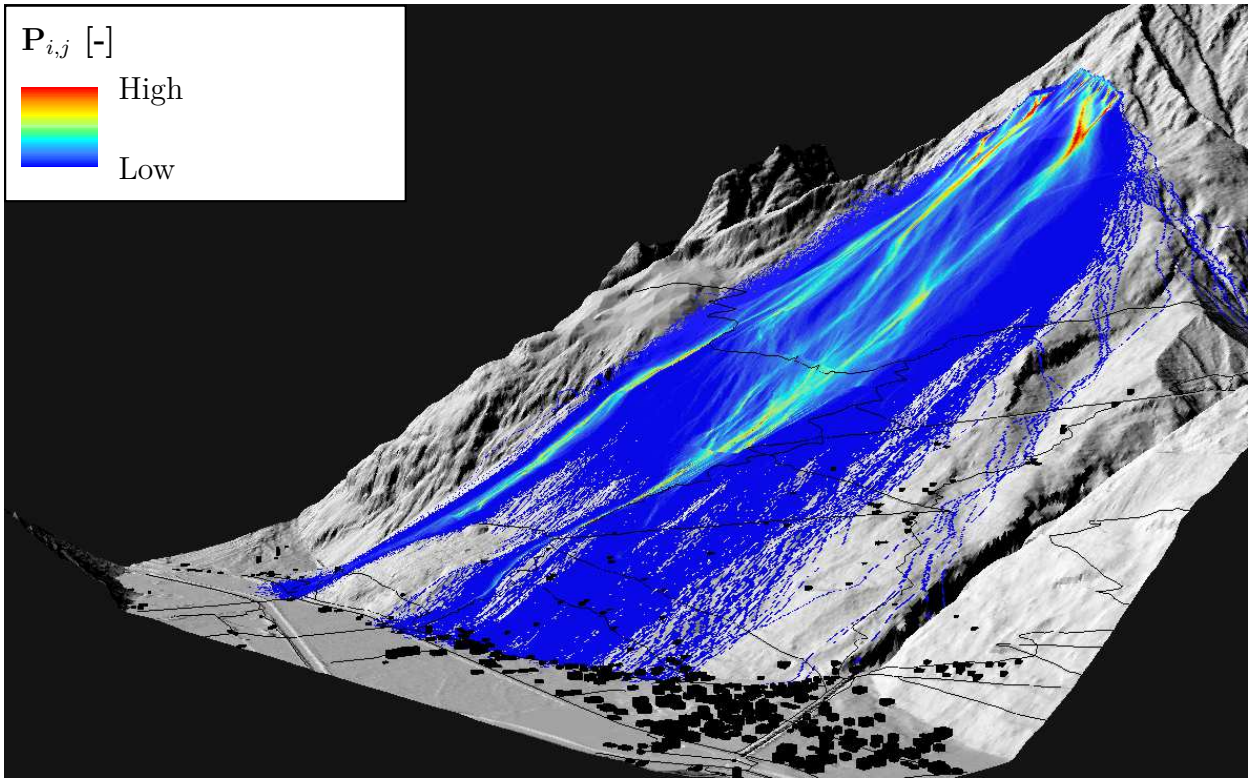

Figure 6.3: Probability $P_{i,j}$ at which a raster cell is affected in a scenario (1–1.5 m^3), obtained from modeling results and Equation (6.5).

$$P_{i,j} = \frac{traj_{i,j}}{traj_{tot}} \tag{6.5}$$

Finally, to control for the cell size in a raster-based approach, a correction factor C_j is applied to the spatial probability $P_{i,j}$. Thereby, in the case of an event reaching a raster cell, only a fraction of this cell or even multiple cells will be affected, depending on raster resolution, block size and the considered event type. For example, a block of half the diameter of a raster cell will affect only half the cell, and a block with twice the diameter of a raster cell will affect two raster cells. Following Jaboyedoff et al. (2005) and the DETEC & FEDRO (2012), the spatial probability $P_{i,j}$ is corrected by the correction factor C_j according to Equation (6.6), which considers the mean block diameter d_j in each scenario and the raster resolution, which is 2×2 m.

$$C_j = \frac{d_j}{2} \tag{6.6}$$

6.2.2 Intensity

The intensity at which a certain raster cell is affected determines the degree of damage that this raster cell will suffer. As different physical vulnerabilities are assumed for discrete intensity classes (Section 3.4), the kinetic energy distribution simulated at each cell was classified into these classes for the risk analysis. More specifically, the 90%-quantile of this distribution was classified into classes of low (0–30 kJ), medium (30–300 kJ) and high (>300 kJ) intensity according to the Swiss guidelines (Lateltin 1997). The resulting intensity map for the above discussed sceanrio (1–1.5 m^3) is shown in Figure 6.4. By considering the 90%-quantile, maximum energy values obtained by the simulations are neglected, which has practical significance. Such values represent extreme unfavourable conditions and would result in high risk estimates and thereby also high costs in the design of protection measures. By considering the 90%-quantile, however, these protection measures will be less costly, but nevertheless be able to guarantee a sufficient degree of protection (Abbruzzese et al. 2009).

6.2.3 Hazard mapping

Having determined the frequency of an event and the corresponding 90%-quantile of the energy distribution for each cell and scenario, the resulting rockfall hazard can be determined according to the hazard mapping scheme introduced in Section 3.2 and shown in Figure 6.5. The frequency of a scenario is thereby expressed with the return period T(M), corresponding to the minimum magnitude of a scenario M_j (DETEC & FEDRO 2012) and accounting for the propagation probability of the scenario at each location (Equation (6.7)). This hazard mapping approach is a quantitative implementation of the Matterock methodology outlined by Abbruzzese et al. (2009). To allow for a numerical solution of the hazard mapping, the Swiss hazard mapping scheme is interpreted to be continuous (i.e. with diagonals), and the worst case over all scenarios is shown on the final hazard map (Abbruzzese & Labiouse 2014).

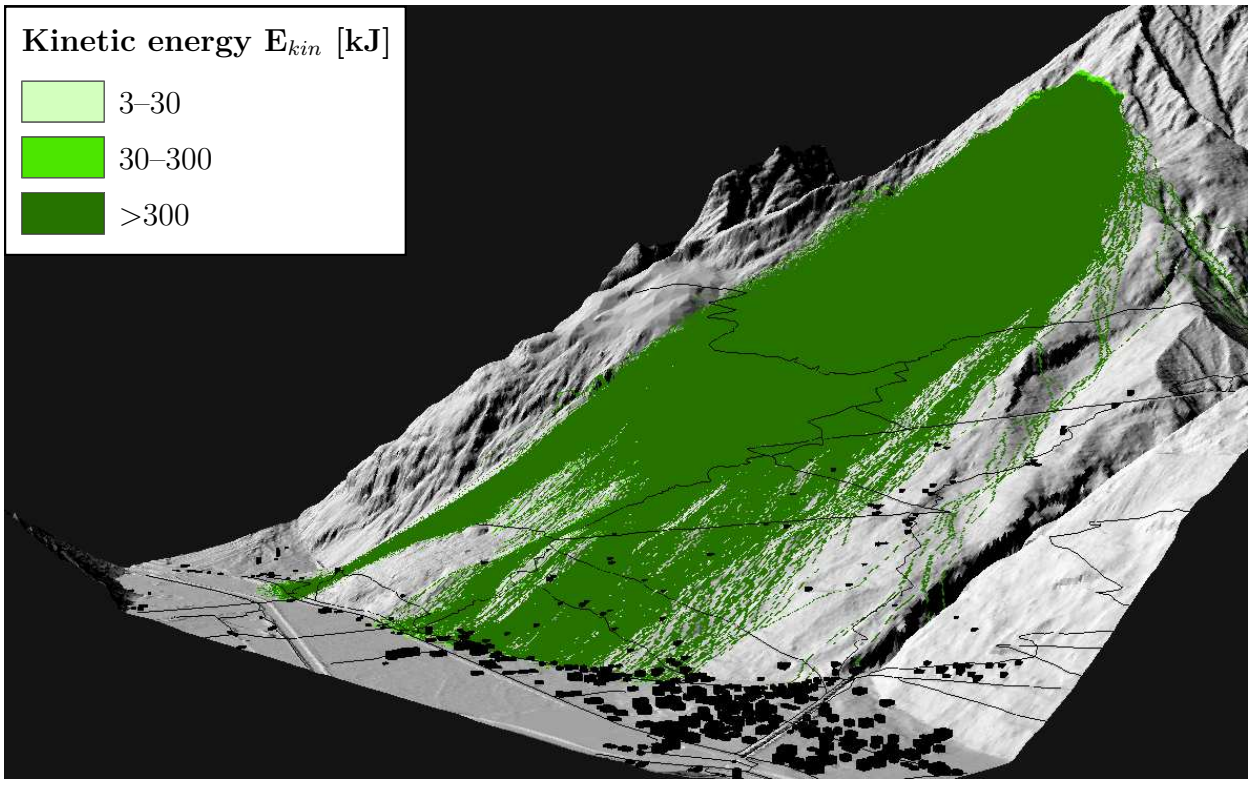

Figure 6.4: Intensity at which a raster cell is affected in a scenario (1–1.5m^3), obtained from the classification of the 90%-quantile of the energy distribution in each cell into classes of low (0–30 kJ), moderate (30–300 kJ) and high (>300 kJ) physical impact.

$$T(M_j) = \frac{1}{F(M_j) \cdot P_{i,j} \cdot C_j} \tag{6.7}$$

6.3 Damage potential

In the following, the quantification of both the value and vulnerability of exposed objects and persons is described, which are implemented into Equation (6.1) by the monetary value A_i of each raster cell and its vulnerability $V_{i,j}$ respectively. At the end of this section, the integration of both of these aspects into the damage potential map is presented.

6.3.1 Object values

The monetary value of each raster cell is basically the sum of object values and the monetized values of persons present in the raster cell. These values were calculated on the basis of EconoME (Bründl et al. 2015), which provides basis values for different object categories (Table 6.1) and persons (5 Mio CHF per person), while in this study only buildings and streets were considered.

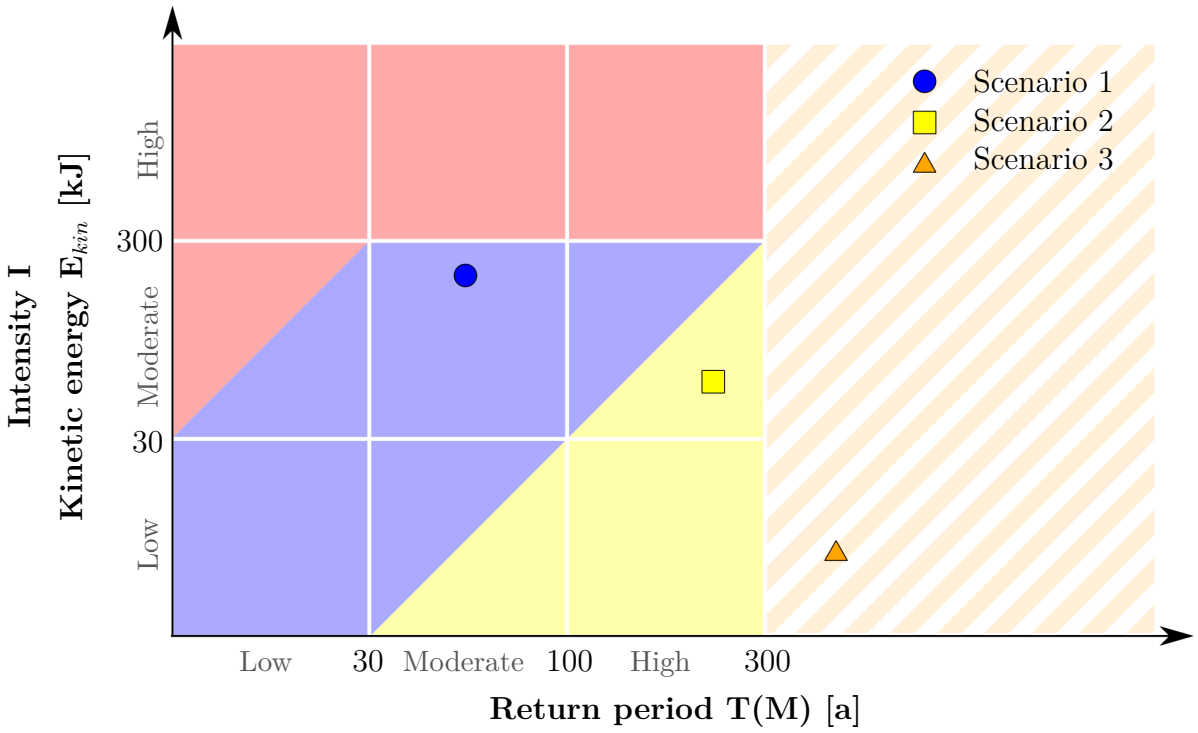

Figure 6.5: Rockfall hazard mapping according to the Swiss hazard mapping scheme: For each raster cell and scenario, a hazard value is obtained, while the worst case (scenario 1 in the above example) is shown on the final hazard map. To allow for a numerical solution of the hazard mapping, the Swiss hazard mapping scheme is interpreted to be continuous (i.e. with diagonals).

The calculation of values for buildings and streets from these basis values requires the estimation of several parameters, which are derived from different data sources listed in Table 6.2 and in more detail described in Section 5.5. The object value of buildings thereby depends on the building category and its volume, for residential buildings additionally on the number of apartments. The value of persons in residential buildings is given by their number and average probability of presence, which is set to 0.8 (equal to 19.2 hours per day) according to the default value in EconoME (Bründl et al. 2015). The object value of streets depends on the street category and its length. The value of persons being exposed on streets is dependent on several assumptions about traffic volume, namely mean daily traffic frequency, mean occupancy and velocity of road vehicles.

Table 6.1: Basis values for different object categories (Bründl et al. 2015).

Object category	Basis value	Unit
Shed	80	$CHFm^{-3}$
MFH	550'000	$CHFapp^{-1}$
Trail (asphalt)	700	$CHFm^{-1}$

Table 6.2: Parameters for determining values of buildings and streets and their sources.

Parameter	**Source**
Building category	Fieldwork
Building volume	swissBUILDINGS3D
Number of apartments for residential buildings	BDS data
Number of persons for residential buildings	BDS data
Street category	Fieldwork, VECTOR25
Street traffic volume	Canton VS

Since direct information about traffic frequencies was only available for the main road, additional assumptions had to be made for smaller trails (Table 6.3). For the main road, the observed mean daily traffic frequency derived from an automatic counting station at St. Niklaus was 4039 vehicles in 2010. Furthermore, a mean occupancy of 1.76 persons per vehicle was assumed according to the default value in EconoME (Bründl et al. 2015) and the speed limit in the relevant section of the road was observed to be 50 kmh^{-1}. For all other road types in the study area, a predominant use as hiking trails was assumed. The Europaweg being the most important hiking trail in the study area, travel frequencies on these trails were assumed to be limited by the capacity of the Europa Hut in Randa, from which Täschgufer and Täschalp are reached within one day. According to the mean number of sunny days on which the hut is open during the hiking season and its capacity (42 beds), a mean annual travel frequency of 5 persons per day was estimated. Furthermore, a walking pace of 4.2 kmh^{-1} was assumed.

Table 6.3: Traffic parameters for different street categories: The value of persons being exposed on streets is dependent on mean daily traffic frequency DTV, mean occupancy and velocity of road vehicles. Assumptions for the main road are based on vehicle counts, while assumptions for hiking trails are based on the capacity of the Europa Hut in Randa and its assumed occupancy.

Street category	**DTV [d^{-1}]**	**Occupancy [pers.]**	**Velocity [kmh^{-1}]**
Road (8 m width)	4039	1.76	50
Trail	5	1	4.2

Given the slightly different data states of the different sources, a homogenisation to the reference year 2009 was applied, which is the data state of the National Map LK25. Thereby, only buildings visible on this map were considered, and information about newer buildings (BDS) was excluded. Furthermore, building heights, which lacked for newer buildings in the swissBUILDINGS3D dataset, were estimated in the field.

6.3.2 Vulnerability

The vulnerability of each raster cell depends on the objects in this cell and the scenario it is exposed to, or more precisely the intensity at which it is affected. In EconoME, for each object category and process intensity, a vulnerability V for objects as well as a lethality L for persons is specified, which denote the expected degree of loss in case that the object or person is exposed to a low, medium, or high physical impact (Table 6.4). With this implementation, as outlined in Section 3.4, only physical vulnerability is considered. Additionally, the approach is based on discrete intensity values, which are only an approximation of the corresponding vulnerability function.

Table 6.4: Vulnerability of objects and lethality of persons for different object categories, denoting the degree of loss in case that the object or person is exposed to low (V(low), L (low)), medium (V(med), L (med)), or high (V(high), L (high)) physical impact (Bründl et al. 2015).

Object category	V(low)	V(med)	V(high)	L(low)	L(med)	L(high)
Shed	0.01	0.8	0.9	1E-3	3.2E-2	5.4E-2
MFH	0.01	0.1	0.2	1E-5	2E-4	2E-2
Trail (asphalt)	0.1	0.5	1	0.1	0.8	1

6.3.3 Damage potential mapping

As described in Section 3.4, no standardized procedures for damage potential mapping exist and existing procedures are highly subjective. For reasons of transparency and facilitated interpretation of the resulting map, it was chosen to map the obtained value A_i of each raster cell as the sum of object and monetized person values, multiplied by the maximum vulnerability V(high) and lethality L(high), respectively. The resulting measure thus represents the expected monetary loss in case of a rockfall event with high intensity. This approach is very similar to assuming the probable maximum loss (Section 3.4) and facilitates mapping, because the resulting map does no longer depend on the rockfall scenario.

6.4 Sensitivity and temporal aspects

To allow for planning in risk management (Section 3.5), a multi-temporal approach is followed in this thesis, focusing on the quantification of observed and anticipated long-term changes between 1880 and 2060. Therefore, distinct time periods around 1880, 1940, 2010 and 2060 are examined, which are thought to represent important changes in the human and natural system. Different influential factors and their changes are considered, the implementation of which into the risk analysis is outlined in the following for changes in hazard potential as well as changes in damage potential. In general, past changes are tried to be quantified based on observations and available data, while future changes are assessed with different scenarios to account for the substantial uncertainties of future developments.

6.4.1 Changes in hazard potential

Hazard potential might change if type, magnitudes or frequencies of expected events change, or if changing slope characteristics (e.g. soil types, forest cover or protection measures) will affect the spatial propagation probability or the distribution of kinetic energy of these events. To assess real and anticipated changes from 1880 to 2060, two factors were considered, namely an expected change in rockfall frequency due to a changing climate, and the effect of the deflection dams, which were built at Täschgufer in late 20$^{\text{th}}$ century.

To estimate changes in rockfall frequency due to a changing climate, a relation between data on long-term rockfall activity and a long-term temperature series (Section 5.3) was established, assuming that warmer temperatures lead to increased rockfall activity at Täschgufer due to thawing of permafrost in the upper parts of the slope. More specifically, a correlation analysis revealed the highest correlation coefficient (0.44) between RCI values and mean summer temperatures (JJA) between 1944 and 2010, where the former are considered to be reliable. Based on this analysis, a simple regression model was fitted to these variables. To meet the requirement of a normal distribution and allow for statements about the model uncertainty, RCI values were transformed with the square root function before applying a linear regression (Figure 6.6 (left)). Although the resulting model is not able to explain the variability of RCI values sufficiently, which is reflected in both a low R^2 (0.187) and wide prediction intervals (Figure 6.6 (right)), it suggests a significant common trend in both series. Therefore, it is argued that an estimation of mean RCI values associated with certain summer temperatures is possible.

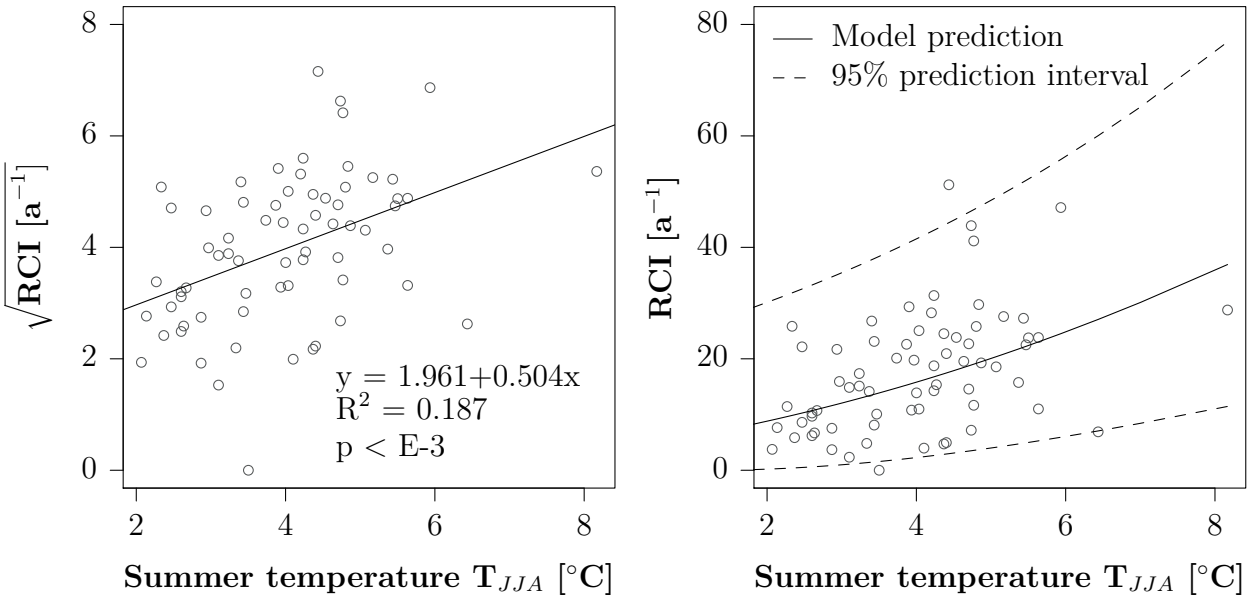

Figure 6.6: Regression model relating mean annual summer temperatures T_{JJA} and RCI values (left), as well as corresponding 95% prediction intervals (right).

To estimate mean rockfall frequencies for all time periods, the model was applied to both the observed past temperature series and the constructed future temperature series (Figure 6.7). By applying the model to the future time series, the domain of the model is barely exceeded, mainly due to the already relatively high summer temperatures observed in summer 2003. Nevertheless, as can be inferred from Figure 6.6 (right), the uncertainty in predicted annual rockfall activity is high. To obtain more robust estimates, predicted annual RCI values were averaged over time periods of 30 years, which are indicated in Figure 6.7. With help of the resulting estimates, the frequency of the rockfall scenarios, namely the parameter a of the MCF distribution, could be adjusted when modeling risk for time periods of 1880, 1940, 2010 and 2060 (Table 6.5).

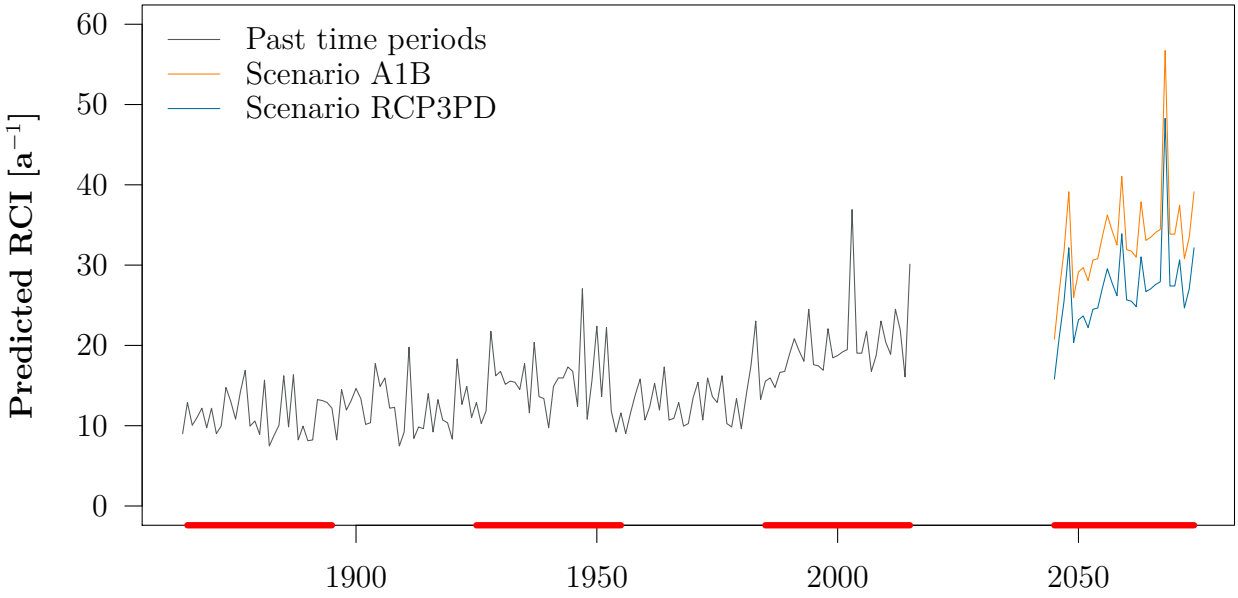

Figure 6.7: Predicted mean annual rockfall frequencies for the investigated time periods: To obtain more robust estimates, predicted mean annual RCI values were averaged over periods of 30 years for both past and future time periods.

Table 6.5: Adjusted MCF distribution for the investigated time periods: The parameter a of the MCF distribution could be adjusted to the investigated time periods according to modeled rockfall activity in these periods.

Times period	**1880**	**1940**	**2010**	**2060**	
Scenario				**RCP3PD**	**A1B**
Predicted mean RCI [a^{-1}]	12	15	20	27	33
Correction factor a [-]	0.6	0.8	-	1.4	1.7
Adjusted a [a^{-1}]	62	83	104	147	177

As mentioned in Chapter 4, several deflection dams were built at Täschgufer in the late 20th century. The comparison of measured dam heights and height profiles in the DEM used in this study (Section 5.2) showed that the deflection dams are quite well represented in the simulation. To examine their effect on rockfall risk, the DEM was manipulated before it was used for modeling in the time periods of 1880 and 1940. Thereby, the dams were removed from the DEM and gaps were filled by linear interpolation (IDW) of elevation values between their lower and upper bounds (Figure 6.8). For correcting the large areas covered by the deflection dams, this method seemed to provide better results than the manipulation of contour lines, which was applied by Kallen (2015) for smaller corrections in a DEM. For future simulation, it is assumed that deflection dams remain in the state of 2010.

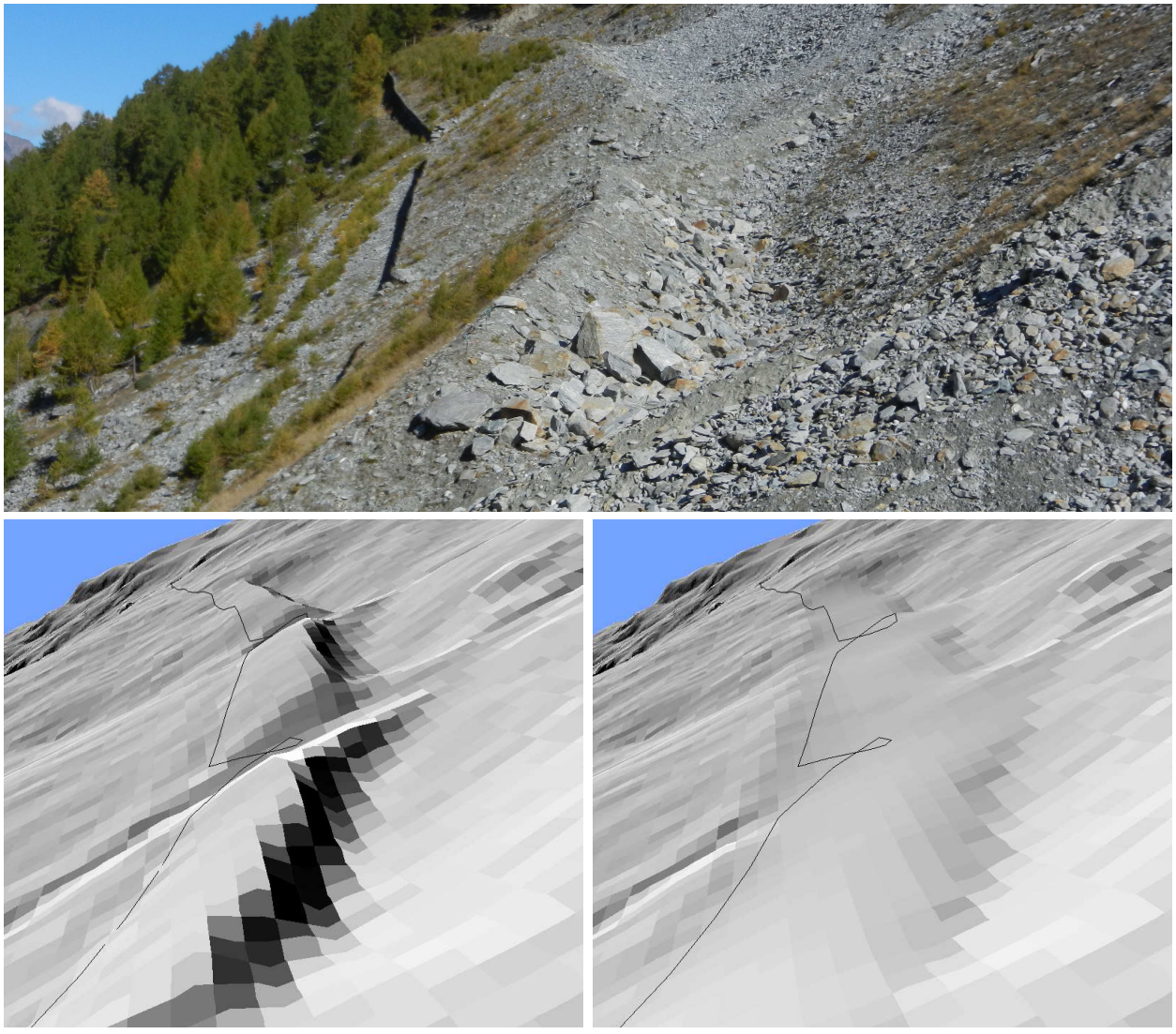

Figure 6.8: Removal of the deflection dams from the digital elevation model (DEM): A segment of the upper dam (top) (photo: M. Fehlmann) and corresponding hillshades of the DEM swissALTI3D before (bottom left) and after (bottom right) removal of the deflection dams.

6.4.2 Changes in damage potential

Damage potential might change if exposure, values or vulnerabilities of objects or persons change. Since changes of values and vulnerabilities are hard to assess and associated with very large uncertainties, they are regarded as constant in the following and only changes in exposure, meaning the number of objects and persons exposed to the rockfall hazard, are examined.

To estimate past changes in the built environment, historical maps were considered (Section 5.4). Similar to Kallen (2015), a unique object ID was assigned to each of the classified objects (buildings and streets) and – with help of information about its building phase (Section 5.5) – it was identified on the historical maps. Thereby, the same object value was assumed, implying for example no changes in building category, number of apartments and persons and also the footprint of the building, which is not reliable on historical maps due to coarser map scales.

To assess future changes in the built environment, three exploratory scenarios were developed, which cover a wide range of fundamental uncertainties in regional socio-economic development. Following the approach of Nussbaumer et al. (2014), the most relevant drivers of regional development and potential development pathways in Täsch were identified based on an expert interview with a local authority and combined into three qualitative scenario storylines, which were then quantified and implemented into the risk analysis with help of existing data.

Based on an expert interview, the following drivers of regional socio-economic development and potential development pathways in Täsch were identified.

Tourism in Zermatt and Täsch: The growth and success of Zermatt as a tourist destination strongly affects demographic developments in Täsch. Since employers in the tourist sector in Zermatt discovered Portuguese employees in the early 1990s, the population of Täsch nearly doubled, around 40% of today's population being of Portuguese origin (FSO, 2016). Täsch is an attractive place of residence for these workers, since residential property in Zermatt is not only rare but also expensive. Apart from Zermatt, Täsch has not yet fully tapped its own tourist potential within the region. Since space is limited in Zermatt, there lack sports fields or a congress center in the region, which could be build in Täsch. Furthermore, a direct connection by mountain railway from Täsch to the skiing region of Zermatt could further integrate the Zermatt-Matterhorn tourist region, which was founded 10 years ago by the communities of Zermatt, Täsch, and Randa.

Traffic routes: Traffic routes ensure a quick and reliable connection between Täsch and Zermatt, which is a basis for a successful employer-employee relationship. Substantial improvements in traffic safety (e.g. foundation of a traffic safety service, building of galleries) were realised since an accident in 1985, which caused 11 fatalities. Furthermore, the Matterhorn-Gotthard railway connects Täsch and Zermatt every 20 minutes

since 2014. As discussed above, fast connections to Zermatt are indispensable for the development of tourism in Täsch, a future highlight of which might be a direct connection to the skiing region of Zermatt.

Political constraints: Political constraints determine construction activities in Täsch. The Swiss federal popular initiative limiting second homes in many tourist resorts triggered substantial construction activity in Täsch previously to its acceptance in 2012. Since all buildings in Täsch and Zermatt built after 2015 are restricted to be used as permanent dwellings for local residents, they are less attractive for investors and as a consequence, construction activity is expected to decrease in the future. This trend is already visible in land prices, which nearly halved during the last 3 years, indicating a decrease in expected benefits. Another regulation is given by national and cantonal land-use planning laws (RPG), which target a high-density construction in already developed areas and can even provoke a reduction of building zones for environmental protection purposes.

Natural hazards: Regional development in Täsch is not independent of natural hazards, since building zones at the valley floor are strongly confined by hazard zones, whereby for example construction of new buildings in the red hazard zone is prohibited. With regard to the current hazard map of Täsch (Figure 4.2), it can be stated that Täsch is affected by many natural hazards (e.g. rockfalls, debris flows and avalanches from Täschgufer as well as flooding of the rivers Täschbach and Vispe). A major hazardous event in the future could lead to an enlargement of the red hazard zone and thereby hinder future construction activity.

The driving forces and development pathways were combined into three land-use scenarios according to Table 6.6, which can be described by the following qualitative storylines. It has to be noted that in none of these scenarios a major revision of the current hazard map is expected, which at least for the rockfall hazard is consistent with different future scenarios (Section 7.1).

Table 6.6: Development pathways of major driving forces and their implications for land-use within the three damage potential scenarios in Täsch.

Driver	**Scenario "-"**	**Scenario "o"**	**Scenario "+"**
Tourism	Decrease in Zermatt Decrease in Täsch	Increase in Zermatt Constant in Täsch	Increase in Zermatt Increase in Täsch
Traffic routes	No significant changes of current routes	No significant changes of current routes	Integration of Zermatt and Täsch
Political constraints	Reduction of current building zones	Reduction of current building zones	No changes of current building zones
Natural hazards	No major events	No major events	No major events

Scenario "-" is characterized by a European-wide crisis in the tourist sector (e.g. due to increasing terrorism), which might lead to a decrease of tourism in the international tourist destination of Zermatt. Less jobs and employees lead to empty flats in Zematt, which will be available on the housing market for low prices. As a consequence, employees in Täsch might afford to move back to Zermatt or – given the tense situation on the labour market – even have to leave the region. Consequently, population will decrease and empty flats will increase in Täsch.

Scenario "o" is characterised by an ongoing success of Zermatt as a tourist destination. Due to limited space and the new regulations in the housing market, especially objects built before 2015 will attract investors, who will buy, renovate or rebuild them, causing an increase in prices and forcing local employers with low wages towards other residential places. Since house prices in Täsch are already on quite a high level and the local population tends to retain rather than to sell their parcels of land, it is expected that these employees will move not only to Täsch, but also further north to Randa or St. Niklaus, where a quick connection to Zermatt is still guaranteed. Moderate population growth is expected in Täsch, leading to a higher building density in already developed areas. However, probably within the next 20 to 30 years, current building zones need to be partly reduced according to the RPG.

Scenario "+" is characterized by the realization of the tourist potential and the creation of jobs in Täsch, meaning that the hotel and service sector will grow as well as the number of apartments and holiday flats will increase within the available building zones. An integration of the Zermatt-Matterhorn tourist region is achieved by a direct connection from Täsch to the skiing region of Zermatt. Population growth in Täsch will continue in the order of past decades. By attracting also people with high income, qualitative growth will be possible, eventually leading to a slightly higher portion of single family than multiple family houses within the limiting conditions of the RPG.

The three land-use scenarios were quantified on the basis of observed developments in the building zones of Täsch since their first delineation in the communal zone plan in 1980. Current building zones as well as the building phase of residential houses within these zones are shown in Figure 6.9 (left). Buildings in the core zone of the village (1) and the adjacent village extension zone south of Täschbach (2) were mostly built before 1981 and future development in these zones is limited by the red hazard zone indicating a potential flooding of Täschbach. Major construction activity since 1981 took place in the northern village extension (3) and residential zone (4), where future development will probably be most pronounced. Since 2010, several new buildings were built in these zones and three large building projects are still ongoing (a-c). The northern (5) and parts of the southern chalet zone (6) are not yet developed and are the first zones to be reduced if population growth in Täsch will be limited in the future.

The quantitative estimates of new buildings for the three damage potential scenarios are shown in Figure 6.10 and Table 6.7, and their spatial allocation is shown in Figure 6.9

Figure 6.9: Mapping of the three damage potential scenarios: For the scenario definition, construction activity in existing building zones since 1981 was analysed (left). According to the resulting scenarios, new buildings were randomly placed in the available building zones (right).

(right). In scenario "-", only already built and planned buildings since 2010 are added to the map. In scenario "+", the observed construction activity is linearly extrapolated until 2060, while the percentage of new buildings in each category as well as average numbers of apartments, persons and building volumes in the reference period (1981–2009) are preserved. New buildings were evenly distributed in the available building zones, with exception of the red hazard zone, where construction of new buildings is prohibited. In scenario "o", the mean number of new buildings of scenario "-" and scenario "+" is allocated to existing building

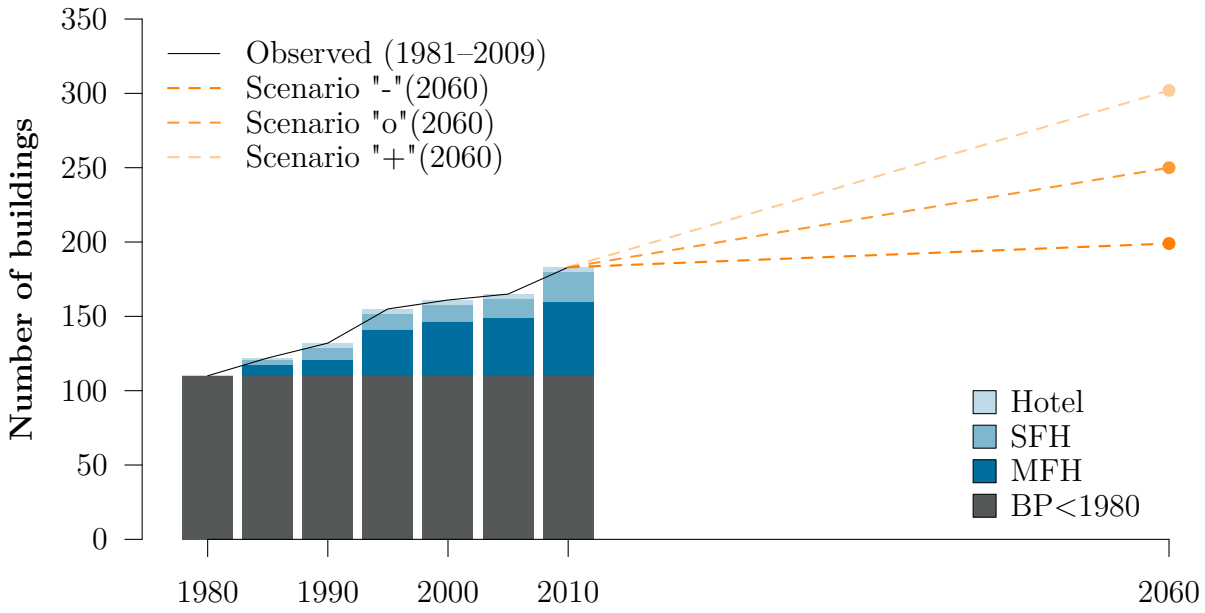

Figure 6.10: Quantification of new buildings in the three damage potential scenarios on the basis of observed construction activity in the reference period (1981–2009): Scenario "-" includes only currently built and planned buildings, scenario "+" corresponds to the trend scenario, and scenario "o" includes the mean number of buildings in scenario "-" and scenario "+". In scenario "o" and "+", the percentage of new buildings in each category is preserved with respect to the reference period.

Table 6.7: Quantification of new buildings in the three damage potential scenarios on the basis of observed construction activity in the reference period (1981–2009) (Figure 6.10).

Times period	**1981–2010**		**2010–2060**	
Scenario		**"-"**	**"o"**	**"+"**
Hotel	+3	+1	+3	+5
	4%	6%	4%	4%
SFH	+20	+2	+18	+33
	27%	13%	27%	27%
MFH	+50	+13	+46	+81
	69%	81%	69%	69%
Total	+ 73	+16	+59	+119
	100%	100%	100%	100%

zones, with exception of the red hazard zone and the northern and southern chalet zones, which are reduced in this scenario. To ensure that the spatial distribution of common new buildings is consistent between the scenarios, they were successively added to the map, meaning that all buildings present in scenario "-" are also included in scenario "o", and all buildings present in scenario "o" are also included in scenario "+".

Observed and anticipated population growth is shown in Figure 6.11 and Table 6.8. The anticipated increase in population basically results from the assumed construction activity and typical occupancy of buildings in the different scenarios. It can be noted that the resulting population in scenario "o" is in good agreement with cantonal projections (FSO 2016*b*). However, for scenario "-", the number of persons in buildings is reduced, corresponding to the emigration of people and the existence of empty flats in Täsch. As employees of predominantly foreign origin, which started to populate Täsch since the early 1990s, are assumed to move to Zermatt or even leave the region in this scenario, the number of persons is reduced according to the percentage of foreigners in 2010 (50.7%), which was evenly subtracted from all buildings in Täsch after adding currently observed and planned buildings to the map. Consequently, population in Täsch is reduced to 668 residents in 2060.

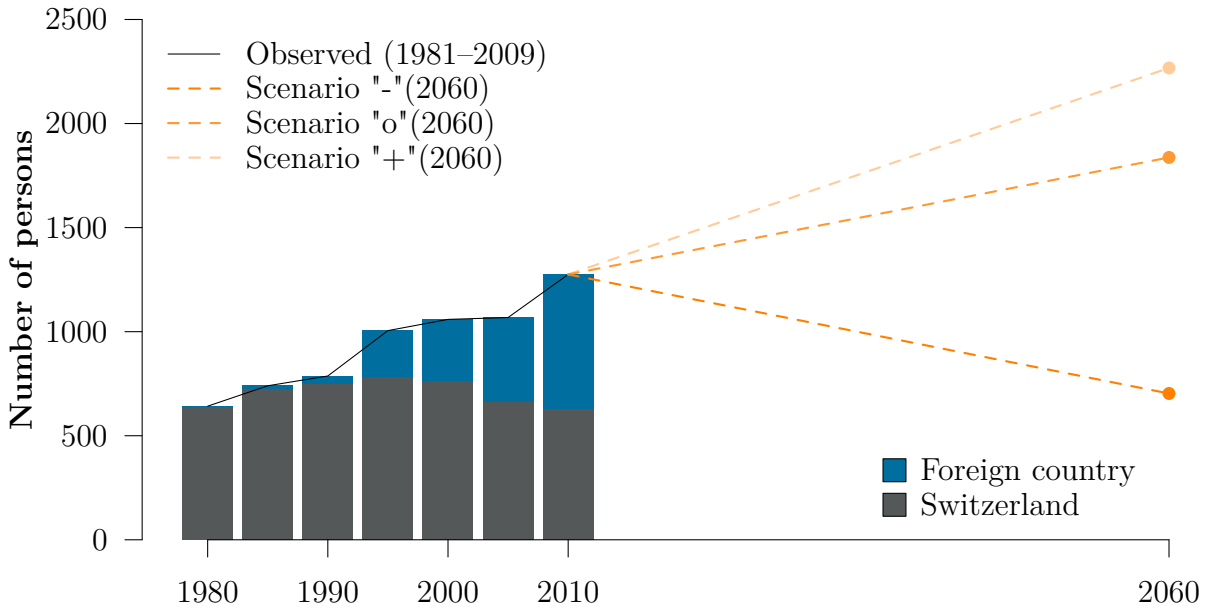

Figure 6.11: Quantification of the population in the three damage potential scenarios on the basis of observed population growth in the reference period (1981–2009): Anticipated population growth in scenario "+" and scenario "o" results from anticipated construction activity and mean number of persons per building category. In scenario "-", the number of persons is reduced according to the percentage of foreigners in 2010.

Table 6.8: Quantification of the population in the three damage potential scenarios on the basis of observed population growth in the reference period (1981–2009) (Figure 6.11).

Time period	**1981–2010**		**2010–2060**	
Scenario		**"-"**	**"o"**	**"+"**
Number of persons	+633	-572	+562	+992

7 Results

In the following, obtained estimates and maps for hazard potential, damage potential and risk are shown for all investigated time periods, namely 1880, 1940, 2010 and 2060. For 2060, results are shown for each of the two hazard potential scenarios (RCP3PD, A1B) and the three damage potential scenarios ("-", "o", "+"), while all combinations of these scenarios are investigated in the risk analysis.

7.1 Hazard potential

Figure 7.1 and Figure 7.2 show the resulting hazard maps for all time periods, which depict the hazard degree at each location according to the Swiss hazard mapping scheme (Section 3.2). The extent of the hazard zones for these periods is shown in Figure 7.3.

The obtained hazard map for the current time period (2010) can be compared to the already existing hazard map in Täsch (Figure 4.2). Thereby, the obtained hazard map is a rather conservative estimate, as the red zone is less pronounced than on the existing hazard map, but general patterns are well reproduced. Furthermore, the extent of the blue zone is very small on the obtained hazard map and the yellow zone is not apparent, which is basically a consequence of the model Rockyfor3D not simulating rock movement at very low energies (<30 kJ) on the investigated slope. Therefore, there is a direct transition from the blue hazard zone to the zone of residual hazard. Although the zone of residual hazard is not shown in the official hazard map, it is interesting to further investigate developments of damage potential (Section 7.2) and risk (Section 7.3) in this zone, particularly because development of infrastructure is not legally prohibited. Thus, damage potential and risk might still increase in this zone, while such developments in the red and blue hazard zones are limited to a certain degree by legal constraints.

Regarding temporal aspects and sensitivity, the hazard maps are not very sensitive to the investigated changes, which can be seen in Figure 7.3, depicting the extent of all hazard zones for all time periods. From 1880 to 1940, changes are only due to increasing rockfall activity and are reflected in a slight increase of the red hazard zone from 100 to 107 ha (+7%). From 1940 to 2010, changes are due to increasing rockfall activity as well as decreasing frequencies below the deflection dams. These effects seem to almost cancel each other out, which is reflected in very similar hazard maps. The slight increase of the red hazard zone from 107 to 108 ha (+1%) is mostly visible at the northern branch of the red hazard zone, which is not influenced by the construction of the deflection dams. Also from 2010 to 2060, estimated future increases in rockfall activity are not significantly influencing the extent of the hazard

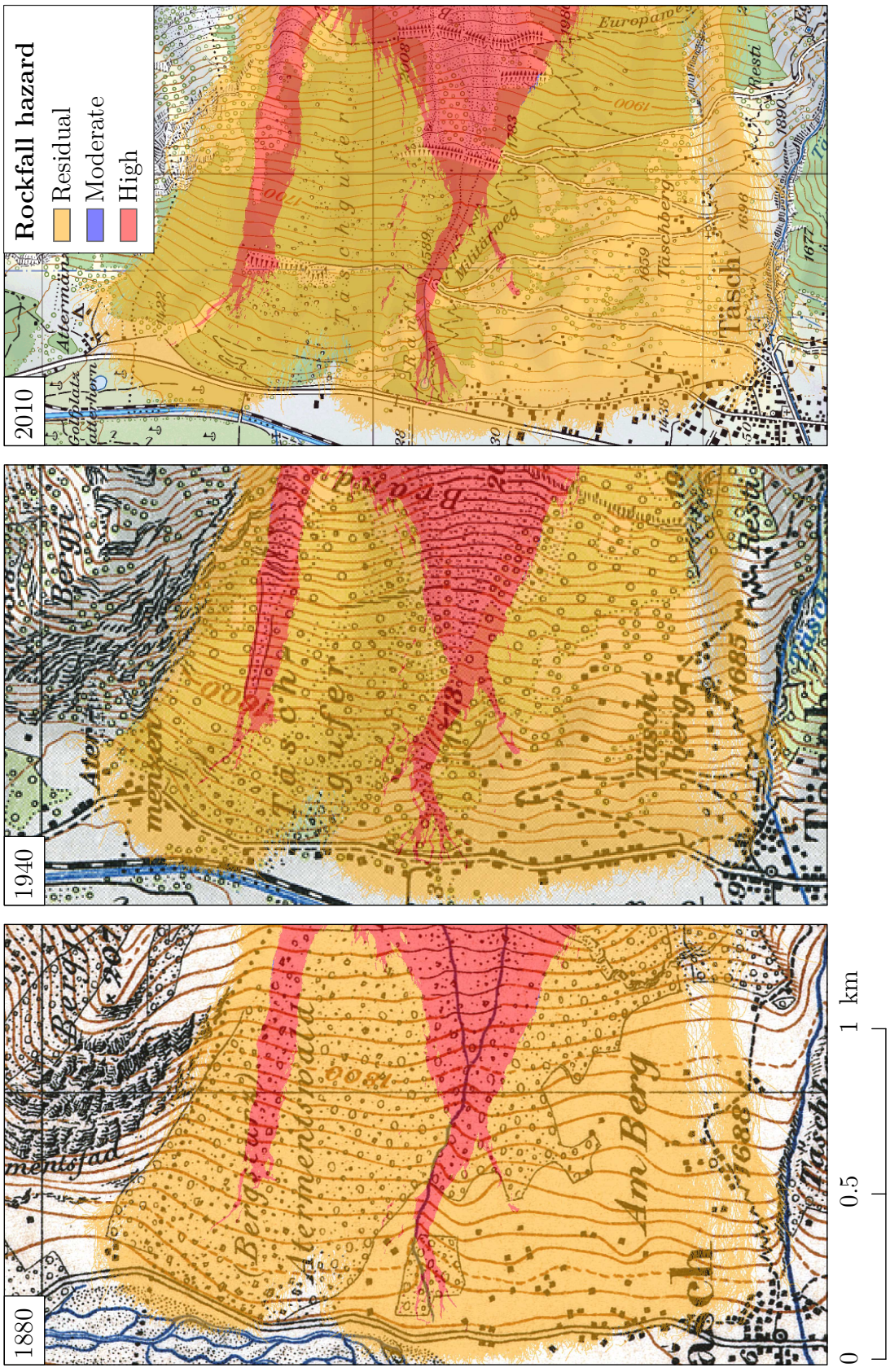

Figure 7.1: Rockfall hazard maps in Täsch for 1880, 1940 and 2010. The hazard maps delineate zones of high, moderate and residual hazard according to the Swiss hazard mapping scheme.

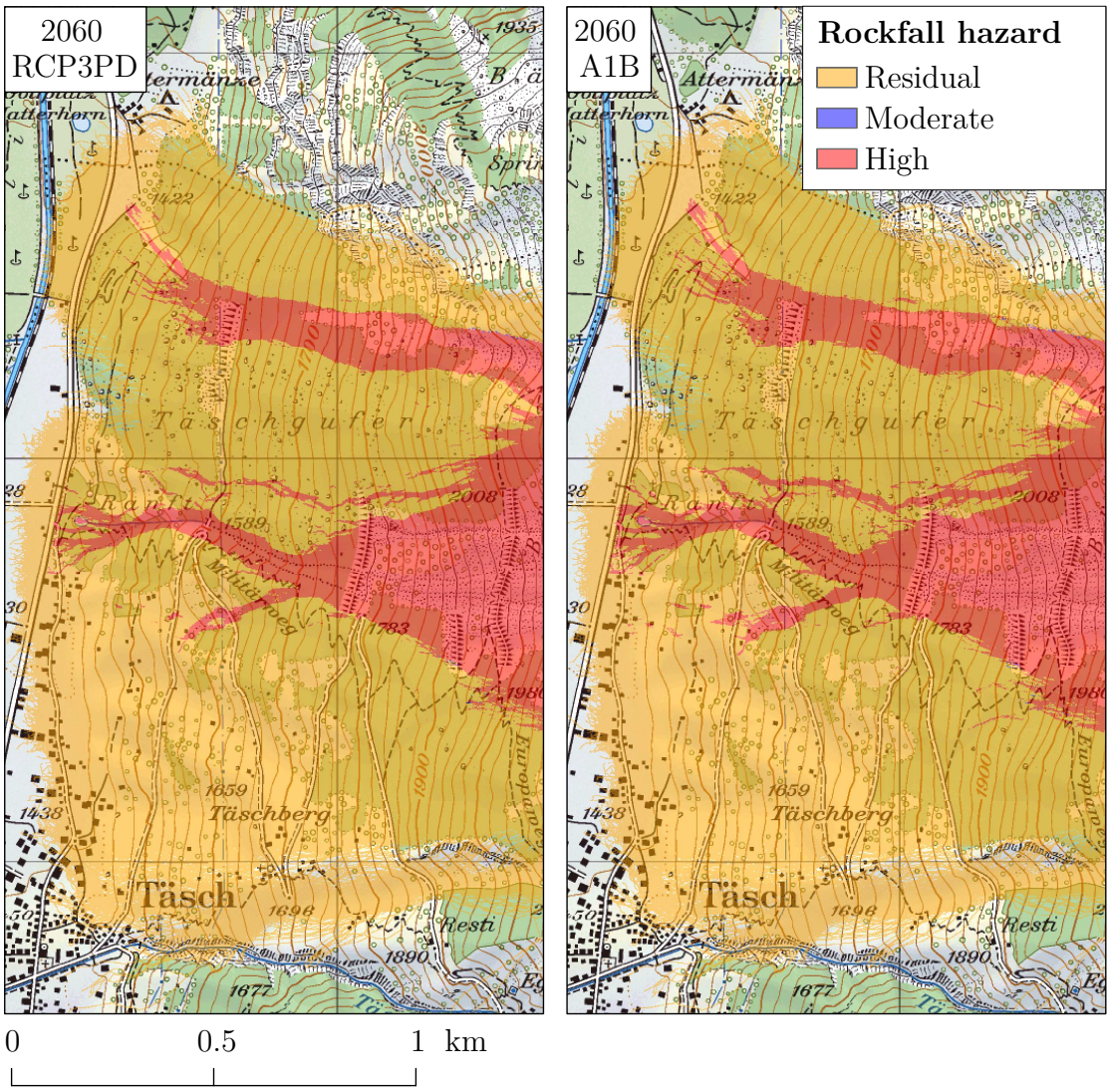

Figure 7.2: Rockfall hazard maps in Täsch for 2060, considering the climate scenarios RCP3PD and A1B. The hazard maps delineate zones of high, moderate and residual hazard according to the Swiss hazard mapping scheme.

zones in both climate scenarios. More precisely, the red hazard zone is estimated to increase to 116 ha (+7%) in scenario RCP3PD and to 122 ha (+13%) in scenario A1B. The total extent of the hazard map is almost the same for all time periods, because it is defined by the run-out of the maximum magnitude, which is assumed to be 20 m^3 for all time periods and is not significantly retained by the deflection dams. Slight deviations in the total extent of the hazard maps between simulations before (1880 and 1940) and after (2010 and 2060) the building of the deflection dams are due to small statistical deviations between the two model runs, mainly in the upper part of the slope. In the next section (Section 7.2), development of damage potential in the delineated hazard zones is investigated.

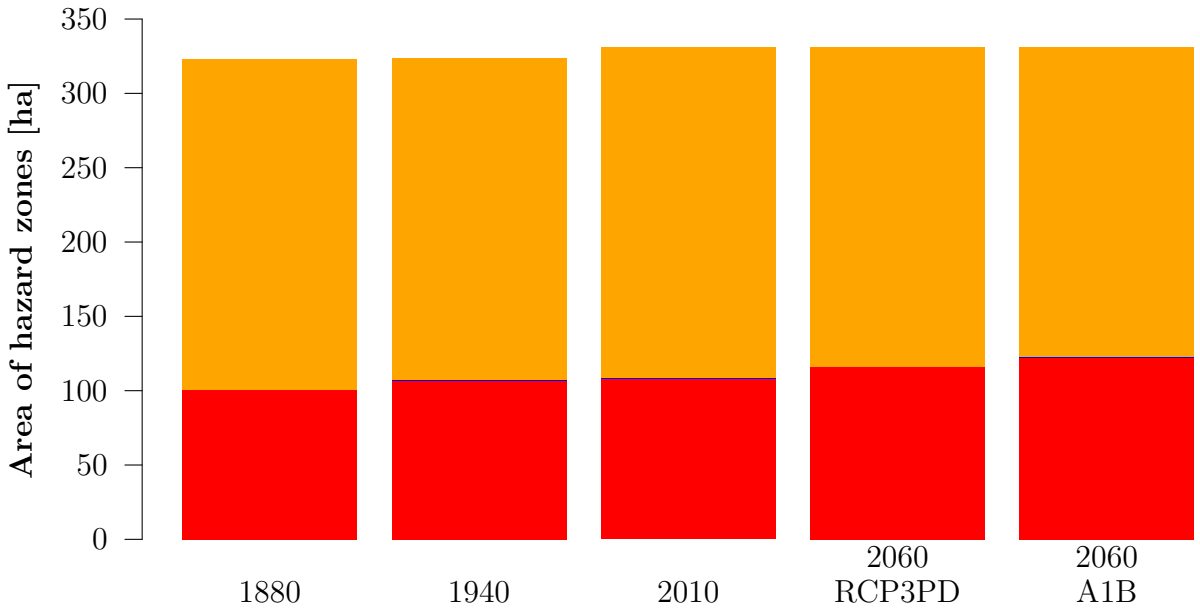

Figure 7.3: Areas of the rockfall hazard zones in Täsch for all time periods. Zones of high (red), moderate (blue) and residual (orange) hazard were determined according to the Swiss hazard mapping scheme.

7.2 Damage potential

Figure 7.4 and Figure 7.5 show the damage potential maps for all time periods. Damage potential thereby describes the expected loss in $CHFm^{-2}a^{-1}$ in case of a high intensity event, as outlined in Section 6.3.3. Figure 7.6 and Figure 7.7 depict the aggregated damage potential within all hazard zones in Mio $CHFa^{-1}$, while it is distinguished between exposed objects and persons as well as different object categories.

In the past, the exposure of infrastructure and people in Täsch was increasing from 1880 to 2010. As can be inferred from Figure 7.4 and Figure 7.6, the main development of the village took place since 1940, probably going along with the success of Zermatt as a tourist destination in the late 20^{th} century. This applies not only to residential buildings to the north and south of the core village, but also to streets, such as the main road built in 1971, and hiking trails, such as the Europaweg built in 1997. In total, damage potential within the hazard zone in the north of the village increased from 6 Mio $CHFa^{-1}$ in 1880 to 9 Mio $CHFa^{-1}$ in 1940 and 138 Mio $CHFa^{-1}$ in 2010. The increase since 1940 is therefore equal to 129 Mio $CHFa^{-1}$ or factor 14. In case of a high intensity event, high damage per area unit is expected from the main road (Figure 7.4), which is only apparent on the most recent map. Being exposed to the rockfall hazard along two segments and over a distance of around 1150 m, it thereby accounts for roughly one third of total damage potential within the hazard zones. Also, residential buildings are a substantial part of damage potential, which almost account for the remaining two thirds of total damage potential within the hazard zones.

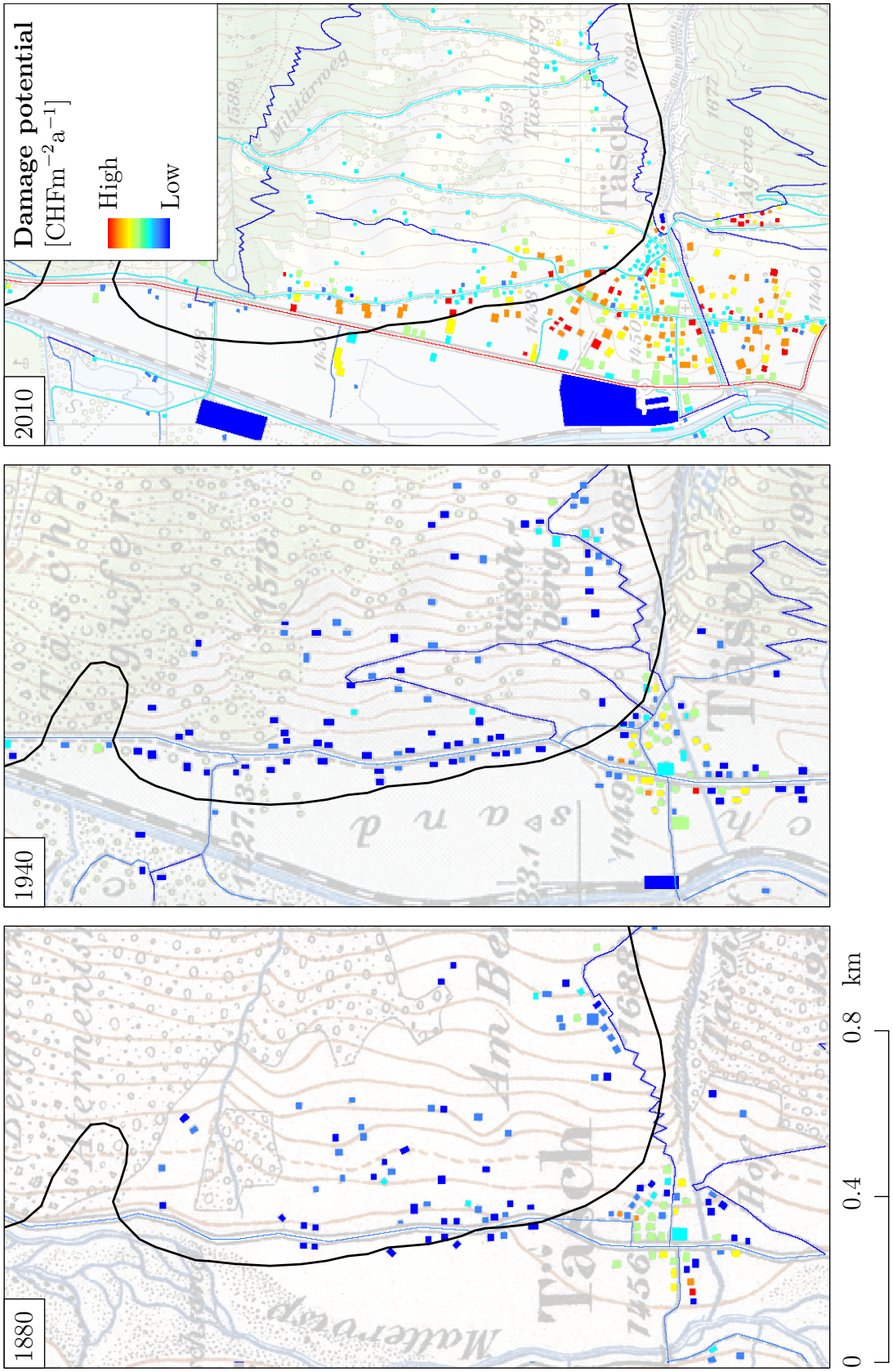

Figure 7.4: Damage potential maps in Täsch for 1880, 1940 and 2010. Damage potential denotes expected losses due to a high intensity impact at each location. The maximum extent of the hazard zone is indicated by a black line.

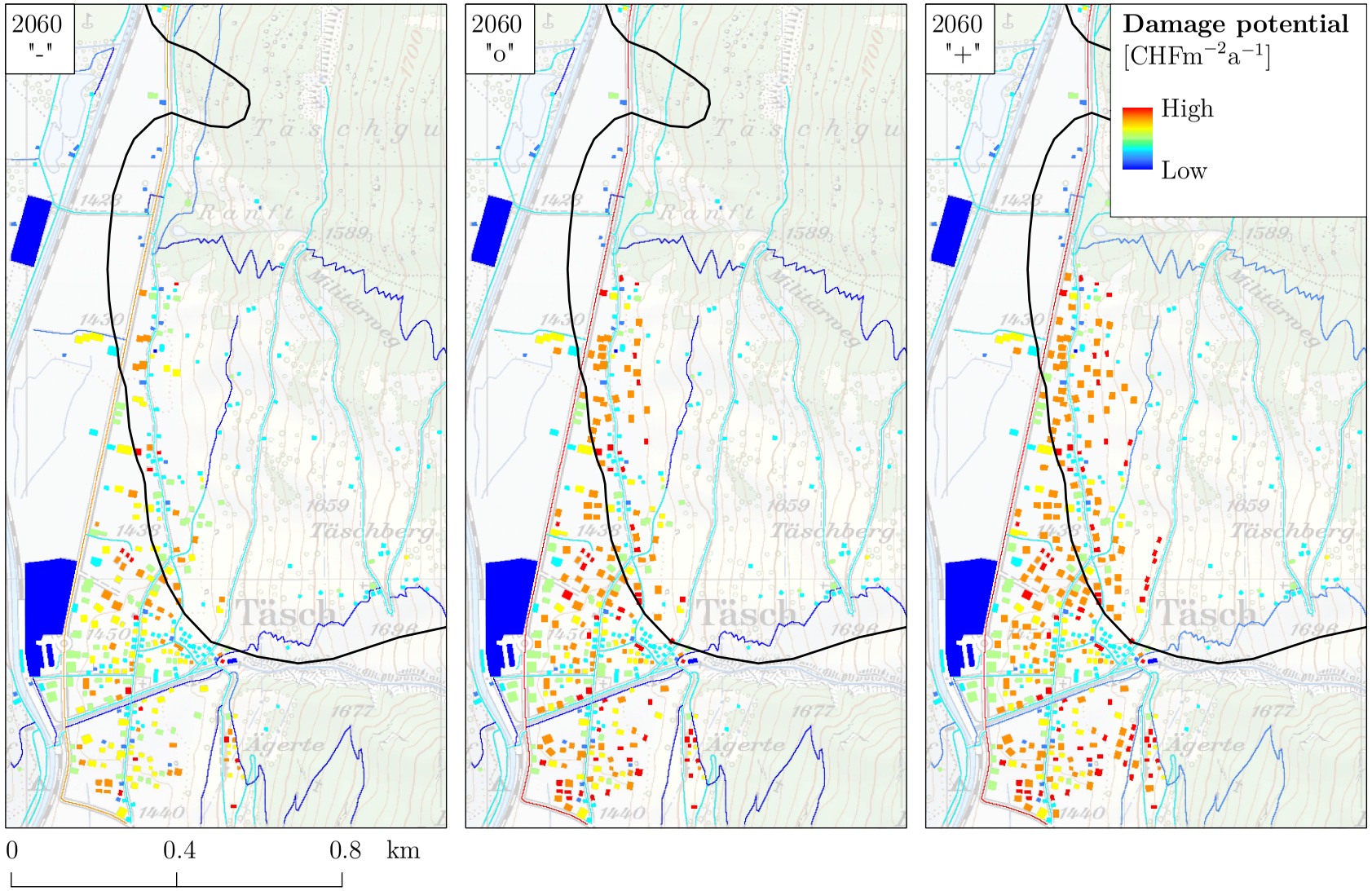

Figure 7.5: Damage potential maps in Täsch for 2060, considering the exposure scenarios "-", "o" and "+". Damage potential denotes expected losses due to a high intensity impact at each location. The maximum extent of the hazard zone is indicated by a black line.

While the building fabric mostly consists of multiple family houses, single family houses are very relevant in terms of damage potential, since the lethality of persons is assumed to be around factor 10 higher according to EconoME. Least damage is expected from smaller roads and hiking trails, such as the Europaweg. However, these trails are frequently built just below the rockfall slope and are thus subject to more frequent events and a higher risk, which is shown in Section 7.3.

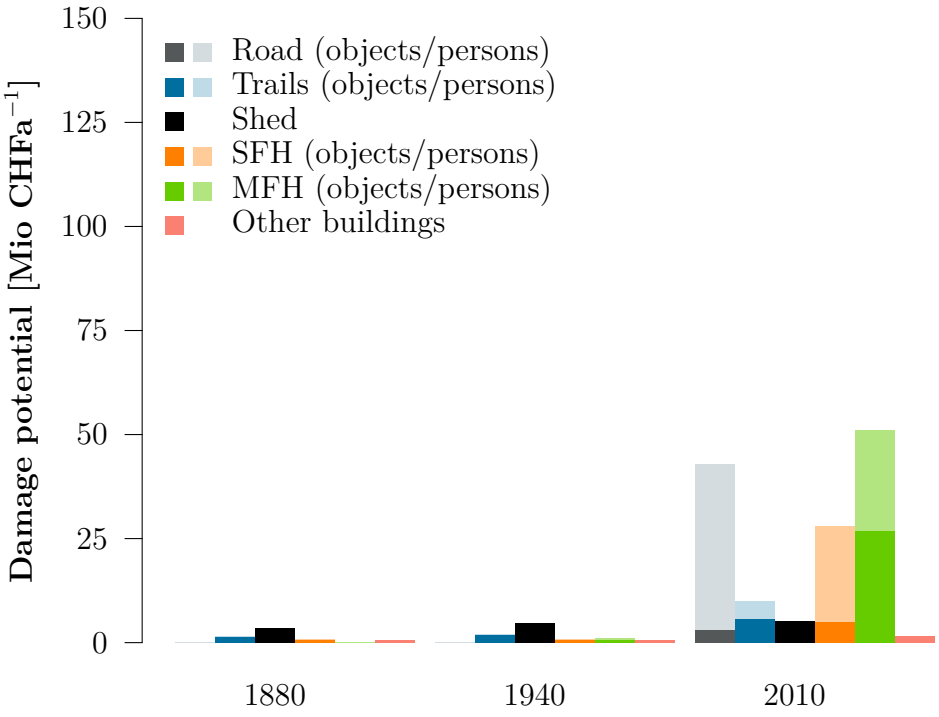

Figure 7.6: Aggregated damage potential within all hazard zones in Täsch for past time periods (1880, 1940, and 2010).

Future development of damage potential is very uncertain and differs considerably between the investigated scenarios (Figure 7.7). In scenario "-", damage potential decreases by 37 Mio CHFa^{-1} or 27% due to decreasing population in residential buildings and decreasing traffic frequencies on roads and hiking trails. In scenario "o" and "+", where further growth of the village is assumed, damage potential increases by 80 Mio CHFa^{-1} (+58%) or 152 Mio CHFa^{-1} (+110%) respectively. This increase is mainly caused by the building of additional residential buildings in the northern building zone of the village, and to a smaller degree by higher traffic frequencies on the cantonal road. As percentages of single and multiple family houses are preserved (Section 6.4.2), it is assumed that more multiple family houses are built in the endangered area for all scenarios. The assumed spatial distribution of new buildings, which is shown in Figure 7.5, is thereby very uncertain and will strongly affect their relevance in terms of risk, which is outlined in the following section (Section 7.3).

Figure 7.7: Aggregated damage potential within all hazard zones in Täsch for 2060, considering the exposure scenarios "-", "o" and "+".

7.3 Risk

In the following section, effects of rockfall risk in Täsch for all investigated time periods (Section 7.3.1) and the relevance of different driving factors between these time periods (Section 7.3.2) are investigated separately.

7.3.1 Effects of risk

Figure 7.8 and Figure 7.9 show the risk maps for all time periods. For reasons of simplicity, future risk maps for 2060 are only shown for the climate scenario A1B. Figure 7.10 and Figure 7.11 depict the aggregated rockfall risk in Täsch for all time periods, while future risk estimates for 2060 are shown for all climate and exposure scenarios separately. As in Section 7.2, it is distinguished between exposed objects and persons as well as different object categories. In general, rockfall risk in Täsch is mainly regarded as residual risk according to the Swiss hazard mapping scheme, as was shown above (Section 7.1).

The effects of rockfall risk in Täsch changed considerably in the past (Figure 7.10). In 1880, predominantly uninhabited sheds were subject to rockfall risk, while developed hiking trails account for roughly one third of total risk in 1940. Until this time, estimated rockfall risk for persons is nearly zero. Although by 2010, risk emerging from some of the exposed sheds is reduced by the effect of the deflection dams, much higher risks emerge from additional

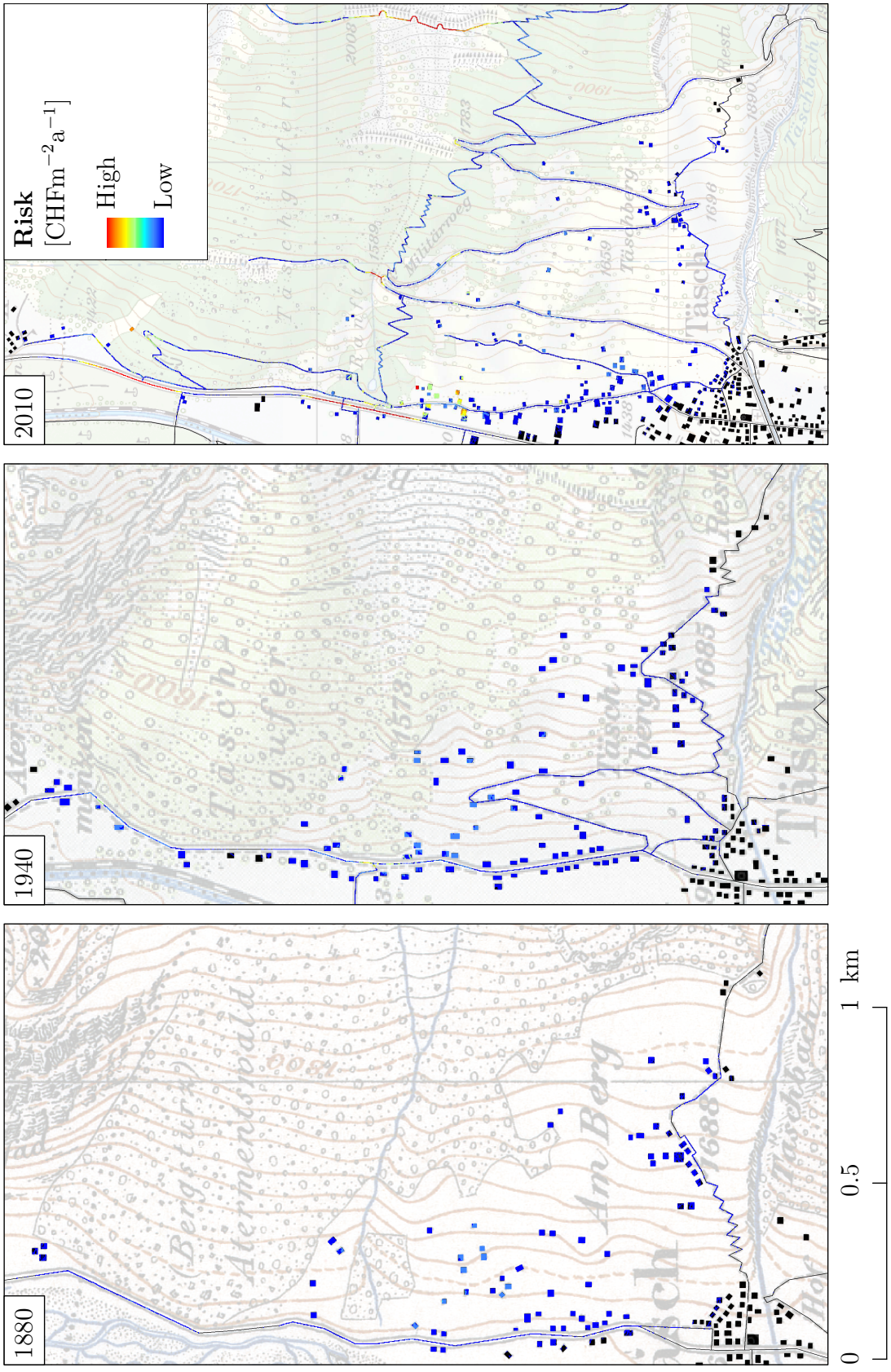

Figure 7.8: Risk maps in Täsch for 1880, 1940 and 2010. Rockfall risk is expressed as mean annual expected losses from rockfall events in the long term.

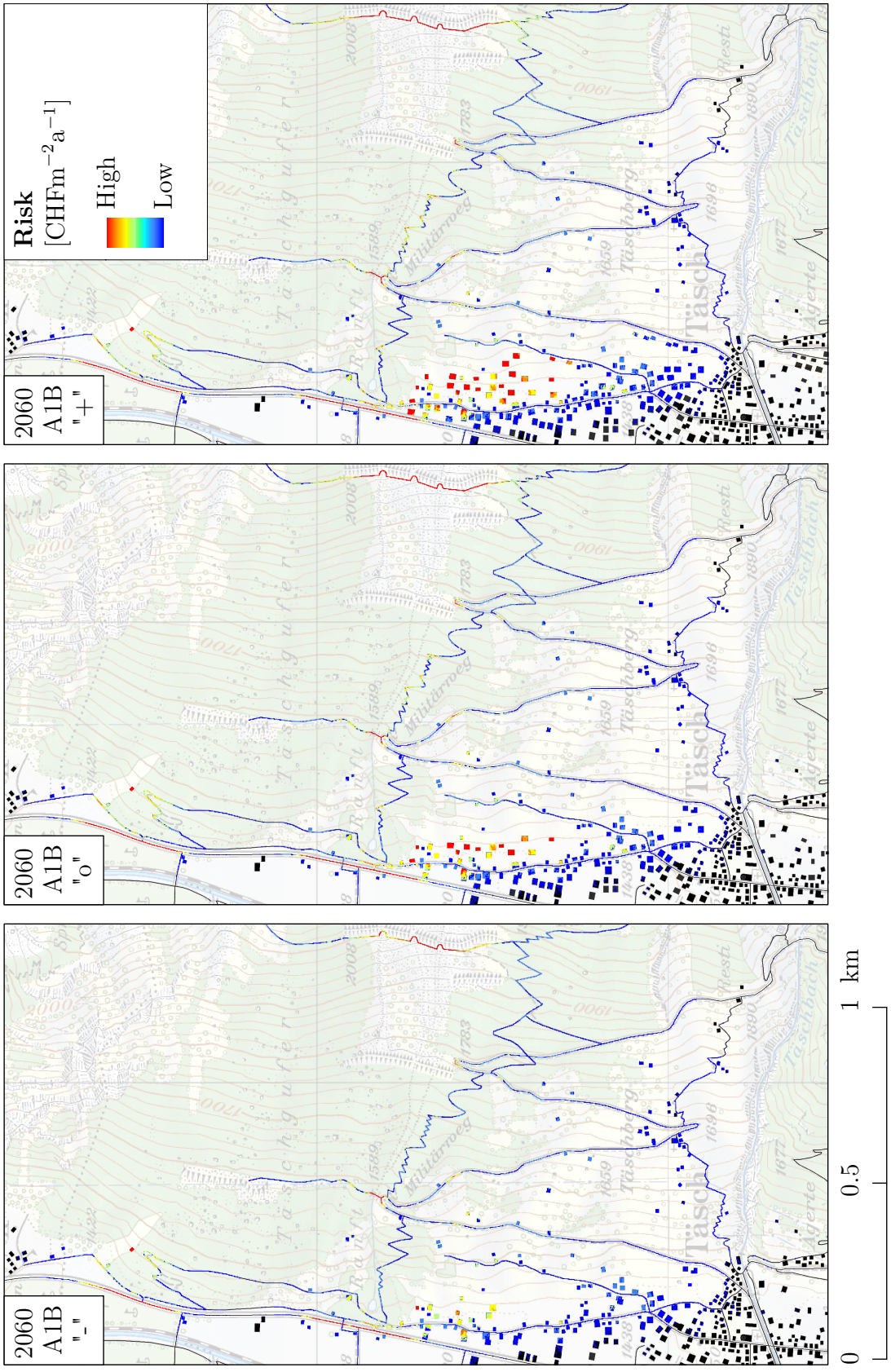

Figure 7.9: Risk maps in Täsch for 2060, considering the climate scenario A1B and the exposure scenarios "-", "o" and "+". Rockfall risk is expressed as mean annual expected losses from rockfall events in the long term.

infrastructure, which was built in northern Täsch until this time. The main increase in risk is observed along roads and hiking trails, hotspots of which are two segments of the main road and the Europaweg (Figure 7.8). Although much more damage is expected from an event at the main road than at the Europaweg, both are equally relevant in terms of risk, accounting for roughly two thirds of total rockfall risk in 2010. The remaining risk is due to buildings, mostly residential houses. Although aggregated damage potential for multiple family houses is higher than for single family houses, the latter are more relevant in terms of risk, which is due to their spatial distribution and further discussed in Section 8.2.

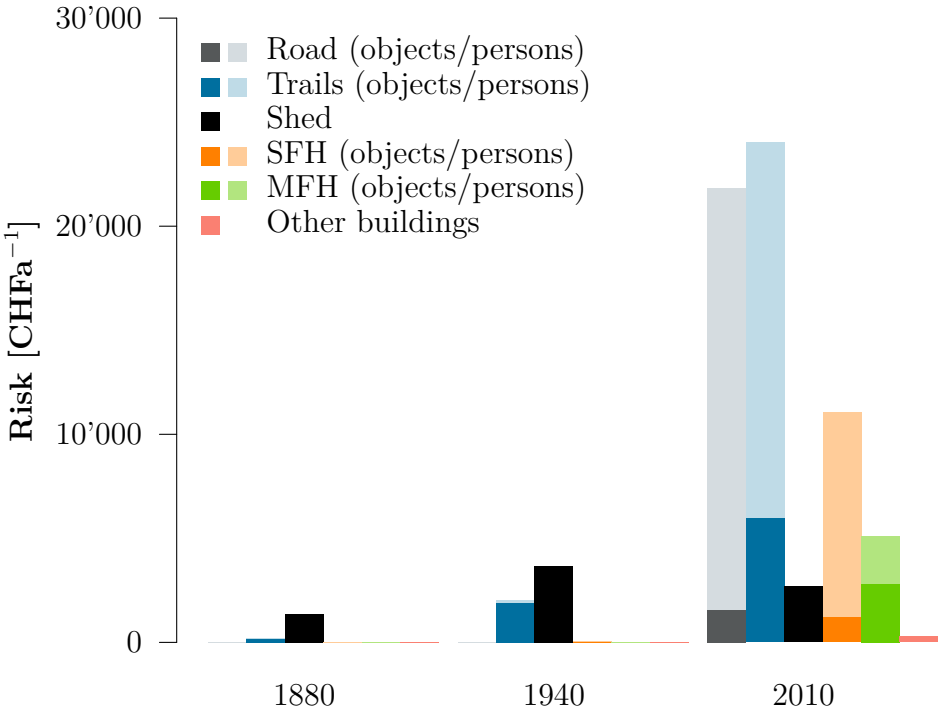

Figure 7.10: Aggregated rockfall risk in Täsch for past time periods (1880, 1940, and 2010).

To investigate future risk, it is most transparent to first consider the effects of changing hazard and damage potential separately with respect to the situation in 2010. Figure 7.11 (top) depicts the effect of increasing hazard potential in both climate scenarios (RCP3PD, A1B). Rockfall risk thereby simply increases proportionally to the assumed increase in rockfall frequencies, since existing infrastructure and people will more frequently be exposed to rockfall events. In the three damage potential scenarios, however, changes in risk are more complex (Figure 7.11 (bottom)). Regarding roads and hiking trails, only risks emerging from exposed persons change, since no further construction is assumed. In scenario "-", such risks are reduced due to emigration, while traffic frequencies and accompanying risk are assumed to increase in scenario "o" and "+" due to increasing population. Regarding buildings, risks decrease in scenario "-" due to emigration, while construction of new buildings in endangered areas causes risks to increase in the scenarios "o" and "+". While in scenario "o", risk from single family houses is still higher than for multiple family houses, the latter is dominant in

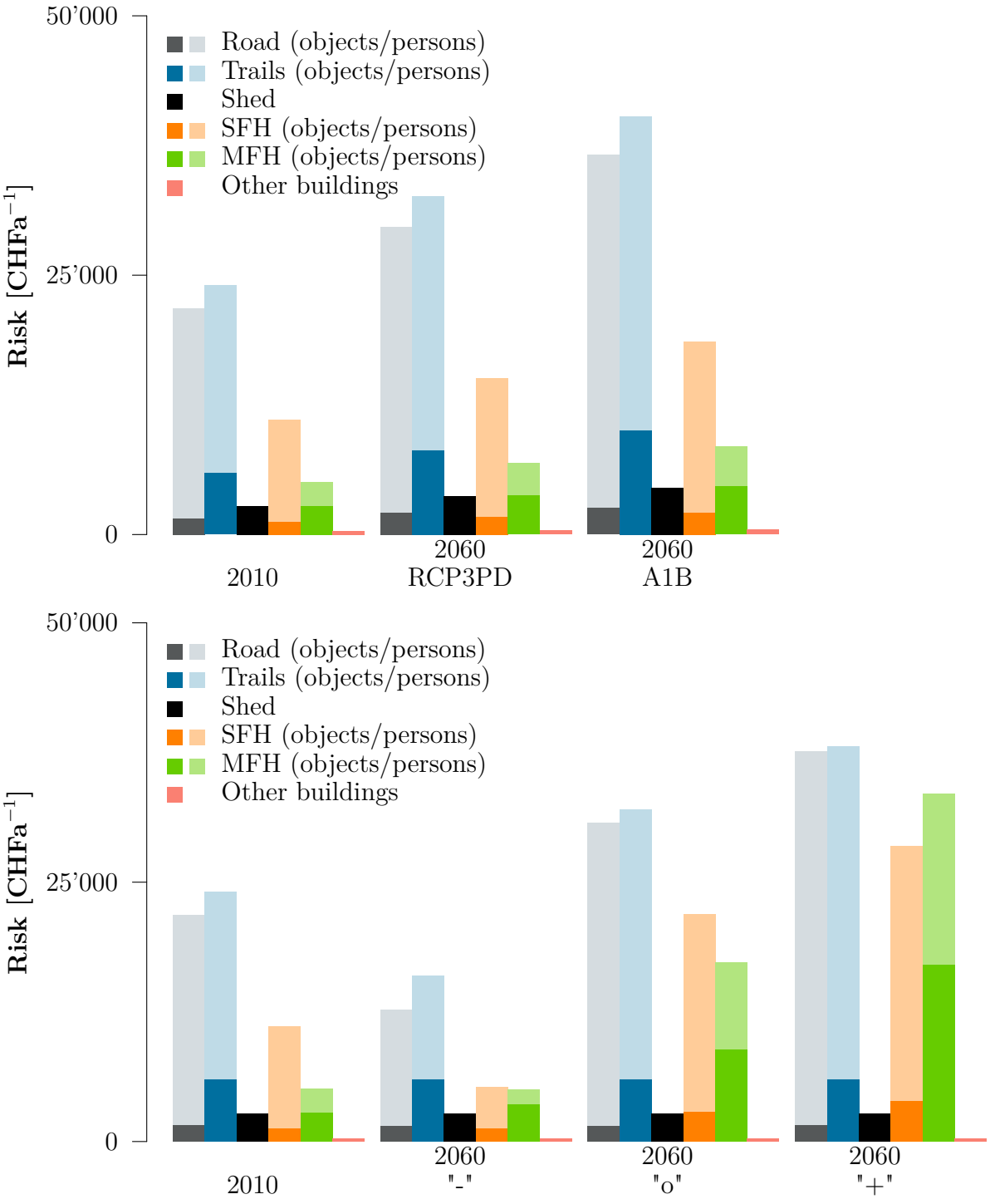

Figure 7.11: Aggregated rockfall risk in Täsch for 2060, considering the climate scenarios (RCP3PD, A1B) and the exposure scenarios ("-", "o", "+") separately with regard to the situation in 2010. When combining different scenarios, the total effect on risk is different than the sum of the individual effects.

scenario "+". Since the percentage of each object category is preserved in both scenarios, this again highlights the importance of where the new buildings are built. It can further be noted that in scenario "+", the relevance of buildings and streets in terms of risk is almost the same, the latter gaining of relative importance with increasing construction activity, which is also clearly visible in Figure 7.9. When combining several scenarios, effects will be more complex than discussed above. For example, when increasing both rockfall frequency and construction activity, more frequent rockfall events will not only affect already existing, but also new buildings. Such effects are in the following referred to as interaction effects and in more detail examined in the next section (Section 7.3.2).

7.3.2 Drivers of risk

Figure 7.12 and Table 7.1 investigate drivers of rockfall risk in Täsch, which can hardly be assessed from previous results, because several parameters (e.g. climate, exposition, protection measures) differ between the different time periods. To isolate individual effects of these parameters, they are changed separately in the analysis and the resulting change in total risk is evaluated with respect to 2010. As mentioned above, the effect of changing several parameters at once is different to the summed individual effects due to interaction effects.

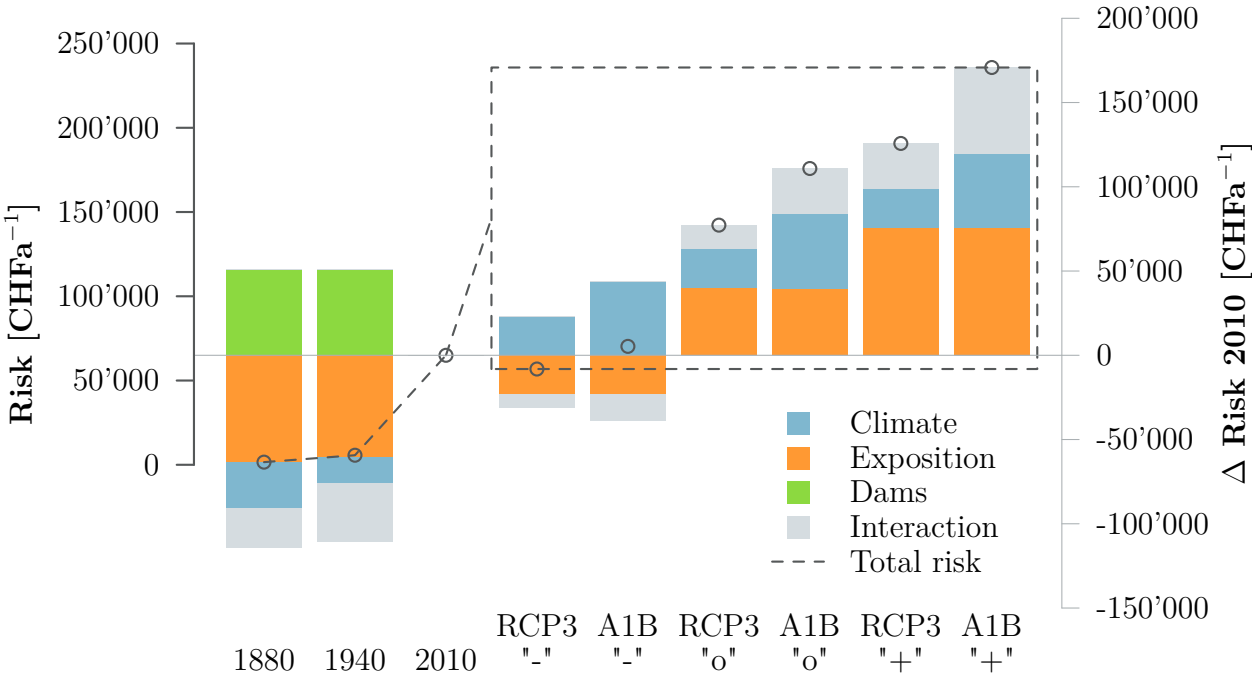

Figure 7.12: Drivers of rockfall risk in Täsch between 1880 and 2060: Total annual rockfall risk for all time periods (left axis) and the difference to 2010 (right axis) are given, while different causes of these changes (i.e. climate, exposition, deflection dams, and interactions) are distinguished. For 2060, all combinations of climate and exposure scenarios are investigated.

Table 7.1: Drivers of rockfall risk in Täsch between 1880 and 2060: Total annual rockfall risk is given in 1000 CHFa^{-1} for all time periods. Furthermore, the absolute and relative difference to 2010 and the the contribution of different drivers to these differences is given (Figure 7.12).

Time period	**1880**	**1940**	**2010**	**2060**					
Scenario				**RCP3 "-"**	**A1B "-"**	**RCP3 "o"**	**A1B "o"**	**RCP3 "+"**	**A1B "+"**
Total risk	2	6	65	57	70	142	176	191	236
Δ Risk 2010	-63	-59	-	-8	+5	+77	+111	+126	+171
	-98%	-91%	-	-13%	+8%	+119%	+171%	+193%	+263%
Climate	-27	-15	-	+23	+44	+23	+44	+23	+44
	-42%	-23%	-	+36%	+68%	+36%	+68%	+36%	+68%
Exposition	-63	-61	-	-23	-23	+40	+40	+76	+76
	-97%	-94%	-	-36%	-36%	+61%	+61%	+116%	+116%
Dams	+51	+51	-	-	-	-	-	-	-
	+79%	+79%	-	-	-	-	-	-	-
Interaction	-24	-34	-	-8	-16	+14	+27	+27	+51
	-37%	-52%	-	-13%	-25%	+23%	42%	+42%	+79%

In the past (1880 and 1940), rockfall risk in Täsch was almost not existent. Compared to 2010, rockfall risk was reduced mainly due to a reduced exposition of infrastructure and people. As described in Section 7.2, almost no residential buildings and only smaller trails were present in the northern part of the village. To a smaller extent, rockfall risk was reduced due to a less frequent rockfall activity, which is related in this study to lower mean annual summer temperatures at these times. When considering recent climate and exposition, the protective effect of the deflection dams is estimated to be roughly 51'000 CHFa^{-1}. Since these dams were not yet present in 1880 and 1940, risk would theoretically have been increased by this amount at these times, assuming everything else to be constant. However, since also much less infrastructure and people would have been protected by the deflection dams in the past, there are large negative interaction effects and almost no rockfall risk in these time periods. This highlights the importance of considering temporal aspects when looking at the benefit of protection measures. While the protective effect of the dams is estimated to be 51'000 CHFa^{-1} in the current time period, it would have been much lower in the past, and will probably be much higher in the future, which is discussed at the end of this section.

Looking at possible rockfall risk developments in the future, all combinations of the two hazard potential scenarios (RCP3PD, A1B) and the three damage potential scenarios ("-","o", "+") are investigated. As seen before, increasing rockfall activity will increase already present risks, while increasing building activities will produce new risks, and the combined effect will be larger due to interaction effects. While in the past, exposition was the dominant factor of

risk reduction, this picture is not so clear any more in the future. More precisely, the climate effect is estimated to be about the same order of magnitude in the future and may even be dominant in certain scenario combinations. The differences in risk estimates, reflecting aleatory uncertainties, are thereby lower between different global emission scenarios than between different local socio-economic scenarios, the latter of which can include population growth as well as a reduction in population. Of course, uncertainties within each climate scenario are very high, in particular resulting from the uncertain relation of climate and rockfall activity (Section 6.4.1), but are not assessed in this study in terms of risk. Finally, it is interesting to look at the interaction effects, which are increasing with increasing individual effects. This implies, that changes in risk due to different factors cannot be estimated by looking at each factor separately. In a scenario combination of highest temperature increases (A1B) and highest construction activity ("+"), interaction effects can even be higher than the individual climate effect, the explanation of which is the following: Only due to warming and more frequent rockfall events, rockfall risk would increase in this case by roughly 44'000 $CHFa^{-1}$ (+68%) due to a higher rockfall frequency at already existing infrastructure and people. However, going along with high construction activity, more frequent events will also affect new buildings, which more than doubles the climate effect.

To conclude this section, the effect of protection measures, namely the deflection dams and the protection forest, is assessed in more detail. Therefore, risk for the current time period has been calculated with and without each protection measure, and the risk reduction is plotted for each scenario or rock volume range. To make the effect comparable among the different scenarios, risk reduction had to be normalized by the volume range of each scenario. Figure 7.13 shows that both protection measures effectively reduce risk for volumes smaller than around 4 m^3. Since these volumes do not reach very far, predominantly hiking trails in the upper part of the rockfall slope are protected by these measures. As mentioned before, the protective effect of the deflection dams is estimated to be roughly 51'000 $CHFa^{-1}$, while the protective effect of the protection forest is estimated to be more than three times higher or 178'000 $CHFa^{-1}$. Covering an area of 142 ha, this is equal to a protective effect of 1250 $CHFha^{-1}a^{-1}$. As mentioned above and illustrated in Table 7.2, the absolute protective effect of both measures changes considerably over time, as more or less infrastructure and people are exposed in different time periods. Also the efficiency of both measures, given in terms of their total relative risk reduction, changes slightly between these periods, which is due to the changing spatial distribution of exposed infrastructure and people to be protected.

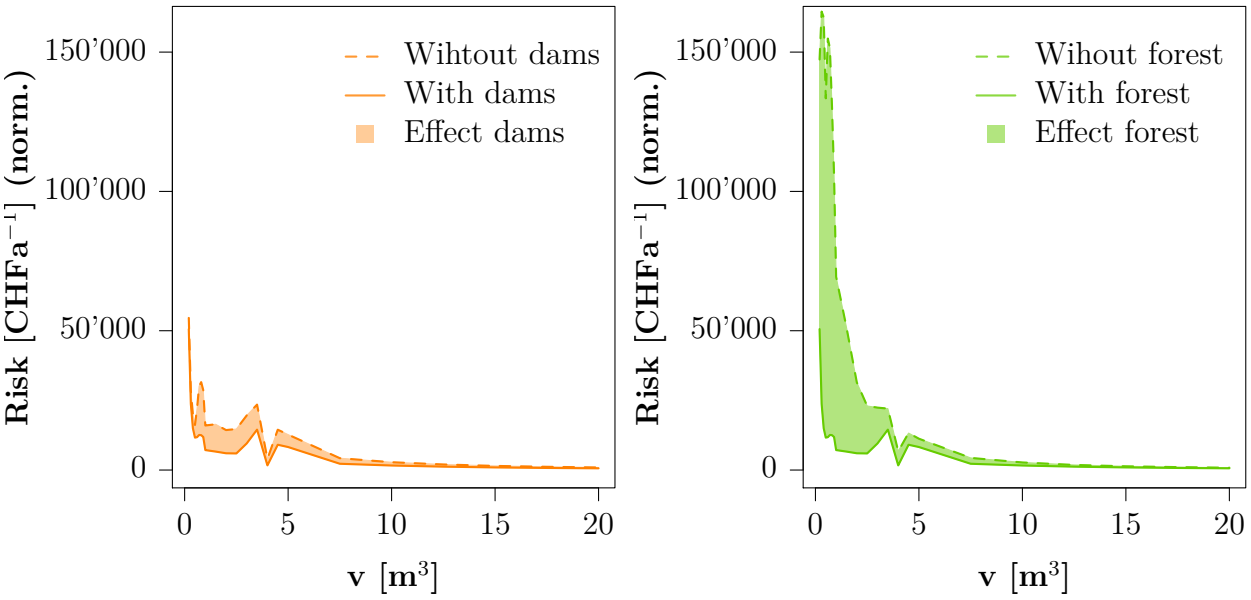

Figure 7.13: The effect of protection measures in Täsch 2010: The recent protective effects of the deflection dams and the protection forest have been calculated in each scenario by comparing annual rockfall risk with and without each measure. To make the effects comparable among the different scenarios, risk reduction had to be normalized by the volume range of each scenario.

Table 7.2: The effects of protection measures in Täsch 1880–2060: Absolute risk reduction in CHFa^{-1} is calculated by comparing total annual rockfall risk with and without each measure for all time periods. Relative risk reduction in % is the risk reduction with respect to the state without the pretection measure.

Time period	**1880**	**1940**	**2010**	**2060**		
Scenario				**"-"**	**"o"**	**"+"**
Dams	1'000	2'000	51'000	55'000	130'000	170'000
	42%	42%	44%	44%	42%	42%
Forest	4'000	11'000	178'000	201'000	522'000	747'000
	81%	78%	73%	74%	75%	76%

8 Discussion

The main purpose of this study was to assess long-term changes (1880–2060) in rockfall hazard and risk at Täschgufer and to create hazard and risk maps for distinct time periods, depicting spatial patterns of these changes. In the following, the most important results of this study are discussed with respect to each of the four research questions, and compared to literature. Thereby, the methodologies and results are discussed for past (Sections 8.1 and 8.2) and future risk development (Sections 8.3 and 8.4).

8.1 Methodology: Past risk developments

Research question 1: How can information from different sources (e.g. field observations, event reports, dendrochronological and socio-economic data, statistical and process-based models) be combined within a consistent, transparent methodology to assess developments of hazard and risk for distinct time periods in the past (1880, 1940 and 2010)?

The presented approach to assess the development of hazard and risk in the past is process-oriented, meaning that it aims to quantify these aspects based on physical and empirical relations. Much more frequently, however, a statistical approach of damage statistics normalization is applied in literature for the same purpose. In the following, these two approaches are compared to each other and general strengths and weaknesses of both are discussed. Then, more specific assumptions and simplifications of the presented methodology are discussed and a final note on the assessment of uncertainties is made.

The presented, process-oriented approach, as for example also applied by Fuchs et al. (2004), aims to quantify hazard potential and damage potential and calculate the resulting risk for distinct time periods in the past. The influence of different factors on the developments of hazard and risk can then systematically be assessed by changing certain variables while holding others constant. To characterise the system, information about past hazard potential, such as rockfall frequencies, and past damage potential, such as exposure of infrastructure and people, is essential. Data on actually observed damages are not explicitly required, since theoretically expected damages are calculated according to physical and empirical formulas, inherent for example in process-oriented models or empirically derived vulnerability functions.

A strength of this process-oriented approach is the spatially explicit characterization of the whole system, including hazard potential, damage potential and the relations between them.

Thereby, a very detailed picture can be given at local scale, including the mapping of individual components, which can facilitate the interpretation of results (Section 8.2). With relatively few additional information and assumptions, it is possible to assess developments of hazard and risk over time scales of decades to centuries. For this purpose, dendrochronological records proved to be valuable in this study, because they provide information on past rockfall activity without being subject to a reporting bias inherent in many alternative sources (Huggel et al. 2015, 2012). This information could directly be used to adjust hazard potential in past time periods, namely MCF distributions and process-oriented modeling. Similarly, historical maps depicting the past exposure of infrastructure could be used to adjust damage potential for past time periods. Having characterized the whole system for different time periods, the influence of any individual component on theoretically expected losses can systematically be assessed, and interaction effects can be quantified. A general limitation of this approach lies in its limited application over larger spatial scales. Especially hazard potential might be difficult to estimate for larger spatial scales, since process-oriented modeling requires detailed and local calibration of the model parameters, and the acquisition of dendrochronological data is time-consuming (Trappmann & Stoffel 2013). The estimation of damage potential on the basis of recent data and historical maps, however, could probably be applied over larger spatial scales with the presented approach.

An alternative, rather statistical approach, which is widely used in literature to assess the development of hazard and risk in the past, is the normalization of available damage statistics (Barthel & Neumayer 2012, Bouwer 2011, Mechler & Bouwer 2015). The idea is to investigate a time series of observed damage records and normalize these records by observed changes in damage potential to eventually reveal changes in hazard potential in the remaining time series. To apply this approach, observations of actual damage records in the study area, such as total economic or injured losses, as well as variables which depict changes in damage potential, typically the price level, population and wealth per capita, are of importance. However, modeling of physical processes and information about past hazard potential is not explicitly required, since changes in hazard potential are thought to be depicted by the normalized time series (Barthel & Neumayer 2012, Bouwer 2011).

A strength of this statistical approach is its possible application on regional to global scales, since information about past damage from natural disasters is more extensive on these scales. Furthermore, since only limited process understanding and modeling is required, multiple processes or groups of processes, such as several climate related hazards, can be studied at once (Barthel & Neumayer 2012, Bouwer 2011). Weaknesses of this approach are manifold. Regarding the input data, damage records of homogeneous quality are often not available over time scales longer than a few decades (i.e. 20–30 years), which makes it statistically difficult to detect systematic changes in hazard potential and eventually relate them to climate change (Bouwer 2011). The completeness of such records is also a critical issue, since disasters are usually only captured in the respective databases in case they had a considerable influence on society, and damages from smaller disasters in earlier time periods are typically underrated (Huggel et al. 2012). Furthermore, the variables used for normalization are of-

ten not directly measurable and have to be represented by proxies. For example, wealth per capita is often represented by GDP per capita and thereby typically underestimated (Barthel & Neumayer 2012). After normalization, the remaining time series is difficult to interpret, since it may include effects that were not accounted for in normalization, such as changes in protection measures and vulnerabilities, which might mask a potential climate signal in the remaining time series (Bouwer 2011, Mechler & Bouwer 2015). Finally, the approach can only in a very limited way reveal or control for spatial patterns, since damage statistics are often aggregated over larger spatial units, such as municipalities or countries. For example, it cannot be judged by such approaches, whether changes in normalized damages result from changes in the frequency or intensity of a hazardous process, or simply from a change of the spatial pattern of its occurrence (Neumayer & Barthel 2011).

To summarize, the presented methodology complements the much wider used normalization approach, being especially suitable for smaller spatial scales, longer temporal scales, and a specific process at investigation. Since a rather theoretical value of expected loss is calculated based on physical and empirical relations, any variables introduced in the system can be controlled for. Especially the effects of changing protection measures and changing vulnerabilities can be evaluated, which are difficult to control for in normalization approaches. Furthermore, mapping of individual components at fine spatial resolution allows for the interpretation of changing spatial patterns. However, resulting risk estimates are relying on many assumptions and represent hypothetical expected losses rather than actual observed losses, statistics of which may either be lacking or difficult to interpret at these small scales. For aggregated spatial units at larger spatial scales, however, damage statistics might be available and can be investigated with normalization approaches. Such statistical approaches overcome the need of modeling physical processes, which is difficult at these larger scales, but suffer from limited data availability and quality as well as a limited ability to control for protection measures, vulnerabilities and spatial patterns.

The presented process-based methodology to quantify rockfall hazard and risk relies on several assumptions and simplifications, the most critical of which are discussed in the following. Regarding the assessment of hazard potential, the estimation of a MCF distribution is fundamental and can be based on different data and statistical methods. In this study, the estimated MCF distribution represents observed rockfall deposits on a deflection dam. As these deposits are located around 1000 m from the cliff, they are regarded as a suitable basis to estimate rockfall magnitudes and frequencies for the risk analysis, because they probably have already been subject to a certain degree of fragmentation. Rockfall fragmentation leads to a higher number but smaller volume of individual blocks, which in turn increases their impact probability but reduces their kinetic energy and run-out distance at the valley floor. Since rockfall models are currently not able to account for the fragmentation process, model results based on initial rock masses will underestimate impact probability and overestimate the rockfall kinetic energy and run-out (Ruiz-Carulla et al. 2015). To estimate the parameter b of the MCF distribuition, the linear regression method was applied. Alternatively, the maximum likelihood estimator method is proposed in literature, which however results

in similar estimates (Dussauge-Peisser et al. 2003, Ruiz-Carulla et al. 2015). The estimated parameter b of 1.085 is rather high compared to other studies (0.4–1) (Dussauge-Peisser et al. 2002), but is thought to be the best estimate for the specific geological setting (e.g. lithology, geological structure) in the study area. The estimated parameter a is difficult to compare with other studies, since it depends on both the area extent and the overall susceptibility of the cliff (Guerin et al. 2014), the former of which had not been estimated. However, the very high agreement between two independent estimation procedures based on either observed rockfall deposits or dendrochronological data gives high confidence in the obtained value. A somewhat arbitrary assumption might be the upper limit of expected rockfall magnitudes, which was set to 20 m^3 according to the largest observed historical record at the valley floor. As confirmed from a geological expert, this estimate is reasonable although larger magnitudes cannot be excluded entirely. The extrapolation of the MCF distribution to larger volumes was regarded as critical due to the rather short observation period of 19 years and possible cutoff effects (Hergarten 2012, 2004, 2003). Also, results show that rockfall risk at the study site is driven by frequent and small rather than rare and large events. When applying the MCF distribution for past time periods, the range of expected magnitudes was not changed, mainly because such changes cannot be inferred from dendrochronological data. Regarding the assessment of damage potential, the consistent methodology of EconoME (Bründl et al. 2015) could be applied in a raster-based approach. When estimating damage potential for past time periods, only changes in exposure could be inferred from historical maps, namely the number and location of buildings and streets. Other parameters such as building types, building volumes and prices, occupancy of residential buildings and vulnerabilities to physical impact are assumed to be constant, which is of course a major simplification. Regarding the calculation of risk, it was also followed the transparent methodology of EconoME. Thereby, like in most risk analyses, only direct physical damage from single falling blocks is considered (Bründl et al. 2015). Other damage patterns, such as blockage of a road from multiple rock fragments, are not considered but might be very relevant depending on the specific situation (Dorren & Wehrli 2012). Also, indirect economic losses resulting for example from a disruption of economic or tourist activity due to such road blockages are not considered.

As follows from the above considerations, the presented risk analysis relies on many assumptions and some major simplifications and thus the resulting monetary risk estimates are highly uncertain (Straub & Schubert 2008). Also, such estimates are difficult to validate, because they represent average values of expected losses in the long term and data on observed losses might be limited, especially at local scale. However, when looking at the resulting risk estimate as a rather theoretical value, its sensitivity to changes of different factors can transparently be assessed with the presented methodology. Thereby, the general aim of the sensitivity analysis is to identify important drivers of the system, to compare different states of the system and to estimate the possible spectrum of future developments rather than to give accurate predictions for distinct time periods.

8.2 Results: Past risk developments

Research question 2: How and how strong are rockfall hazard and risk in the study area affected by different factors such as climate change, building of deflection dams, protection forest and changing construction activity?

Developments of past rockfall risk in the study area are mainly driven by increasing exposure of infrastructure and people in the second half of the 20th century, while increasing rockfall activity in the 1940s and especially the last 30 years is thought to have had a minor influence. These developments are in more detail described in the following and compared to other findings on local, regional and global scale.

Past developments of rockfall hazard and risk in Täsch were assessed for time periods around 1880, 1940 and 2010. While estimated rockfall risk was yet very low in 1880 and 1940, it increased by one order of magnitude until 2010, mainly because of settlement development in the northern part of the village. This part of the village is mostly affected by residual rockfall risk as defined by Swiss Federal Guidelines, but can nevertheless be reached by larger boulders from Täschgufer, which was demonstrated by a very recent event in 2013. Until 1940, the only relevant infrastructure in this area were few uninhabited sheds and some smaller trails. The construction of residential buildings in this area until 2010 can explain roughly one third of total risk increase, while the other two thirds are equally explained by the construction of the main road (1971) and the Europaweg (1997), which is also the reason why risks from exposed persons are clearly the major concern in 2010. The amount that an increase in damage potential will lead to an increase in risk is thereby very much dependent on spatial patterns. For example, the main road crossing the zone of residual hazard is much more frequently travelled by people than the Europaweg, but the latter is crossing Täschgufer in the zone of high hazard just 1000 m below the delineated rockfall release area and thus much more frequently exposed to rockfall events. Besides the increased construction activity, dendrochronological data provides evidence that rockfall activity increased around the 1940s, and especially in the last 30 years (Stoffel et al. 2005), which is consistent with more regional studies in the Alps and is thought to be connected with periods of higher temperatures and permafrost-degradation (Huggel et al. 2012). Thereby, increasing rockfall activity increases the average number of rockfall events affecting existing infrastructure and people. Although this effect is modeled to be about 4 times smaller than the effect of additional construction between 1940 and 2010, it probably was the dominant effect of risk increase between 1880 and 1940, where almost no changes in exposure occurred. Besides changes in exposure and rockfall activity, deflection dams build at Täschgufer in the late 20th century have affected the development of rockfall risk. The protective effect of the deflection dams in the recent time period is estimated to be roughly 51'000 CHFa^{-1}, which is only about one third of the effect of the current protection forest. However, it is possible that the protective effect of the dams is underestimated in this study because of their smoothed representation in the digital elevation model. Both protection measures are most effective in retaining small blocks (smaller than around 4 m^3) and thereby mainly protect hiking trails not too distant from the rockfall release area, which in the case of protection forest is consistent with

previous findings in the study area (Stoffel et al. 2006). Finally, it is argued in this study that the effect of protection measures on risk development is complex and strongly linked to settlement development. For example, the protective effect of the deflection dams being 51'000 CHFa^{-1} in 2010 is estimated to be up to 170'000 CHFa^{-1} in 2060, because more infrastructure will be protected by these dams in the future. Implications of this finding for the planning of protective measures are further discussed in Section 8.4.

Findings regarding past development of hazard and risk generally confirm findings from studies regional to global scales, but nevertheless must not generally hold true for other locations. An important finding of this study is that rockfall risk at the study site substantially increased due to settlement development in the second half of the 20$^{\text{th}}$ century and despite the implementation of protection measures in the 1980s and 1990s. This finding is consistent with results from many studies on regional to global scales, including Switzerland, which identify population growth and settlement expansion or compaction as the main driver of increasing losses from natural hazards (Ammann 2001, Barbolini et al. 2002, Bouwer 2011, Keiler & Fuchs 2008, White et al. 2001). Thereby, this study was explicitly able to account for the effect of protection measures, which is generally not possible in regional or global studies and might distort results on these scales, especially in developed countries (Mechler & Bouwer 2015, Neumayer & Barthel 2011). However, it cannot be concluded that this finding is generally true on the local scale, since other local case studies come to different conclusions. For example, local studies of avalanche risk development from 1950–2000, which are also able to account for protection measures, find no general trend in avalanche risk in Galtür, Austria (Keiler et al. 2006), or even a substantial decrease in avalanche risk in Davos, Switzerland (Fuchs et al. 2004), despite increasing damage potential. One reason for these inconsistent findings on the local scale is the site-specific spatial distribution of exposed objects, which strongly affects the effectiveness of the protection measures (Fuchs et al. 2004, Keiler et al. 2006). This issue is confirmed by this study, resulting in different relative risk reduction of both deflection dams and protection forest for different time periods. Also, small changes in other assumptions, such as values at risk and related vulnerabilities, which are held constant in this study, might considerably differ between different sites and have been shown to strongly affect the resulting risk (Fuchs et al. 2004, Keiler & Fuchs 2008, Keiler et al. 2006, Mechler & Bouwer 2015). Therefore, general statements referring to larger areas might be difficult to derive from local case studies (Fuchs et al. 2004).

From the above findings on past developments of hazard and risk, the following three implications for the analysis of their future developments (Section 8.3) can be pointed out and are all supported by this study. First, developments of damage potential and social aspects are certainly an important driver of risk that should be taken into account when making statements about future losses from natural hazards. Second, spatial patterns of such developments are important to consider, since they not only determine the relevance of damage potential in terms of risk, but also the effectiveness of existing or planned protection measures. Third, the inability of many global and regional studies to attribute past increases in losses to climate change does not ensure with certainty that climate change had no impact on

disaster losses, mainly due to the rather short observation periods and factors that cannot be controlled for on these scales, such as protection measures, vulnerabilities and spatial patterns of exposed infrastructure and people. Even more importantly, the absence of a climate signal in the past does not imply its absence in the future. In the case of the rockfall hazard, as in other cases, climate sensitivity is expected both from theoretical perspective and observations (Chapter 2) and should be considered when projecting future losses from natural hazards. To account for the high uncertainty in future developments of both hazard potential and damage potential, the definition of several scenarios might be reasonable.

8.3 Methodology: Future risk developments

Research question 3: On which scientific basis can plausible future climate and exposure scenarios (2060) be defined and implemented into the assessment of hazard and risk?

In this study, future development of hazard and risk was assessed based on different climate and exposure scenarios, which is considered important but not yet very common in literature (Bouwer 2013). In the following, both the definition of climate and exposure scenarios are summarized and critically discussed.

Two different scenarios of future hazard potential were based on the Swiss Climate Change Scenarios CH2011, which are derived from regional climate models (RCMs), and a relation of rockfall frequencies and mean summer temperatures, which was derived from observations. RCMs are currently among the most comprehensive tools to project climate on regional scales (Allen & Huggel 2013, Bouwer 2013). A major limitation of the Swiss Climate Change Scenarios CH2011 is, however, that future changes in temperature and precipitation are only given in terms of changes in their mean values, while their statistical distribution (e.g. variability, skewness, shape) is assumed to remain unchanged (C2SM et al. 2011). In fact, the statistical distribution of temperature and precipitation may change in many fashions, and especially changes in variability are more important than changes in mean values when it comes to extreme events, such as the unusually hot summer 2003 (Katz & Brown 1992, Schär et al. 2004). The inability to make statements about future extreme events on the basis of CH2011 was only one of many difficulties when coupling climate change scenarios to rockfall activity in this study. For this purpose, a regression model was established between mean annual summer temperatures and reconstructed annual rockfall activity. Being statistically significant, the relation between these two variables revealed that higher mean annual summer temperatures tend to go along with higher annual rockfall activity, which could reflect processes of permafrost-degradation at the study area (Section 6.4.1). However, the very low R^2 (0.187) of the regression model indicates that the variability of mean annual summer temperatures can only very poorly explain the variability of annual rockfall activity, for which three reasons are suggested. First, the reconstruction of annual rockfall activity from dendrochronological data relies on many uncertainties and assumptions, including the choice of sampling strategies and methods and assumption made when statistically estimating the number of missed events (Morel et al. 2015, Stoffel & Perret 2006,

Trappmann et al. 2013). Second, the relation of rockfall activity and climate is complex and involves many different processes and their interactions. Apart from mean summer temperatures, extreme temperature and precipitation events, the frequency of freeze-thaw cycles and the timing and duration of snow cover might be other influential factors (Chapter 2). Since 90% of annual rockfall in the study area occurs in spring (Stoffel et al. 2005), winter temperatures, related freeze-thaw cycles and extreme precipitation events in spring could be of particular importance (Gruner 2008). However, the existing model could neither be improved by including mean annual winter temperature nor by including the number of days with extreme precipitation during different seasons, based on available data from the station in Grächen. A third reason for the poor model performance could be the presence of delayed effects, since especially processes related to warming and permafrost-degradation are acting on different scales of time and depth (Chapter 2). Cross-correlations revealed that mean annual summer temperatures might influence annual rockfall activity with a lag of up to 4 years, but the simple inclusion of lagged variables could also not improve the model. More sophisticated statistical methods might be applied to account for lagged effects, but some of them might suffer from over-parametrization (Bhaskaran et al. 2013). Given the poor model performance, predictions of future rockfall frequencies are subject to large uncertainty (Section 6.4.1). However, as the model is not used to predict exact annual rockfall frequencies but average values over 30 years associated with warming, more robust estimates are possible. Finally, being calibrated with dendrochronological data, no changes in rockfall magnitudes can be predicted by the model. As was discussed in Section 2.3, such changes are generally difficult to estimate based on available data, although they could be expected from a theoretical perspective due to warming and thawing of permafrost at depth.

Three different scenarios of future damage potential were based on observed socio-economic development in the past 30 years and an expert interview. Thereby, the most crucial steps are the quantification and spatial allocation of new infrastructure and people in the different scenarios. Regarding their quantification, it is common practise to define a trend scenario, in which observed trends in population growth, building activity or land-use change are extrapolated (Nussbaumer et al. 2014, Seher & Löschner 2016). However, it is very uncertain whether observed trends will continue, since boundary conditions might change in the future. Therefore, the trend scenario is usually accompanied by further scenarios, which include changes in important drivers of socio-economic development (Nussbaumer et al. 2014). In this study, it could reasonably be argued on the basis of an expert interview that the trend scenario rather represents the upper boundary of expected socio-economic development (scenario "+"), and a more persistent development or even a decrease in population can be assumed in scenario "o" and scenario "-", respectively. The inclusion of a scenario with negative growth is not common in literature (Bouwer 2013). However, such developments are regarded as plausible also for other alpine regions in Switzerland (ARE & DETEC 2008, Lehmann et al. 2007, Hayek et al. 2011). Regarding the spatial allocation of new infrastructure, it is important to account for legal planning constraints, such as legally defined construction areas (Nussbaumer et al. 2014). In this study, it was accounted for the fact that such constraints are politically contested and can be adapted with

respect to the anticipated future socio-economic development. Within given construction areas, plausible spatial allocation of new buildings was regarded as especially challenging in this study and strongly affects resulting risk estimates. Thereby new buildings were simply uniformly distributed to existing building zones. Such procedures might be backed by the use of more detailed cadastral maps and in-situ knowledge of local decision makers (e.g. building authorities, spatial planning consultants) (Seher & Löschner 2016). As is argued for other assumptions, however, transparency and consistency between scenarios is regarded as more valuable than the achievement of a realistic as possible spatial distribution. To assure that differences between the scenarios are not affected by changing spatial patterns and facilitate the interpretation of results, new buildings were successively added to the map (Section 6.4.2). Similarly, emigration of people in scenario "-" is assumed to take place evenly in space, since emigration patterns are difficult to estimate. With these procedures, only changes in exposure of infrastructure and people are assessed, while their value and vulnerability is assumed to remain constant. Based on the expert interview, it could be expected that risk developments will be accentuated by changes in land and housing prices, meaning that they will tend to increase in a scenario of strongly positive economic growth and decrease in a scenario of negative growth (positive feedback). In contrast, risk developments might be stabilized by changes in vulnerabilities, since capabilities to construct and maintain protection measures are higher in scenarios of higher economic growth (negative feedback), which is also supported by findings of Neumayer & Barthel (2011) on global scale.

To summarize, this study combines different hazard potential and damage potential scenarios in the projection of future rockfall hazard and risk, which is considered important in literature to account for the large uncertainties in these developments (Bouwer 2013). More precisely, it is accounted for changing process frequencies and exposure of infrastructure and people, while changes in process magnitude and vulnerabilities could theoretically also be assessed with the presented methodology. Regarding the hazard potential scenarios, a major methodological problem was the coupling of future climate scenarios and rockfall activity. Although increasing mean air temperatures are thought to have an impact on rockfall activity in many high-mountain regions of the world (Huggel et al. 2012), the relation of climate and the rockfall hazard is more complex and was difficult to quantify on the basis of available local data (Chapter 2). Clearly more research is needed in this field to reduce epistemic uncertainty. While more empirical research on regional scales and including data on extreme events might be promising (Huggel et al. 2012), forecasting of changes in hazard frequencies and magnitudes is also likely to depend on improved process-based modeling (Harris et al. 2009). Regarding the damage potential scenarios, the quantification and spatial allocation of future infrastructure and people is also uncertain, mainly because socio-economic developments are influenced by human actions and behaviour, which are not easily predictable. The inherent uncertain nature of such processes is a form of natural or aleatory uncertainty (Bouwer 2013), which can be assessed by including multiple scenarios and thereby by accounting for a wide range of possible developments. Inclusion of local stakeholders in this process is considered important (Nussbaumer et al. 2014, Seher & Löschner 2016, Walz et al. 2007) and was achieved with an expert interview in this study.

8.4 Results: Future risk developments

Research question 4: By combining different climate and exposure scenarios and evaluating their influence on rockfall hazard and risk, which conclusions can be drawn with respect to future research and risk management in the study area?

Projected risk in the study area increases on average by +124% until 2060, being on average equally driven by both climate and socio-economic change. However, large differences in risk developments and the relative importance of these driving factors can be observed between different development pathways, depending on both global CO_2 emissions and local socio-economic developments at the study site. Projected risk developments are in more detail described in the following and compared to similar studies, before some implications for risk management are outlined.

Projected risk at the study site in 2060 ranges from a decrease of -13% to an increase of +263%. Although changes in exposure were identified as the dominant driver of risk developments in the past, climate change may become equally or even more important under certain future development pathways. When continuing economic growth is assumed in Täsch, increasing exposure remains the major driver of risk development and may cause a risk increase of +116%. When assuming moderate economic growth, this might still hold true for a climate scenario of low CO_2 increase (RCP3PD). However, under the emission scenario A1B, which is still moderate when compared to recently observed CO_2 increases (Mani & Caduff 2015), increasing rockfall activity due to higher temperatures is modeled to become the dominant driver, causing an increase in rockfall risk by +68%. Also when assuming low economic growth and emigration, risk increases due to climate change remain equally or more important than decreases in risk due to emigration of people. Apart from the individual effects of climate change and socio-economic developments, it is interesting to see that considerable interaction effects exist between these drivers. For example, effects of increasing rockfall activity are more severe when assuming increasing construction activity at the same time or vice versa. Although this insight is quite intuitive, it is interesting to see that interaction effects might become even more important than individual effects under extreme conditions, for example when combining the emission scenario A1B and the socio-economic scenario "+". Effects of changing protection measures are not investigated, since such changes are difficult to anticipate without concrete planning options. However, it could be shown that absolute protective effects of existing measures vary considerably between the different scenarios. To a minor degree, also their efficiency of protection or relative risk reduction varies between the scenarios, depending on the spatial distribution of the infrastructure to be protected.

Results from projected losses are difficult to compare with other studies, since no comparable local projection of rockfall risk from 2010 to 2060 is published. There are only few studies on regional to global scales, which project risk for other climate-related natural hazards (e.g. tropical and extra-tropical cyclones or floods) from 2000 to 2040, taking both climate change and socio-economic changes into account (Bouwer 2013). Results from these studies

are in good agreement with the above findings, indicating that future anthropogenic climate change might become almost equally important in driving risk development than changes in exposure of infrastructure and people. The average projected risk increase from seven studies is estimated to be +125% due to climate change and +164% due to changes in exposure. These estimates are higher than average individual effects of both about 50% reported in this study, especially when considering the slightly shorter time horizon of these projections. However, variability of projected relative risk increases between studies is quite high. Only three studies investigated interaction effects, highlighting that the combined effect of changes in hazard and exposure is higher than a simple summation of their individual effects, which is also shown in this study.

Regarding risk management, it is argued in the following that scenarios can be helpful when planning both passive and active protection measures. Different hazard potential scenarios are thereby useful to assess the robustness of existing hazard maps to future changes. In this study, the existing rockfall hazard map is found to be robust with respect to increasing rockfall frequencies. This result is comparable with a study in the Bernese Alps of Switzerland, concluding that existing hazard zones for rockfall and other hazardous processes in high-alpine areas are barely expected to change in the future (VOLBE 2015). Although further construction within these zones is to a certain degree limited in Switzerland since the 1990s (Raetzo et al. 2002), risk from such processes can nevertheless increase in the zone of residual hazard, where further construction is not subject to any structural obligations (Fuchs et al. 2004, Keiler & Fuchs 2008). Different damage potential scenarios are thereby useful to anticipate such developments and help local authorities to make informed decisions regarding allocation of land, relocation or reinforcement of buildings in this zone (Schwendtner et al. 2013, Seher & Löschner 2016). Finally, both different hazard potential and different damage potential scenarios are useful for the planning of active protection measures, such as deflection dams or protection forest care. When planning such measures, costs are typically compared to benefits. However, as was shown in this study, changes in both hazard and damage potential can affect future benefits of such measures and should therefore be considered in the planning process. While such multi-temporal approaches exist (Aerts et al. 2014), they are not yet very common in Switzerland, where applications with EconoME usually take only the current situation into account (Bründl et al. 2015). In addition, changing spatial patterns of the built environment can affect the efficiency of protection measures and might be helpful to consider to find sustainable solutions.

9 Conclusions

In this study, a transparent and consistent methodology was developed to assess long-term developments of rockfall hazard and accompanying risk. The developed methodology allows to determine resulting rockfall hazard and risk with a raster-based approach, and thereby to create hazard and risk maps for the area at investigation. Furthermore, the relative importance of different driving factors of rockfall hazard and risk, such as changes in climate and exposure of infrastructure and people, can be assessed. Being in accordance with well-established general concepts of hazard and risk in Switzerland, the methodology can be transferred to other climate-related natural hazards and adjusted to available data, according to which hazard and damage potential for each time period are estimated. The minimum requirements for its application are thereby several event scenarios, eventually in the from of a MCF distribution, a process-based model or another method to determine spatial patterns of the impact and process intensities, and a more or less detailed categorization of damage potential in the area at investigation. To assess the climate impact on related hazards and risks, a coupling of process frequencies and/or process magnitudes to at least one climate variable is further required. Finally, to account for the substantial aleatory uncertainties in future projections of hazard and risk, the assessment of several hazard potential and damage potential scenarios is proposed.

The methodology was applied at Täschgufer, a highly active rockfall slope in the southern Swiss Alps, where detailed field observations, event records, dendrochronological and socio-economic data provide a sound data basis. The analysis of the rockfall hazard revealed that the northern part of the village of Täsch is affected by mostly residual rockfall hazard, as defined according to the Swiss hazard mapping scheme. A recent event in 2013 confirmed that larger boulders may reach the valley floor in this area and endanger people, infrastructure and the environment. Results of the multi-temporal risk analysis (1880, 1940, 2010 and 2060) show that rockfall risk in this area substantially increased in the late 20^{th} century, mainly due to socio-economic development and despite the building of several deflection dams in the 1980s and 1990s. From present to 2060, however, projected rockfall risk is estimated to be equally driven by climatic and socio-economic factors, leading to a further risk increase by a factor of 2.2 over all scenarios. Climate change is thereby expected to cause increasing rockfall frequencies in the study area, where release zones of rockfall are located in periglacial environments, which is supported by both theoretical considerations and dendrochronological observations. Results therefore suggest that a lacking climate signal in past losses from natural hazards does not necessarily imply the same finding for the future under continuing climate and socio-economic change.

Existing disaster loss studies are mainly focusing on regional to global scales, but risk has typically many local-scale characteristics, and therefore important aspects are likely not covered. This study fills this gap by proposing a methodology for the assessment of local-scale risk evolution. Results show that local socio-economic development is equally or more important in driving rockfall risks at the study site, but is subject to large aleatory uncertainty. For the village of Täsch, plausible future scenarios include both further growth of the village as well as emigration of people, depending on the future development of tourism and traffic routes, potential changes in political constraints or the occurrence of major hazardous events. Additionally, spatial patterns of future growth or emigration are important for the risk evolution, since they determine how strong a change in damage potential is affecting accompanying risk. The construction of the Europaweg in the red hazard zone at Täschgufer illustrates for example, how a relatively small increase in damage potential can become very relevant in terms of risk. Finally, the construction of active protection measures, such as deflection dams or protection forest, can significantly influence risk development, while both their absolute and relative risk reduction is linked to the development of hazard and damage potential and changing over time. For these reasons, results of this study are very site-specific and must not generally hold true for other locations, although they are in good agreement with findings on regional to global scales.

The presented study points out potential for future research in several fields. The application of a consistent methodology to both past and likely future developments of hazard and risk is not yet common, but allows for consistent statements about potential changes in such developments. Thereby, the investigation of time periods longer than several decades might provide interesting insights, especially in terms of climate change. On one hand, past climate signals are likely to be less obscured by changing protection measures and vulnerabilities in the early than in the late 20^{th} century. On the other hand, the majority of future changes in extreme weather events associated with climate change will likely occur after the first half of the 21^{st} century. The impact of climate change on the rockfall hazard, however, remains highly uncertain and requires further investigation. While more empirical research on regional scales and including data on extreme events might be promising, improved process-based modeling is likely to be equally important in this regard. Apart from the investigation of climate impacts, results of this study underline the need for the inclusion of socio-economic factors in risk analyses. While such factors are commonly accounted for in analyses of past disaster losses, it is striking that they are neglected in most of the studies projecting future disaster losses from climate-related natural hazard. As it is likely that changes in exposure will be equally or even more important than changes in climate in driving such losses, only the consideration of socio-economic scenarios and their interactions with climate scenarios can provide reasonable projections. In other words, research that only considers changes in climate performs a sensitivity test only, and in fact does not provide a projection. Finally, it could be shown that spatial aspects of hazard potential and damage potential are essential in determining rockfall risk at the local scale. The inclusion of such aspects into risk analyses seems crucial but might be challenging on regional to global scales, since it requires process modeling as well as information about the location of infrastruc-

ture and people over larger areas. With some abstractions in the presented methodology, such as the use of conceptual models and aggregated socio-economic data, however, its application on larger scales (e.g. entire mountain valleys) seems possible with reasonable effort.

Results of this study have further implications for practical risk management. In general, the importance of risk management is highlighted by the large influence of active protection measures and the spatial configuration of damage potential on the development of rockfall hazard and risk. Associated aleatory uncertainties might at first sight seem challenging from the perspective of research, but only reflect the large scope of actions from the perspective of risk management. Therefore, instead of providing exact estimates of future hazard and risk, multi-temporal risk analyses can provide a valuable basis for risk management by considering several future scenarios. For example, long-term benefits of protection measures can be evaluated and compared to their long-term costs by considering scenarios of future climate and socio-economic change, which is not yet common practice in Switzerland. To make such an integrative risk management possible, however, methodologies of risk analyses need to keep up with the changing perception of risk from natural hazards, which is increasingly interpreted in a social context, and in particular allow for the inclusion of climatic and social aspects, both of which significantly affect local dynamics of hazard and risk.

Bibliography

Abbruzzese, J. M. & Labiouse, V. (2014), 'New Cadanav methodology for quantitative rock fall hazard assessment and zoning at the local scale', *Landslides* **11**(4), 551–564.

Abbruzzese, J. M., Sauthier, C. & Labiouse, V. (2009), 'Considerations on Swiss methodologies for rock fall hazard mapping based on trajectory modelling', *Natural Hazards and Earth System Science* **9**(4), 1095–1109.

Aerts, J. C., Botzen, W. W., Emanuel, K., Lin, N., Moel, H. d. & Michel-Kerjan, E. O. (2014), 'Evaluating flood resilience strategies for coastal megacities', *Science* **344**(6183), 473–475.

Alcántara-Ayala, I. (2002), 'Geomorphology, natural hazards, vulnerability and prevention of natural disasters in developing countries', *Geomorphology* **47**(2), 107–124.

Allen, S. & Huggel, C. (2013), 'Extremely warm temperatures as a potential cause of recent high mountain rockfall', *Global and Planetary Change* **107**, 59–69.

Ammann, W. (2001), 'Integrales Risikomanagement - Der gemeinsame Weg in die Zukunft', *Bündnerwald* **54**(5), 14–17.

ARE & DETEC (2008), *Raumkonzept Schweiz: Eine dynamische und solidarische Schweiz, Entwurf*, Federal Office for Spatial Development (ARE) & Federal Department of the Environment, Transport, Energy and Communications (DETEC), Bern.

Barbolini, M., Natale, L. & Savi, F. (2002), 'Effects of release conditions uncertainty on avalanche hazard mapping', *Natural Hazards* **25**(3), 225–244.

Bartelt, P., Bieler, C., Bühler, Y., Christen, M., Dreier, L., Gerber, W., Glover, J. & Schneider, M. (2015), *RAMMS::ROCKFALL User Manual*, WSL Institute for Snow and Avalanche Research SLF, Davos.

Barthel, F. & Neumayer, E. (2012), 'A trend analysis of normalized insured damage from natural disasters', *Climatic Change* **113**(2), 215–237.

Bhaskaran, K., Gasparrini, A., Hajat, S., Smeeth, L. & Armstrong, B. (2013), 'Time series regression studies in environmental epidemiology', *International journal of epidemiology* **42**(4), 1187–1195.

Bouwer, L. M. (2011), 'Have disaster losses increased due to anthropogenic climate change?', *Bulletin of the American Meteorological Society* **92**(1), 39–46.

Bouwer, L. M. (2013), 'Projections of future extreme weather losses under changes in climate and exposure', *Risk Analysis* **33**(5), 915–930.

Bründl, M. (2009), *Risikokonzept für Naturgefahren - Leitfaden*, National Platform for Natural Hazards (PLANAT), Bern.

Bründl, M., Ettlin, L., Burkard, A., Oggier, N., Dolf, F. & Gutwein, P. (2015), *EconoMe - Wirksamkeit und Wirtschaftlichkeit von Schutzmassnahmen gegen Naturgefahren, Formelsammlung*, Bern.

C2SM, MeteoSwiss, ETH, NCCRClimate & OcCC (2011), *Swiss climate change scenarios CH2011*, Center for Climate Systems Modeling (C2SM), Federal Office of Meteorology and Climatology (MeteoSwiss) ETH Zurich (ETH), National Centre of Competence in Research Climate (NcCCRClimate) & Advisory Body on Climate Change (OcCC), Zurich.

Cardona, O. D., van Aalst, M. K., Birkmann, J., Fordham, M., McGregor, G., Perez, R., Pulwarty, R. S., Schipper, E. L. & Sinh, B. T. (2012), Determinants of risk: Exposure and vulnerability, *in* C. B. Field, V. Barros, T. F. Stocker, D. Qin, D. J. Dokken, K. L. Ebi, M. D. Mastrandrea, K. J. Mach, G. K. Plattner, S. K. Allen, M. Tignor & P. M. Midgley, eds, 'Managing the risks of extreme events and disasters to advance climate change adaptation. A special report of working groups I and II of the Intergovernmental Panel on Climate Change (IPCC)', Cambridge University Press, Cambridge, UK and New York, NY, USA, pp. 65–108.

Carrea, D., Abellan, A., Derron, M. H. & Jaboyedoff, M. (2015), Automatic rockfalls volume estimation based on terrestrial laser scanning data, *in* G. Lollino, D. Giodran, G. B. Crosta, J. Corominas, R. Azzam, J. Wasowski & N. Sciarra, eds, 'Engineering geology for society and territory', Vol. 2, Springer, Cham, pp. 425–428.

Davies, M. C., Hamza, O. & Harris, C. (2001), 'The effect of rise in mean annual temperature on the stability of rock slopes containing ice–filled discontinuities', *Permafrost and Periglacial Processes* **12**(1), 137–144.

DETEC & FEDRO (2012), *Naturgefahren auf den Nationalstrassen, Risikokonzept: Methodik für eine risikobasierte Beurteilung, Prävention und Bewältigung von gravitativen Naturgefahren auf Nationalstrassen*, Federal Department of the Environment, Transport, Energy and Communications (DETEC) & Federal roads office (FEDRO), Bern.

Dorren, L. (2016), *Rockyfor3D (v5.2) revealed: Transparent description of the complete 3D rockfall model*, International EcorisQ Association (ecorisQ), Geneva.

Dorren, L., Berger, F., Jonsson, M., Krautblatter, M., Mölk, M., Stoffel, M. & Wehrli, A. (2007), 'State of the art in rockfall – forest interactions', *Schweizerische Zeitschrift fur Forstwesen* **158**(6), 128–141.

Dorren, L. & Wehrli, A. (2012), *Wirkungsbeurteilung Steinschlag-Schutzwald Britterwald (GL), Kurzbericht*, Federal Office for the Environment (FOEN), Bern.

Dussauge-Peisser, C., Grasso, J. R. & Helmstetter, A. (2003), 'Statistical analysis of rockfall volume distributions: Implications for rockfall dynamics', *Journal of Geophysical Research: Solid Earth* **108**(B6), 1–11.

Dussauge-Peisser, C., Helmstetter, A., Grasso, J. R., Hantz, D., Desvarreux, P., Jeannin, M. & Giraud, A. (2002), 'Probabilistic approach to rock fall hazard assessment: Potential of historical data analysis', *Natural Hazards and Earth System Science* **2**(1/2), 15–26.

Fischer, L., Purves, R. S., Huggel, C., Noetzli, J. & Haeberli, W. (2012), 'On the influence of topographic, geological and cryospheric factors on rock avalanches and rockfalls in high-mountain areas', *Natural Hazards and Earth System Science* **12**(1), 241–254.

FOEN (2016), *Web-GIS*, retrieved from http://www.map.geo.admin.ch.

FSO (2016*a*), *Buildings and Dwellings statistic (BDS)*, retrieved from http://www.bfs.admin.ch/bfs/portal/de/index/infothek.html.

FSO (2016*b*), *Szenarien zur Bevölkerungsentwicklung der Kantone der Schweiz 2015-2045*, retrieved from http://www.bfs.admin.ch/bfs/portal/de/index/infothek.html.

Fuchs, S., Bründl, M. & Stötter, J. (2004), 'Development of avalanche risk between 1950 and 2000 in the Municipality of Davos, Switzerland', *Natural Hazards and Earth System Science* **4**(2), 263–275.

Gruber, S. & Haeberli, W. (2007), 'Permafrost in steep bedrock slopes and its temperature-related destabilization following climate change', *Journal of Geophysical Research: Earh Surface* **112**(F2), 1–10.

Gruber, S., Hoelzle, M. & Haeberli, W. (2004), 'Permafrost thaw and destabilization of alpine rock walls in the hot summer of 2003', *Geophysical Research Letters* **31**(13), 1–4.

Gruber, S., Peter, M., Hoelzle, M., Woodhatch, I. & Haeberli, W. (2003), Surface temperatures in steep Alpine rock faces - A strategy for regional-scale measurement and modelling, *in* '8th International Conference on Permafrost - Conference Proceedings', Vol. 1, pp. 325–330.

Gruner, U. (2008), Climatic and meteorological influences on rockfall and rockslides ('Bergsturz'), *in* '11th International Converence Interpraevent - Conference Proceedings', Vol. 2, pp. 147–158.

Gsponer, P. (2013), *Ereignisrapport zum Ereignis vom 03.08.2013*, Täsch.

Gubler, S., Fiddes, J., Keller, M. & Gruber, S. (2011), 'Scale-dependent measurement and analysis of ground surface temperature variability in alpine terrain', *The Cryosphere* **5**(2), 431–443.

Guerin, A., D'Amato, J., Hantz, D., Rossetti, J. P. & Jaboyedoff, M. (2014), Investigating rockfall frequency using terrestrial laser scanner (Grenoble area, France), *in* '1st Vertical Geology Conference - Conference Paper'.

Haeberli, W., Wegmann, M. & Vonder Mühll, D. (1997), 'Slope stability problems related to glacier shrinkage and permafrost degradation in the Alps', *Eclogae Geologicae Helvetiae* **90**(3), 407–414.

Harris, C., Arenson, L. U., Christiansen, H. H., Etzelmüller, B., Frauenfelder, R., Gruber, S., Haeberli, W., Hauck, C., Hölzle, M., Humlum, O., Isaksen, K., Kääb, A., Kern-Lütschg, M. A., Lehning, M., Matsuoka, N., Murton, J. B., Nötzli, J., Phillips, M., Ross, N., Seppälä, M., Springman, S. M. & Vonder Mühll, D. (2009), 'Permafrost and climate in Europe: Monitoring and modelling thermal, geomorphological and geotechnical responses', *Earth-Science Reviews* **92**(3-4), 117–171.

Hayek, U. W., Jaeger, J. A., Schwick, C., Jarne, A. & Schuler, M. (2011), 'Measuring and assessing urban sprawl: What are the remaining options for future settlement development in Switzerland for 2030?', *Applied Spatial Analysis and Policy* **4**(4), 249–279.

Hegglin, E. & Huggel, C. (2008), 'An integrated assessment of vulnerability to glacial hazards: A case study in the Cordillera Blanca, Peru', *Mountain Research and Development* **28**(3), 299–309.

Hergarten, S. (2003), 'Landslides, sandpiles, and self-organized criticality', *Natural Hazards and Earth System Science* **3**(6), 505–514.

Hergarten, S. (2004), 'Aspects of risk assessment in power-law distributed natural hazards', *Natural Hazards and Earth System Science* **4**(2), 309–313.

Hergarten, S. (2012), 'Topography-based modeling of large rockfalls and application to hazard assessment', *Geophysical Research Letters* **39**(13), 1–5.

Huggel, C., Allen, S., Deline, P., Fischer, L., Noetzli, J. & Ravanel, L. (2012), 'Ice thawing, mountains falling - are alpine rock slope failures increasing?', *Geology Today* **28**(3), 98–104.

Huggel, C., Raissig, A., Rohrer, M., Romero, G., Diaz, A. & Salzmann, N. (2015), 'How useful and reliable are disaster databases in the context of climate and global change? A comparative case study analysis in Peru', *Natural Hazards and Earth System Science* **15**(3), 475–485.

Huggel, C., Salzmann, N., Allen, S., Caplan-Auerbach, J., Fischer, L., Haeberli, W., Larsen, C., Schneider, D. & Wessels, R. (2010), 'Recent and future warm extreme events and high-mountain slope stability', *Philosophical Transactions of the Royal Society of London A: Mathematical, Physical, and Engineering Sciences* **368**(1919), 2435–2459.

Jaboyedoff, M., Dudt, J. P. & Labiouse, V. (2005), 'An attempt to refine rockfall hazard zoning based on the kinetic energy, frequency and fragmentation degree', *Natural Hazards and Earth System Science* **5**(5), 621–632.

Kallen, I. (2015), Risikoentwicklung im Schatten des Geschiebesammlers: Die Veränderung des Risikos über die Zeit des Geschiebesammlerbaus im Richenbach in Reichenbach i.K. bis heute, Master's thesis, University of Bern, Bern.

Katz, R. W. & Brown, B. G. (1992), 'Extreme events in a changing climate: Variability is more important than averages', *Climatic Change* **21**(3), 289–302.

Keiler, M. & Fuchs, S. (2008), Variabilität des Schadenpotentials: Methodik im Rahmen des integralen Risikomanagements, *in* '11th International Converence Interpraevent - Conference Proceedings', Vol. 2, pp. 371–382.

Keiler, M., Sailer, R., Jörg, P., Weber, C., Fuchs, S., Zischg, A. & Sauermoser, S. (2006), 'Avalanche risk assessment - A multi-temporal approach, results from Galtür, Austria', *Natural Hazards and Earth System Science* **6**(4), 637–651.

Kienholz, H., Zeilstra, P. & Hollenstein, K. (1998), *Begriffsdefinitionen zu den Themen Geomorphologie, Naturgefahren, Forstwesen, Sicherheit und Risiko*, Swiss Agency for Environment, Forests and Landscape (SAEFL) & Federal Forestry Administration, Bern.

Künzler, M., Huggel, C. & Ramírez, J. M. (2012), 'A risk analysis for floods and lahars: Case study in the Cordillera Central of Colombia', *Natural Hazards* **64**(1), 767–796.

Lari, S., Frattini, P. & Crosta, G. B. (2014), 'A probabilistic approach for landslide hazard analysis', *Engineering Geology* **182**(A), 3–14.

Lateltin, O. (1997), *Empfehlungen 1997: Berücksichtigung der Massenbewegungsgefahren bei raumwirksamen Tätigkeiten*, Federal Office for Spatial Development (ARE), Federal Office for Water and Geology (FOWG) & Swiss Agency for the Environment, Forests and Landscape (SAEFL), Bern.

Lehmann, B., Steiger, U. & Weber, M. (2007), *Landschaften und Lebensräume der Alpen: Zwischen Wertschöpfung und Wertschätzung*, vdf Hochschulverlag AG, Zurich.

Magnin, F., Brenning, A., Bodin, X., Deline, P. & Ravanel, L. (2015), 'Statistical modelling of rock wall permafrost distribution: Application to the Mont Blanc massif', *Geomorphologie* **21**(2), 145–162.

Malamud, B. D. (2004), 'Tails of natural hazards', *Physics World* **17**(8), 31–35.

Mani, P. & Caduff, U. (2015), *Klimasensitivität Naturgefahren*, geo7 AG, Bern.

Matsuoka, N. & Sakai, H. (1999), 'Rockfall activity from an alpine cliff during thawing periods', *Geomorphology* **28**(3), 309–328.

Mechler, R. & Bouwer, L. M. (2015), 'Understanding trends and projections of disaster losses and climate change: Is vulnerability the missing link?', *Climatic Change* **133**(1), 23–35.

Morel, P., Trappmann, D., Corona, C. & Stoffel, M. (2015), 'Defining sample size and sampling strategy for dendrogeomorphic rockfall reconstructions', *Geomorphology* **236**, 79–89.

Neumayer, E. & Barthel, F. (2011), 'Normalizing economic loss from natural disasters: A global analysis', *Global Environmental Change* **21**(1), 13–24.

Noetzli, J. & Gruber, S. (2009), 'Transient thermal effects in alpine permafrost', *The Cryosphere* **3**(1), 85–99.

Nussbaumer, S., Schaub, Y., Huggel, C. & Walz, A. (2014), 'Risk estimation for future glacier lake outburst floods based on local land-use changes', *Natural Hazards and Earth System Science* **14**(6), 1611–1624.

Peduzzi, P. & Herold, H. D. C. (2005), 'Mapping disastrous natural hazards using global datasets', *Natural Hazards* **35**(2), 265–289.

PERMOS (2016), *Permos database - Borehole temperature data from the Swiss Permafrost Monitoring Network*, Swiss Permafrost Monitoring Network (PERMOS), Davos.

Raetzo, H., Lateltin, O., Bollinger, D. & Tripet, J. (2002), 'Hazard assessment in Switzerland - Codes of Practice for mass movements', *Bulletin of Engineering Geology and the Environment* **61**(3), 263–268.

Ruiz-Carulla, R., Corominas, J. & Mavrouli, O. (2015), 'A methodology to obtain the block size distribution of fragmental rockfall deposits', *Landslides* **12**(4), 815–825.

Sass, O. (2005), 'Temporal variability of Rockfall in the Bavarian Alps, Germany', *Arctic, Antarctic and Alpine Research* **37**(4), 564–573.

Schär, C., Vidale, P. L., Luthi, D., Frei, C., Häberli, C., Liniger, M. A. & Appenzeller, C. (2004), 'The role of increasing temperature variability in European summer heatwaves', *Nature* **427**(6972), 332–336.

Schiermeier, Q. (2003), 'Alpine thaw breaks ice over permafrost's role', *Nature* **424**(6950), 712.

Schneuwly, D. M. & Stoffel, M. (2008), 'Spatial analysis of rockfall activity, bounce heights and geomorphic changes over the last 50 years - A case study using dendrogeomorphology', *Geomorphology* **102**(3), 522–531.

Schwendtner, B., Papathoma-Köhle, M. & Glade, T. (2013), 'Risk evolution: How can changes in the built environment influence the potential loss of natural hazards?', *Natural Hazards and Earth System Science* **13**(9), 2195–2207.

Seher, W. & Löschner, L. (2016), Settlement dynamics in floodplains: From assessing future flood hazard exposure to developing spatial adaptation measures, *in* '13th International Conference Interpraevent - Conference Proceedings', Vol. 1, pp. 837–844.

Stoffel, M. (2006), 'A review of studies dealing with tree rings and rockfall activity: The role of dendrogeomorphology in natural hazard research', *Natural Hazards* **39**(1), 51–70.

Stoffel, M. & Huggel, C. (2012), 'Effects of climate change on mass movements in mountain environments', *Progress in Physical Geography* **36**(3), 421–439.

Stoffel, M. & Perret, S. (2006), 'Reconstructing past rockfall activity with tree rings: Some methodological considerations', *Dendrochronologia* **24**(1), 1–15.

Stoffel, M., Schneuwly, D. M., Bollschweiler, M., Lièvre, I., Delaloye, R., Myint, M. & Monbaron, M. (2005), 'Analyzing rockfall activity (1600–2002) in a protection forest - A case study using dendrogeomorphology', *Geomorphology* **68**(3), 224–241.

Stoffel, M., Tiranti, D. & Huggel, C. (2014), 'Climate change impacts on mass movements - Case studies from the European Alps', *Science of the Total Environment* **493**, 1255–1266.

Stoffel, M., Wehrli, A., Kühne, R., Dorren, L., Perret, S. & Kienholz, H. (2006), 'Assessing the protective effect of mountain forests against rockfall using a 3D simulation model', *Forest Ecology and Management* **225**(1), 113–122.

Straub, D. & Schubert, M. (2008), 'Modeling and managing uncertainties in rock-fall hazards', *Georisk: Assessment and Management of Risk for Engineered Systems and Geohazards* **2**(1), 1–15.

swisstopo (2010), *swissBUILDINGS3D: Vereinfachte 3D-Gebäude der Schweiz*, Federal Office of Topography (swisstopo), Bern.

swisstopo (2016*a*), *Aerial photos*, retrieved from http://www.swisstopo.admin.ch.

swisstopo (2016*b*), *Background information on the National Map*, retrieved from http://www.swisstopo.admin.ch.

swisstopo (2016*c*), *Background information on the Siegfried Map*, retrieved from http://www.swisstopo.admin.ch.

swisstopo (2016*d*), *swissALTI3D: Das hoch aufgelöste Terrainmodell der Schweiz*, Federal Office of Topography (swisstopo), Bern.

Thouret, J.-C., Enjolras, G., Martelli, K., Santoni, O., Luque, J. A., Nagata, M., Arguedas, A. & Macedo, L. (2013), 'Combining criteria for delineating lahar- and flash-flood-prone hazard and risk zones for the city of Arequipa, Peru', *Natural Hazards and Earth System Science* **13**(2), 339–360.

Trappmann, D., Corona, C. & Stoffel, M. (2013), 'Rolling stones and tree rings: A state of research on dendrogeomorphic reconstructions of rockfall', *Progress in Physical Geography* **37**(5), 701–716.

Trappmann, D. & Stoffel, M. (2013), 'Counting scars on tree stems to assess rockfall hazards: A low effort approach, but how reliable?', *Geomorphology* **180**, 180–186.

Trappmann, D., Stoffel, M. & Corona, C. (2014), 'Achieving a more realistic assessment of rockfall hazards by coupling three-dimensional process models and field-based tree-ring data', *Earth Surface Processes and Landforms* **39**(14), 1866–1875.

van Westen, C. J., van Asch, T. W. & Soeters, R. (2006), 'Landslide hazard and risk zonation - Why is it still so difficult?', *Bulletin of Engineering Geology and the Environment* **65**(2), 167–184.

VOLBE (2015), *Klimawandel und Naturgefahren - Veränderungen im Hochgebirge des Berner Oberlandes und ihre Folgen*, Division of natural hazards of the Canton Bern (VOLBE), Bern.

Walz, A., Lardelli, C., Behrendt, H., Grêt-Regamey, A., Lundström, C., Kytzia, S. & Bebi, P. (2007), 'Participatory scenario analysis for integrated regional modelling', *Landscape and Urban Planning* **81**(1), 114–131.

Wegmann, M., Gudmundsson, G. H. & Haeberli, W. (1998), 'Permafrost changes in rock-walls and the retreat of alpine glaciers: A thermal modelling approach', *Permafrost and Periglacial Processes* **9**(1), 23–33.

White, G. F., Kates, R. W. & Burton, I. (2001), 'Knowing better and losing even more: The use of knowledge in hazards management', *Global Environmental Change Part B: Environmental Hazards* **3**(3), 81–92.

Acknowledgements

I would like to thank Christine Moos for her assistance during fieldwork, support in modeling and the many fruitful discussions. For her assistance during fieldwork, I would also like to thank Jacqueline Ernst. I also gratefully acknowledge the statistical consulting provided by Dr. Christof Bigler and Florian Gerber. Thoughtful comments on an early version of this thesis were further given by Prof. Dr. Luuk Dorren and his research group. A special thank goes to my interview partner, who made a sincere effort to develop plausible local socio-economic scenarios for Täsch. Climate data has been accessed through the IDAWEB portal of the Federal Office of Meteorology and Climatology (MeteoSwiss) and the CH2011 data were obtained from the Center for Climate Systems Modeling (C2SM).

Personal declaration

I hereby declare that the submitted thesis is the result of my own, independent work. All external sources are explicitly acknowledged in the thesis.

Date: _____ Signature: _____